

**Mitral Cell Dendritic Processing in the Olfactory Bulb**

By

Jason Mathew Christie

A DISSERTATION

Presented to the Neuroscience Graduate Program

and the Oregon Health and Science University

School of Medicine

in partial fulfillment of the

requirements for the degree of

Doctor of Philosophy

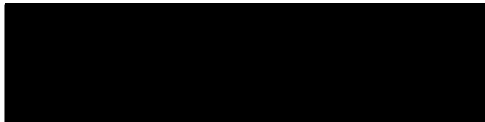
January 2005

School of Medicine  
Oregon Health and Science University


**CERTIFICATE OF APPROVAL**

This is to certify that the Ph.D. thesis of Jason M. Christie has been approved.

---

  
\_\_\_\_\_  
(Gary Westbrook)  
Professor in charge of thesis

  
\_\_\_\_\_  
(Laurence Trussell)

Member  
  
\_\_\_\_\_  
(John T. Williams)  
Member

  
\_\_\_\_\_  
(Craig E. Jahr)  
Member

## **TABLE OF CONTENTS**

Acknowledgements	Page iv
Abstract	Page v
Introduction	Page 1
Chapter 1	Page 15
Chapter 2	Page 32
Chapter 3	Page 56
Chapter 4	Page 89
Conclusions	Page 127
References	Page 131

## **ACKNOWLEDGEMENTS**

I thank my wife Ellen and my daughter Chloe for their love and support.

Gary Westbrook provided excellent guidance and maintained an environment conducive for high quality research. I thank past and present members of the Westbrook lab for their advice and assistance, including Nathan Schoppa, who proved to be an excellent mentor for a young, impressionable graduate student.

Let it known that Drs. Christine Bark, Sheriar Hormuzdi, and Ingo Helbig as part of a collaboration between the Westbrook laboratory and the laboratory of Dr. Hanna Monyer, contributed the data presented in Figures 2 and 4 in Chapter 3.

## **ABSTRACT**

The olfactory bulb serves as the initial center for organizing signals that determines our sense of smell. Mitral cells, the principal neurons of the olfactory bulb, integrate input received from olfactory receptor neurons and convey output to higher brain centers. Mitral cells influence the activity of other mitral cells via excitatory and inhibitory circuits located on both apical and lateral dendrites. To what extent these mitral cell dendritic interactions transform and encode odorant information remains controversial. The unique synaptic architecture of mitral cell dendrites and the olfactory bulb make this both a fascinating question as well as an enigma. I used whole-cell voltage and current-clamp recordings in rodent olfactory bulb slices to study dendritic information processing in both apical and lateral dendrites. My results in mitral and tufted cells indicate that lateral inhibition, the process by which one mitral cell inhibits another through feedforward input, is constrained by the extent of the lateral dendritic arbor. In addition, action potentials were attenuated in distal segments of lateral dendrites due to A-type potassium conductances. Action potential attenuation could have profound consequences on the extent of lateral inhibition by dampening the excitability of lateral dendrites. Mitral cell apical dendrites project to the glomerular region, a distinct second processing region in the olfactory bulb. In this region, I found that mitral cell apical dendrites are the site of connexin36-mediated electrical junctions that allow the instantaneous transmission of currents from an active mitral cell to all other cells with overlapping apical dendrites. Interestingly, mitral cells that share electrical junctions also share a common afferent input. Electrical coupling plays an important role in organizing mitral cell output in a temporally coordinated manner. Without electrical coupling, mitral cell spike

synchronization is lost. Electrical coupling also plays a critical role propagating excitation throughout the electrical syncytium thereby enhancing mitral cell excitability. This work provides insight into mitral cell dendritic circuit interactions and begins to clarify how information is processed in the bulb.

## INTRODUCTION

Animals detect their environment through a variety of senses including smell or olfaction. Olfaction is useful, even essential, for survival and in many species allows for identification of food sources, mates and predators. The neuronal systems that mediate olfaction are exquisitely sensitive, capable of detecting odorants at extremely low concentrations. Also, these neuronal systems allow discrimination between extensive numbers of odorants. Odor detection and discrimination requires a hierarchical neuronal network that samples odorant molecules, encodes the odorant message, and interprets the code in high order processing centers.

In vertebrates, olfaction begins in the nasal turbinates where odorant molecules interact with odorant receptors expressed by olfactory receptor neurons (ORNs) located in the nasal epithelium. Olfactory receptors are encoded by a large family of genes (Buck and Axel 1991). These receptors have seven transmembrane-spanning regions and are coupled to specialized G-proteins ( $G_{olf}$ ). The major signaling pathway (G-protein activation, stimulation of adenylyl cyclase, opening of cyclic nucleotide-gated-ion channels) evokes a prolonged excitatory response in ORNs (Firestein 2001). Odor-evoked action potentials propagate down ORN axons that extend through the cribriform plate and into the main olfactory bulb, the first processing center in the olfactory pathway. Olfactory bulb output neurons, including mitral and tufted cells, directly receive sensory information from ORN afferents and convey information out of the bulb to the thalamus and neocortex. However, the bulb should not be considered a simple relay station. Through complex local circuit interactions, the olfactory bulb plays a prominent

role in transforming incoming unorganized signals into coherent output. How these circuits interact to transform information is an area of continuing study.

Mitral cells are considered the central cellular integrators of the olfactory bulb and therefore it is critical to understand the circuits that mediate their activity. Mitral cells are highly compartmentalized neurons with extensive dendritic projections. Excitatory and inhibitory communication between both local interneurons and other mitral cells, processes that mediate information transformation, occurs along mitral cell dendrites. The unique structures and circuits of the olfactory bulb, including those of mitral cells, are well maintained in *in vitro* slice preparations and therefore are amenable to physiological study.

### **Organization of the olfactory bulb**

Neurons in the mammalian olfactory bulb are organized into distinct laminae that provide the structural basis for circuit interactions (Mori 1987, Scott and Harrison 1991, Shepherd and Greer 1998). These include from the surface inward: the ORN nerve layer (ONL), glomerular layer (GL), external plexiform layer (EPL), mitral cell layer (MCL), and granule cell layer (GCL). The laminae, including the cell bodies and processes that define them, are well defined and recognizable under DIC optics facilitating experimental investigations.

The ONL is composed of thousands of ORN afferents that course along the surface of the bulb. These afferent projections terminate in one of approximately 2400 glomeruli found in the GL. Glomeruli are spheroid bundles of neuropil that do not contain neuronal cell bodies. However, they are densely packed with ORN afferent



terminals, mitral cell dendrites, and numerous dendritic processes of juxtglomerular cells (Pinching and Powell 1971a, Pinching and Powell 1971b). In glomeruli, ORN axons contact dendrites of both mitral cells and juxtglomerular cells. Mitral cell dendrites and juxtglomerular cells also form synaptic connections between one another here as well (Kosaka et al. 2001). Aggregated cell bodies of juxtglomerular cells surround the neuropil and serve to determine the physical separation between neighboring glomeruli. At the ultrastructural level glomeruli are invaginated and internally divided by glial sheaths that appear to demarcate chemical subcompartments (Chao et al. 1997, Kasowski et al. 1999). ORN synapses form a “sensory-synaptic” compartment and dendrodendritic synapses between mitral cells and juxtglomerular cells form a “central-synaptic” compartment.

Juxtglomerular cells, a generic term for cells surrounding the glomerulus, are represented by diverse cell types in the GL. Juxtglomerular cells are primarily composed of periglomerular cells, an inhibitory class of local interneurons composed of dopaminergic and GABAergic types (Kosaka et al. 1998). Periglomerular cell dendritic projections are limited to individual glomeruli where they make synaptic contacts with mitral cell dendritic tufts and are also the site of excitatory input from ORNs. Periglomerular cells project axons to neighboring glomeruli and thereby provide a pathway for interglomerular interactions.

The EPL is the site of synaptic contact between mitral cells and granule cells. Granule cells are usually considered as a chemically homogeneous class of axon-less GABAergic interneurons (but see Didier et al. 2001). Although granule-cell bodies are located in the GCL, their dendrites project to the EPL where they make dendrodendritic

synapses with mitral cells. The EPL also contains the somata and dendritic processes of tufted cells. This class of output cell is heterogeneous in composition, including deep, superficial, and internal variants, with subtypes defined by somatic position (Scott and Harrison 1991). Tufted cells share several common features with mitral cells and therefore are frequently referred to as displaced mitral cells. However, recent data suggests that they have distinct roles (Hayar et al. 2004). Tufted cell lateral dendrites are reduced in length as compared to mitral cells (Mori et al 1983; Orona et al 1984).

Mitral cells are arranged in a compact layer (MCL) only a few cell bodies deep adjacent to the EPL. Mitral cells have a miter-shaped morphology including a large cell body, a single axon, a single apical (primary) dendrite and several lateral (secondary) dendrites. Apical dendrites project superficially to glomeruli via a direct unbranched path through the EPL. Upon reaching the glomerulus apical dendrites ramify extensively to form a tuft of thin processes and are the site of ORN afferent synaptic contact. In addition, mitral cell extend several lateral dendrites into the EPL. The lateral dendrites are oriented tangentially to the axis of apical dendrites and branch several times. Mitral cells extend lateral dendrites for long distances (>1000  $\mu$ m) in EPL and the disc-like radial extent of a single mitral cell can encompass a large fraction of olfactory bulb surface area (Mori et al. 1983, Orona et al. 1984). Lateral dendrites are the site of synaptic interaction with granule cell dendrites. Mitral cell bodies give rise to single axons that project to superficial layers of olfactory cortex including the anterior olfactory nucleus, piriform cortex. Axons pass through the GCL and then coalesce into a large fiber bundle termed the lateral olfactory tract (LOT) upon leaving the bulb.

It is apparent that the mitral cell is divided into separate processing areas based on its distinct dendritic morphology and segregation of inputs (Shepherd and Greer 1998). The glomerular tuft receives and processes ORN input, the apical dendrite and axon of a mitral cell provides a direct and exclusive pathway for information transfer from ORNs to cortex, and the lateral dendrites are concerned with the mediating interactions with vast numbers of granule cells.

### **The glomerular unit**

Odorant receptors are narrowly tuned to a group of odorants and, in some cases, show preferences for single odorants (Malnic et al. 1999). However, ORs are not single-odorant specific. Single odorants may be recognized by several different receptors (Kajiya et al. 2001) thus combinatorial activation of receptors may contribute to odor coding (Malnic et al. 1999). Consistent with the tuning properties of ORs, *in vivo* olfactory bulb imaging studies of odor-induced activity recapitulate the combinatorial activation of multiple glomeruli by individual odorants (Johnson et al. 1998, Rubin and Katz 1999, Wachowiak and Cohen 2001, Fried et al. 2002). Together, these results suggest that odorant receptors encode particular combinations of odorant features (Korsching 2002) and that different odorants are encoded by unique sets of odorant receptors (Duchamp-Viret et al., 1999, Malnic et al 1999).

The olfactory bulb shows a striking modular organization with glomeruli considered as functional units (Mori et al. 1999, Bozza and Mombaerts 2000, Xu et al. 2000). ORNs in olfactory epithelium express one odorant receptor (OR) subtype out of a large gene repertoire (>1000) and ORNs expressing the same olfactory receptor project

their axons to one of two symmetrically oriented glomeruli per olfactory bulb (Buck and Axel 1991, Vassar et al. 1994, Mombaerts et al. 1996). Mitral cells project an apical dendrite to a single glomerulus so that mitral cells are organized as odorant-specific glomerular units. Therefore, these glomerular units represent a single olfactory receptor and the sheet of glomeruli surrounding the olfactory bulb represent a map of odorant receptors.

From an anatomical perspective of the glomerular unit, it may be presumed that the activity of mitral cells directly reflects the activity of ORNs. Consistent with this observation, comparisons of mitral cell responses with the glomerular activation map show that odor responses of mitral cells are highly correlated with those of their principal glomerulus (Lou and Katz 2001). However, there is still considerable debate whether the olfactory bulb simply serves as a relay or is involved in the extraction and/or amplification of more complex features. That is, how might the olfactory bulb extract the olfactory code from the anatomical map? Interactions between individual mitral cells and groups of mitral cells could potentially refine odor codes. Imaging of output neurons in honeybees has showed that postsynaptic activity leads to contrast enhancement and a more confined odor representation when compared to presynaptic signals (Sachses and Galizia 2002). In contrast, second-order neuronal responses in *Drosophila* are more broadly tuned and complex than those recorded in afferents (Wilson et al. 2004). Both of these results are indicative of a transformation process. Presumably, the interaction of excitatory and inhibitory activity within the structured anatomical organization determines how the odorant map is transformed into a sensory code. Aspects of this question are addressed in Chapters 1 and 2 in this text.

## **Mitral-mitral cell communication- lateral inhibition**

Mitral cell activity is regulated by inhibitory and excitatory interactions between interneurons and other mitral cells in the bulb. These cell-to-cell interactions are mediated primarily at dendritic locations, in contrast to the conventional axo-dendritic mode of intercellular communication in the CNS. Interestingly, dendritic interactions of mitral cells are segregated in two different regions, those of the apical dendritic tuft in the glomerulus and those of the lateral dendrites in the EPL reflecting two distinct layers of bulb processing. In the course this of thesis I examined several aspects of mitral cell inhibition and excitation in these discrete functional layers.

Crucial to regulating inhibition in the bulb is the dendrodendritic synapse. These unique synapses are found between periglomerular cells and mitral cell apical dendrites as well as granule cells and mitral cell lateral dendrites. Periglomerular and granule cells contact mitral cells via large spiny structures, termed gemmules, that express both pre- and postsynaptic specializations with mitral cells. Anatomical studies have noted that on gemmules, postsynaptic densities and active zones are segregated but are within extremely close proximity ( $<1 \mu\text{m}$ ) (Price and Powell 1970, Sassoe-Pognetto and Ottersen 2000). Mitral cell dendrodendritic active zones occur on aspiny dendrites and are closely clustered to inhibitory postsynaptic densities (Price and Powell 1970). Mitral cells release glutamate onto interneuronal gemmules (Wellis and Kauer 1994, Isaacson and Strowbridge 1998, Schoppa et al. 1998) that express both AMPA and NMDA receptors (Sassoe-Pognetto and Ottersen 2000, Sassoe-Pognetto et al. 2003). When depolarized, interneuronal gemmules release GABA onto mitral cell dendrites (Jahr and

Nicoll 1982, Wellis and Kauer 1993). The cellular mechanisms that link the postsynaptic periglomerular/granule cell response to vesicle release are still being elucidated. GABA release is mediated by voltage-gated calcium channel activation (Isaacson and Strowbridge 1998, Schoppa et al. 1998, Isaacson 2001) driven primarily and most effectively by NMDA receptors (Isaacson and Strowbridge 1998, Schoppa et al. 1998, Schoppa and Westbrook 1999, Isaacson 2001). In addition, recent results suggest that calcium entry via NMDA-receptors can, under certain conditions, directly contribute to vesicle release (Chen et al. 2000, Halabisky et al. 2000).

Mitral cell depolarizations are followed by prolonged barrages of inhibition because of the synaptic arrangement of the dendrodendritic microcircuit (Isaacson and Strowbridge 1998, Schoppa et al. 1998). The prolonged kinetics of NMDA receptors that drive GABA release from the interneuron, and thus contribute to prolonged inhibition (Schoppa et al. 1998, Schoppa and Westbrook 1999). Reciprocal inhibition results from the direct feedback release of GABA onto the excited mitral cell. Because interneurons can make synaptic contacts with many mitral cells, if sufficiently excited, GABA will be released throughout the entire interneuron dendritic arbor thereby inhibiting all connected mitral cells. This feedforward inhibitory response, termed lateral inhibition, allows one excited mitral cell to influence many other mitral cells.

Lateral inhibition may mediate a center-surround inhibition between mitral cells (Luo and Katz 2001) similar to that of on-type retinal ganglion cells (Kuffler 1953). Conceptually, the olfactory bulb may utilize surround-inhibition to provide contrast enhancement or tuning of the olfactory code (Wilson and Leon 1987; Yokoi et al. 1995). For example, odorant receptors that respond to similar odorants are highly homologous

(Malnic et al. 1999). Likewise, in the few cases studied to date, olfactory receptor neurons that express highly related odorant receptors appear to project their axons to glomeruli that are in close proximity (Tsuboi et al. 1999). Consistent with active local inhibitory interactions, neighboring principal cells that respond to n-aliphatic aldehydes are often inhibited by aldehydes whose aliphatic chain is one or more carbon shorter (Yokoi et al. 1995). Lateral inhibition may also perform more global functions such as synchronization of neuronal activity between different glomerular areas (Kashiwadani et al. 1999).

Because granule cells far outnumber periglomerular cells it is generally assumed that mitral cell inhibition is mediated primarily by the activity of granule cells (Shepherd and Greer 1998). The extreme extent of lateral dendritic projections allows mitral cells to activate vast numbers of granule cells and thereby neighboring mitral cells. Activation of mitral-granule transmission depends on calcium entry that is triggered by action potentials propagating into the lateral dendrites. Key to understanding lateral inhibition is a detailed analysis of lateral dendrites including how excitation is propagated and what factors, both morphological and physiological, control excitability in these dendrites. These aspects were examined in chapters 1 and 2 of this thesis,

### **Mitral-mitral cell communication- spillover excitation**

The glomerular layer provides the anatomical substrate for interactions between same-glomerulus subsets of mitral cells. Glomeruli appear to be organized as chemical compartments (Chao et al. 1997, Kasowski et al. 1999) with the apical dendritic

processes of mitral cell densely packed and in close proximity. The consequences of this anatomical organization to odorant coding may be great.

Mitral cell glutamate release not only excites the postsynaptic complement of receptors on interneurons but also activates both AMPA and NMDA autoreceptors expressed on the mitral cell itself (Nicoll and Jahr 1982, Isaacson 1999, Friedman and Strowbridge 2000, Salin et al. 2001, Schoppa and Westbrook 2001, Schoppa and Westbrook 2002). Functional studies indicate that these glutamatergic autoreceptors are found on both apical and lateral dendrites (Salin et al. 2001, Schoppa and Westbrook 2002). Moreover, anatomical studies indicate that autoreceptors can be found on dendrites near dendrodendritic synapses although their exact spatial relationship is not known (Montague and Greer 1999, Sassoe-Pognetto and Ottersen 2000).

In addition to autoexcitation, mitral cell glutamate release can excite adjacent mitral cells (Isaacson 1999, Schoppa and Westbrook 2001, Urban and Sakmann 2002). Anatomical investigations have not identified synaptic connections between mitral cells (Price and Powell 1970, Pinching and Powell 1971). Therefore, release of glutamate onto adjacent extrasynaptic autoreceptors (spillover) provides the best explanation for cross-excitation mediated between pairs of mitral cells. Mitral cell spillover-excitation, mediated by NMDA receptors (Isaacson 1999, Schoppa and Westbrook 2001,) or both NMDA and AMPA receptors (Urban and Sakmann 2002) has been interpreted as involving mitral cells that share the same dendritic glomerular projection (Schoppa and Westbrook 2001, Urban and Sakmann 2002). The highly compartmentalized structure of glomeruli (Chao et al. 1997, Kasowski et al 1999) in which glial ensheathed bundles of



primary dendrites may provide a compartment for glutamate accumulation supports this idea (Carlson et al. 2000, Schoppa and Westbrook 2002).

### **Mitral-mitral cell communication- electrical coupling**

In addition to chemical synapses, the olfactory bulb is the site of an extensive gap junctional (electrical) network of cells. Gap-junctions, mediated by members of the connexin (Cx) family, can rapidly transmit currents from one cell to all other cells within the syncytium and are well known to mediate synchronized cellular activity (Bennett and Zukin 2004, Hormuzdi et al. 2004). Mitral cells express many connexin subtypes (Paternostro 1995, Miragall 1996, Parenti et al. 2000, Teubner et al. 2000, Zhang and Restrepo 2002, Zhang and Restrepo 2003) and dye injections have revealed gap-junction-mediated indicator coupling (Paternostro et al. 1995). In addition, direct mitral-mitral cell electrical coupling has been shown in paired recordings. Interestingly, mitral cell electrical coupling only occurred between cells projecting to the same glomerulus indicating an apical dendritic localization (Schoppa and Westbrook 2002).

### **The glomerular unit- shared mitral cell activity**

The concept of a mitral cell glomerular unit extends beyond that of anatomical organization. Mitral cells projecting to the same glomerulus share synchronized intraglomerular excitation. When excited by ORN stimulation, all mitral cells that project to a given glomerulus respond in a patterned network response consisting of large, slow oscillating depolarizations that are highly synchronized (Schoppa and Westbrook 2001). In addition, mitral cells that project to the same glomerulus spike in a highly correlated

manner (Schoppa and Westbrook 2002). Thus, mitral cells within the same glomerular unit temporally coordinate both slow and rapid excitatory activity (Schoppa and Westbrook 2001, Schoppa and Westbrook 2002; Carlson et al., 2001). Mechanisms governing ORN induced oscillations and spike synchrony in mitral cells are beginning to be examined and appear to involve both chemical and electrical components (Schoppa and Westbrook 2001, Schoppa and Westbrook, 2002). However, the balance of these interactions is not yet understood.

The precise synchronization of specific output cell subsets is thought to contribute to encoding and discriminating odorants (Laurent et al. 2001). However, the processes that allow the synchronization *in vivo* is an area of continuing study. Understanding the mechanisms of coordinated activity within glomerular sets of mitral cells provides one approach to this problem. In chapters 3 and 4, I investigated factors governing same-glomerulus mitral cell synchrony, including electrical coupling and spillover.

### **Course of thesis**

This thesis is organized in four chapters: The first chapter examines tufted cell dendrodendritic inhibition and provides insight into morphological factors limiting lateral inhibition. Chapter 2 examines action potential backpropagation in lateral dendrites. Chapter 3 examines electrical coupling and synchrony in pairs of mitral cells. Chapter 4 provides insight into factors that contribute to mitral cell cross-excitation.

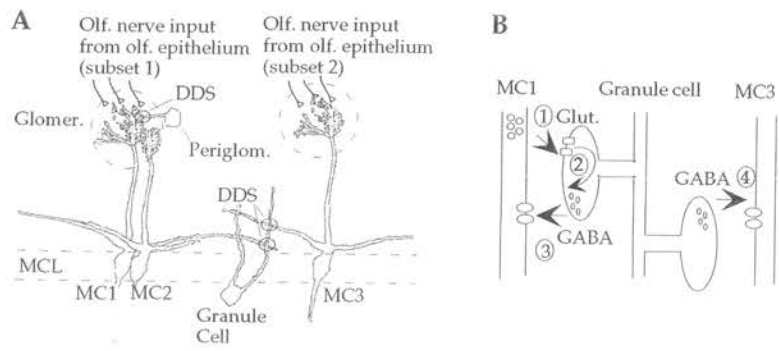
### **Figure Legends**

**Fig. 1.** Olfactory bulb circuitry and the dendrodendritic synapse.

(A). Mitral cells (MC) project single primary dendrites to glomeruli (Glomer.), the site of contact with the terminals of olfactory receptor neurons. Each glomerulus-specific group of mitral cells receives input from a single type of odorant receptor. Mitral cells also make dendrodendritic synapses (DDS, small circles) with periglomerular cells (Periglom.) at their primary dendrite and granule cells at their secondary dendrites. (B). Diagram of a typical dendrodendritic synapse. When excited, glutamate is released from the dendrites of MC1 (*right 1*). This excites the spines of periglomerular and granule interneurons (*right 2*). GABA is then recurrently released back onto the dendrite of MC1 (*right 3*) resulting in inhibition. GABA can also be released onto neighboring mitral cells (*right 4*) resulting in lateral inhibition.

# Figures

## Fig. 1



## **CHAPTER 1**

### **Tufted cell dendrodendritic inhibition in the olfactory bulb is dependent on NMDA receptor activity**

J.M. Christie, N.E. Schoppa and G.L. Westbrook

Vollum Institute, Oregon Health Sciences University

Portland, OR 97201 USA

Address for Correspondence:

Jason M. Christie

Vollum Institute

Oregon Health Sciences University

3181 SW Sam Jackson Park Road

Portland, OR 97201

phone (503) 494-5436

fax (503) 494-1243

email: christij@ohsu.edu

Running Title: Dendrodendritic inhibition in tufted cells

## **Abstract**

Mitral and tufted cells constitute the primary output cells of the olfactory bulb. While tufted cells are often considered as 'displaced' mitral cells, their actual role in olfactory bulb processing has been little explored. We examined dendrodendritic inhibition between tufted cells and interneurons using whole-cell voltage clamp recording. Reciprocal IPSCs generated by a depolarizing voltage steps in a tufted cell were completely blocked by the NMDA receptor antagonist *D,L*-AP5 whereas the AMPA receptor antagonist NBQX had no effect. Tufted cells in the external plexiform layer (EPL) and in the periglomerular region (PGR) showed similar behavior. These results indicate that NMDA receptor-mediated excitation of interneurons drives inhibition of tufted cells at dendrodendritic synapses as it does in mitral cells (Isaacson and Strowbridge 1998; Schoppa et al. 1998). However, the spatial extent of lateral inhibition in tufted cells was much more limited than in mitral cells. We suggest that the sphere of influence of tufted cells, while qualitatively similar to mitral cells, is centered on only one or a few glomeruli.

## **Introduction**

The two classes of primary output neurons in the main olfactory bulb, mitral cells and tufted cells, share several common features. Each receives sensory input from olfactory nerve axons in the neuropil of the glomerular layer and in turn project their axons to piriform cortex. Within the bulb, dendrodendritic synapses form between interneurons and the primary and secondary dendrites of both mitral and tufted cells. Mitral cells are located in a compact layer referred to as the mitral cell layer (MCL) whereas tufted cells are dispersed throughout the external plexiform layer (EPL) and the periglomerular region (PGR) (Cajal 1911). Tufted cells are also considerably more diverse in their morphology (Scott and Harrison 1991).

Our understanding of olfactory bulb function is largely based on studies of mitral cells and the dendrodendritic synapses between mitral and granule cells. At this unique synapse, release of glutamate from mitral cell dendrites drives GABA release from granule cells that then leads to reciprocal and lateral inhibition of mitral cells. Dendrodendritic inhibition of mitral cells can be quite prolonged and follows the slow kinetics of NMDA receptors on granule cells (Mori and Takagi 1978; Schoppa et al. 1998). Dendrodendritic inhibition provides the first step in the network processing of odorant responses that are mapped onto glomeruli in a highly ordered manner (Vassar et al. 1994). As a result, the duration and spatial extent of GABAergic inhibition is likely to have a major impact on sensory integration.

The role of tufted cells in olfactory processing is not well characterized, but there is reason to think their function is distinct from mitral cells. For example, the distribution of dendrites in the bulb suggest that the dendrites of principal cells may preferentially

interact with different sets of interneurons. Granule cell dendrites are present either in the deep zones of the EPL where secondary mitral cell dendrites are located, or in more superficial zones in the EPL where tufted cells secondary dendrites are located (Mori et al. 1983; Orona et al. 1983). Furthermore, dendrodendritic synapses of tufted cells in the PGR may be restricted to periglomerular cell interneurons (Price and Powell 1970; Pinching and Powell 1971a). Distinct interneuronal circuits may also underlie the differences in IPSP size in these two types of principal cells (Ezeh et al. 1993). We examined dendrodendritic inhibition in tufted cells in both the EPL and PGR using whole-cell recording from slices of young rats. Tufted cells were identified visually by their location; morphological subtypes were classified using intracellular dye injections.

## **Materials and Methods**

Slices of the main olfactory bulb (400  $\mu$ M) were prepared from Sprague-Dawley rat pups (PND 10-14) as described (Schoppa et al. 1998). Tufted cells, visualized by infrared DIC optics, were identified by location and morphology (Scott and Harrison 1991). All experiments were performed at room temperature (21-24° C). Whole-cell voltage clamp recordings were made in an oxygenated, magnesium-free solution containing 125 mM or 140 mM NaCl, 25 mM NaHCO<sub>3</sub>, 25 mM glucose, 2.5 mM KCl, 1.25 mM NaH<sub>2</sub>PO<sub>4</sub>, 2 mM CaCl<sub>2</sub> (pH 7.3). Patch pipettes (4-8 M $\Omega$ ) were filled with an intracellular solution containing 140 mM KCl, 10 mM EGTA, 10 mM HEPES, 2 mM MgCl<sub>2</sub>, 2 mM CaCl<sub>2</sub>, 2 mM NaATP, 0.5 mM NaGTP (pH 7.3). In some cases, tufted cells were filled with the dye Alexa 568 hydrazide (Molecular Probes, Eugene, OR) (0.1



mg/ml) and visualized after fixation using confocal microscopy (Odyssey XL, Noran Instruments, Middleton, WI). To verify the location of tufted cell dendrites, slices were counterstained with the nucleic acid stain SYTO-13 (1:4000, Molecular Probes, Eugene, OR).

To evoke reciprocal IPSCs, a depolarizing voltage step (0 mV, 5 ms) was applied to the soma of a voltage clamped tufted cell. To examine lateral inhibition, IPSCs were evoked by stimulating the glomerular layer with a tungsten electrode (0.5 M $\Omega$ , WPI, Sarasota, FL) centered on a single glomerulus. Stimulation pulses (100 V, 100  $\mu$ s) were generated by a stimulation isolation unit (Winston Electronics, Millbrae, CA). IPSCs were recorded with an Axopatch 1B (Axon Instruments, Foster City, CA), filtered with the built-in 4 pole Bessel filter and digitized at 2 kHz. Access resistance ( $R_s$ ) was constantly monitored; recording was terminated when  $R_s$  was >15 M $\Omega$ . All data was analyzed using AXOGRAPH (Axon Instruments). IPSC charge was estimated by integrating the baseline-subtracted current. Statistical significance was determined using standard Student's t-tests or repeated measures ANOVA as appropriate (Microsoft Excel, Redmond, WA).

## **Results**

### *Dendrodendritic inhibition in tufted cells is driven by NMDA receptors*

We first examined tufted cells with cell bodies located in the intermediate zone of the EPL (Fig. 1a). In whole-cell voltage clamp, a depolarizing voltage step (0 mV, 5 ms) elicited a slowly decaying, reciprocal inhibitory post synaptic current (IPSC) due to activation of dendrodendritic synapses. Bath application of bicuculline (40  $\mu$ M) completely blocked the

IPSC, consistent with activation of GABA<sub>A</sub> receptors ( $5 \pm 2.9$  % of control, n=3). The selective NMDA receptor antagonist *D,L*-AP5 (50  $\mu$ M) completely and reversibly abolished the reciprocal IPSC, whereas the AMPA receptor antagonist NBQX (10  $\mu$ M) had no effect (Fig. 1b-d). The dependence of dendrodendritic inhibition on NMDA receptor activation is also observed in mitral cells under the same conditions (see Schoppa et al. 1998). The amplitude and time course of the reciprocal IPSCs were similar to those recorded in mitral cells (not shown; see Schoppa et al. 1998).

As for mitral cells, dendrodendritic inhibition of tufted cells may occur either on primary dendrites in the glomerular layer or on secondary dendrites in the EPL (Macrides and Schneider 1982; Mori et al. 1983; Orona et al. 1984). However, tufted cells can be subtyped into three groups based on their somatic location and dendritic arbors (Scott and Harrison 1991): T<sub>s</sub>, soma and dendrites in the superficial EPL; T<sub>m</sub>, soma and dendrites in the intermediate EPL (Fig. 2a); and T<sub>i</sub>, soma in internal portion of the EPL with dendrites in intermediate EPL. In addition, there is at least one morphologically distinct subtype in the PGR (Fig. 2b) that is characterized by a single large primary dendrite that projects to a single glomerulus and branches repeatedly within it. Secondary dendrites are rare on PGR tufted cells (Pinching and Powell 1971a), thus inhibitory input must be largely from periglomerular cells, rather than granule cells.

Reciprocal IPSCs generated in tufted cells with somata in the EPL ( Fig. 3 a<sub>1</sub> *top*) shared similar characteristics to those generated in tufted cells located within the PGR (example Fig. 3 a<sub>1</sub> *bottom*). The IPSC decay time constant, time to peak, peak amplitude, and IPSC charge were similar for both groups as shown in Figure 3a2. *D,L*-AP5 (50  $\mu$ M) completely and reversibly abolished the reciprocal IPSCs in tufted cells in the periglomerular

region and in all zones of the EPL. In contrast, NBQX (10  $\mu$ M) had no effect (Fig. 3b). Thus, despite the differences in morphology, all types of tufted cells generate reciprocal dendrodendritic inhibition with similar receptor pharmacology and kinetics.

*The spatial extent of lateral inhibition in tufted cells is less than mitral cells*

Our results demonstrate that the general features of reciprocal inhibition are similar in mitral and in tufted cells. However, morphological differences, such as the longer secondary dendrites of mitral cells, could affect the extent of lateral inhibition. Hence, we compared the spatial extent of lateral inhibition in mitral cells with that of tufted cells in the intermediate EPL. A bipolar electrode was used to stimulate individual glomeruli at varying lateral distances ( $\Delta L$ ) from the test cell (Fig. 4a<sub>1</sub>). Under our conditions, the bipolar electrode was expected to directly activate the primary dendrites of principal cells within an underlying glomerulus. Because the primary dendrites of principal cells project only to a single glomerulus (Scott and Harrison 1991), lateral movement of the stimulating electrode can be used to quantify the spatial extent of lateral inhibition. As shown for an intermediate tufted cell ( $T_m$ ) in Fig. 4a<sub>2</sub>, an IPSC generated by stimulation at a lateral separation ( $\Delta L$ ) of 250  $\mu$ m was markedly smaller than at the control location ( $\Delta L=0$   $\mu$ m). The relative degree of lateral inhibition in intermediate tufted cells ( $T_m$ ) was less than mitral cells for all distances examined (Fig. 4b,c). Inhibition in tufted cells was completely eliminated at  $\Delta L \approx 400$   $\mu$ m while inhibition in mitral cells was approximately half-maximal at the same distance (Fig. 4b). For all intervals (100–400  $\mu$ m, binwidth 100  $\mu$ m), the extent of lateral inhibition in tufted cells was significantly less than that of mitral cells (Fig. 4c).

## **Discussion**

*NMDA receptor dependence is a general property of dendrodendritic inhibition in the olfactory bulb*

Previous reports have demonstrated an unusual dependence of mitral cell dendrodendritic inhibition on NMDA receptor activity in granule cells (Isaacson and Strowbridge 1998; Schoppa et al. 1998). Our results indicate that inhibition in tufted cells shares this property regardless of their morphology or location. Mitral and tufted cells receive inhibitory input from granule and periglomerular cells. Direct recordings from granule cells have demonstrated that EPSCs from single mitral cells are conventional in that they have both AMPA and NMDA components, but that the AMPA receptors act primarily to facilitate the depolarization necessary to relieve magnesium block of NMDA receptors. Both the long duration of the NMDA receptor-mediated EPSC as well as its calcium permeability appear to contribute to the release of GABA at dendrodendritic synapses in the bulb (Schoppa and Westbrook 1999; Chen et al. 2000; Halabisky et al. 2000).

Although we did not examine EPSCs in PG cells evoked by stimulation of single tufted cells, PG cells also express NMDA receptor subunits (Giustetto et al. 1997). Thus we expect that tufted cells also drive the activation of NMDA receptors on these interneurons, leading to GABA release. As for mitral cells, stimulation of only a single tufted cell was sufficient in the absence of extracellular magnesium to evoke a reciprocal dendrodendritic IPSC. In physiological magnesium, it is expected that stronger stimulation such as activation of many mitral or tufted cells by olfactory nerve activity will be required to depolarize the principal cell sufficiently to activate reciprocal and lateral inhibition. Our recordings were performed in slices from rat pups (PND 10-14). However a similar pattern of NMDA receptor dependence

has been observed in young adult rats using *c-fos* mRNA expression as a measure of cell activity (Schoppa et al. 1998). In those experiments, pretreatment with MK-801 increased *c-fos* mRNA expression in mitral cells consistent with their disinhibition. Close examination also revealed increased cellular activity in scattered large cells throughout the EPL and in periglomerular region, suggesting that there was simultaneous disinhibition of tufted cells.

NMDA receptors are also present on mitral cell dendrites and contribute an autoexcitatory response that may influence the excitability of the mitral cell dendrite as well as resulting interneuronal activity (Nicoll and Jahr 1982; Isaacson 1999). We have also recorded autoexcitatory responses in tufted cells in the EPL (JM Christie, unpublished observation), providing further evidence that the organization of synaptic glutamate receptors is common to both mitral and tufted cells.

*Morphological differences between classes of principal cells have functional consequences on signal processing*

Although morphological differences between subtypes of interneurons (Mori et al. 1983; Orona et al. 1983; Kosaka et al. 1998) as well as principal cells in the olfactory bulb have been long recognized, the functional consequences of this cellular diversity remains poorly understood. In our experiments, tufted cells located in the PGR, whose dendrodendritic synapses are limited to PG cells (Pinching and Powell 1971b), were not functionally distinct from tufted cells in the EPL that contact PG cells and granule cells (Mori et al. 1983; Orona et al. 1983). Tufted cells in the EPL, while similar in overall morphology to mitral cells, have shorter secondary dendrites (Mori et al 1983; Orona et al 1984) which might predict differences in lateral inhibition. Consistent with this idea, we found that the spatial extent of

lateral inhibition in tufted cells located in the intermediate zone of the EPL was less than mitral cells. Secondary dendrites of tufted cells in superficial zones of the EPL are even shorter than those in deeper zones (Mori et al 1983; Orona et al 1984). Thus the spatial extent of lateral inhibition may be even less in superficial tufted cells than in the tufted cells in the intermediate EPL. We were not able to explore this issue using direct glomerular stimulation because of the likelihood of electrical artifacts in superficial tufted cells adjacent to the stimulator. Our results suggest that the extent of lateral inhibition of intermediate tufted cells is local, extending for several glomeruli ( $\approx 400 \mu\text{M}$ ), whereas the extent of lateral inhibition of mitral cells extends more broadly ( $\approx 750 \mu\text{M}$ ). Our experiments were performed in magnesium-free solutions which enhance NMDA receptor responses. However lateral inhibition is also present in mitral cells in physiological extracellular magnesium, although the spatial extent of lateral inhibition is somewhat reduced. (Schoppa, unpublished).

The precise spatial map of odorant receptors onto glomeruli in the bulb is thought to provide the basis for the odorant code. However lateral inhibition is likely to be important in tuning of the glomerular map. Several lines of evidence suggest that local interglomerular interactions mediated by tufted cells could occur. For example, odorant receptors that respond to similar odorants are highly homologous (Malnic et al. 1999). Likewise, olfactory receptor neurons that express highly related odorant receptors appear to project their axons to glomeruli that are in close proximity (Tsuboi et al. 1999). Consistent with active local inhibitory interactions, neighboring principal cells that respond to n-aliphatic aldehydes are often inhibited by aldehydes whose aliphatic chain is one or more carbon shorter (Yokoi et al., 1995). Such issues are presumably important in odor detection and discrimination as odorants activate

multiple glomeruli (Mori et al. 1999; Rubin and Katz 1999) in order to generate the combinatorial code that constitutes a perceived odor (Malnic et al. 1999).

### **Acknowledgments**

This work was supported by National Institute of Health grant NS26494.

### **Figure Legends**

**Fig. 1.** NMDA receptor activation is required for dendrodendritic inhibition in tufted cells ( $T_m$ ) in the external plexiform layer (EPL) of the olfactory bulb.

(*a,b*) A tufted cell in the EPL was voltage clamped at -70 mV. Depolarizing voltage steps (5 ms, to 0 mV) triggered glutamate release from tufted cell dendrites and activation of synaptically-coupled granule cells (G) and/or periglomerular cells (PG). The resulting GABA release caused a reciprocal IPSC in the tufted cell. This was recorded as a slow inward GABA<sub>A</sub> current in the chloride-loaded tufted cell. The reciprocal IPSC was completely blocked by *D,L*-AP5 (50  $\mu$ M), but not by NBQX (10  $\mu$ M). Each trace is an average of several trials. (*c,d*) The reduction in charge (pA-sec) by AP5 was completely reversible as shown for the same cell as in part b. Summary data for 13 intermediate tufted cells is shown in d. Charge values were generated by integrating the reciprocal IPSC. LOT, lateral olfactory tract; MCL, mitral cell layer.

**Fig.2.** Tufted cells filled with Alexa 568 hydrazide illustrate the distinct morphologies of tufted cells.

(a) A tufted cell with soma located in the external plexiform layer (EPL) had a single primary dendrite that projected into the periglomerular region and secondary dendrites that extended laterally in the EPL. The process extending toward the mitral cell layer is the presumptive axon. (b) Tufted cell with soma in periglomerular region (PGR) had a branched primary dendrite extending locally in the PGR, but no apparent laterally-projecting secondary dendrites. The axon in this cell is not visualized in this image. The margins of glomeruli were visualized by staining with the nucleic acid marker SYTO-13 that labeled the cell bodies of interneurons and glia surrounding each glomerulus.

**Fig. 3.** The characteristics of reciprocal IPSCs were similar for different tufted cell subtypes

(a<sub>1</sub>) Representative reciprocal IPSCs in tufted cell in the PGR (top) and (bottom) tufted cell in the EPL (bottom) showed a similar timecourse. (a<sub>2</sub>) The decay time constants, time-to-peak, peak amplitude and total charge were not statistically different for the tufted cell subtypes. For this analysis, tufted cells in all layers of the EPL were pooled.

(b) The relative sensitivity of the reciprocal IPSCs to AP5 and NBQX were also indistinguishable between subtypes. Tufted cells were subtyped based on the location of their soma. T<sub>p</sub>, tufted cell in PGR; T<sub>s</sub>, tufted cell in superficial zone of EPL; T<sub>m</sub>, tufted cell in intermediate zone of EPL; T<sub>i</sub>, tufted cell in the deep zone of EPL.

**Fig. 4.** The spatial extent of lateral inhibition in tufted cells was significantly less than mitral cells.



( $a_1$ ). Bipolar electrode stimulation of a single glomerulus triggered both a reciprocal IPSC as well as a lateral component arising from the activation of neighboring tufted cells. Lateral movement of the stimulation electrode was used to assess the spatial extent of lateral inhibition.

( $a_2$ ). An IPSC in a tufted cell in the intermediate EPL was evoked by stimulating the glomerulus to which its primary dendrite projected (Glom. A). However, only a small IPSC was recorded when the stimulating electrode was moved 250  $\mu\text{m}$  laterally to an adjacent glomerulus (Glom. X). On return to Glom. A, the IPSC amplitude was unchanged, indicating stability of the recording.

( $b$ ). The spatial extent of lateral inhibition in tufted cells ( $n=8$ ) was less than that of mitral cells ( $n=10$ ).

( $c$ ). At all distance intervals (binwidth = 100  $\mu\text{m}$ ), the magnitude of inhibition in intermediate tufted cells was significantly less than mitral cells (ANOVA analysis). The stimulation artifact was blanked for the current trace ( $\Delta L=250$ ) as indicated by the '=' sign

# Figures

## Fig. 1

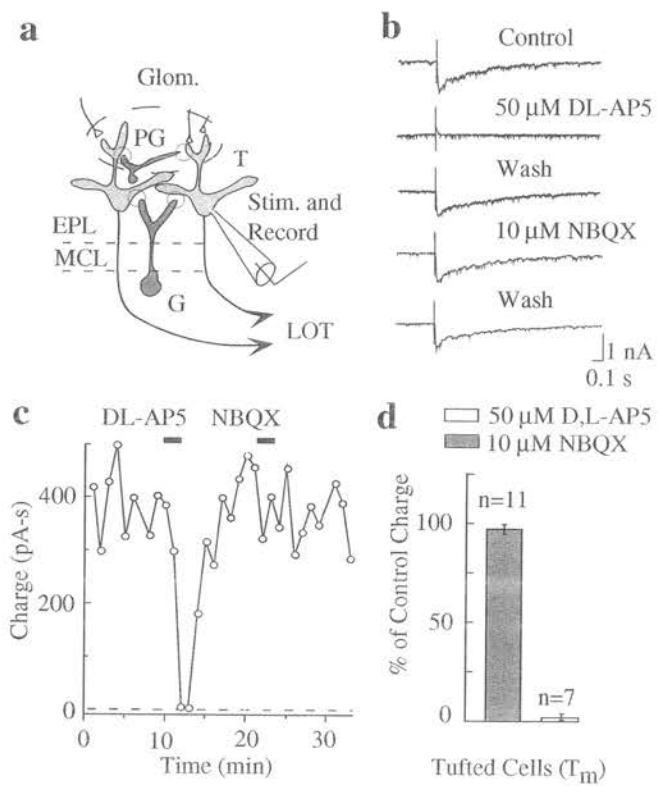
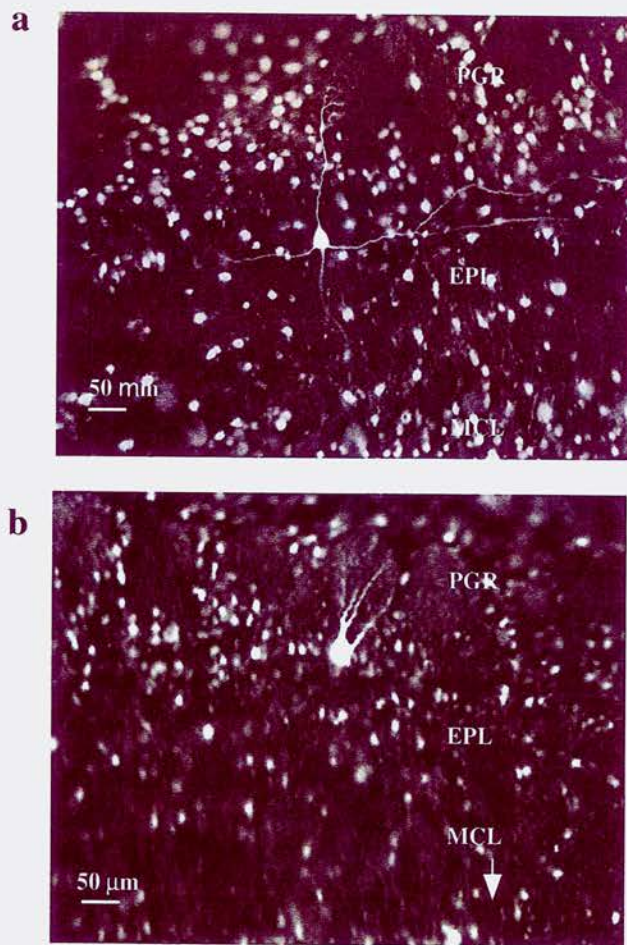
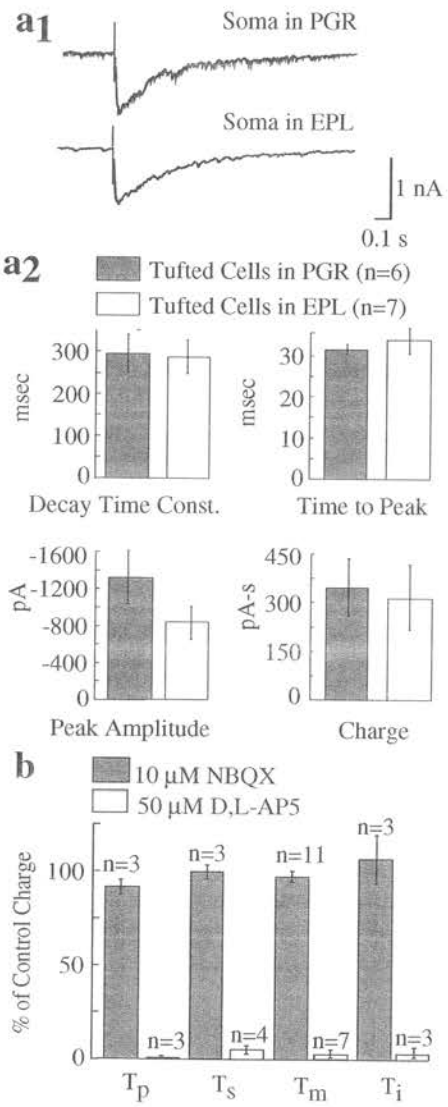


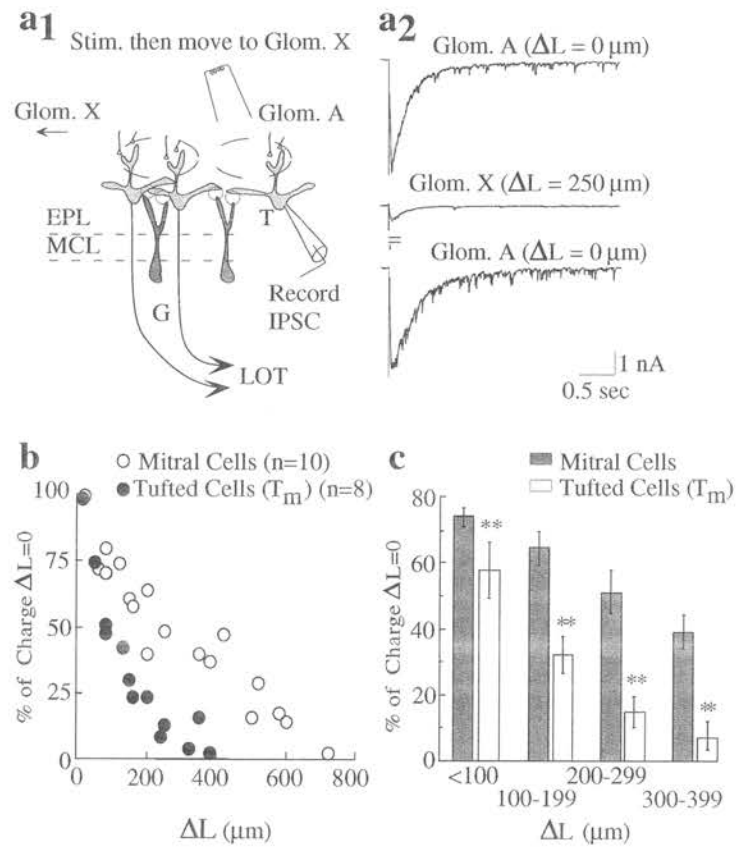
Fig.2



**Fig. 3**



**Fig. 4**



## **CHAPTER 2**

### **Regulation of backpropagating action potentials in mitral cell lateral dendrites by A-type potassium currents**

J.M. Christie and G.L. Westbrook

Vollum Institute, Oregon Health & Science University

Portland, OR 97201 USA

Address for Correspondence:

Jason M. Christie

Vollum Institute

Oregon Health & Science University

3181 SW Sam Jackson Park Road

Portland, OR 97201

phone (503) 494-5436

fax (503) 494-1243

email: christij@ohsu.edu

Running Title:  $I_A$  attenuates action potentials in mitral cell lateral dendrites

Key Words: dendrodendritic, inhibition, olfactory bulb, calcium imaging

## **Abstract**

Dendrodendritic synapses, distributed along mitral cell lateral dendrites, provide powerful and extensive inhibition in the olfactory bulb. Activation of inhibition depends on effective penetration of action potentials into dendrites. Although action potentials backpropagate with remarkable fidelity in apical dendrites, this issue is controversial for lateral dendrites. We used paired somatic and dendritic recordings to measure action potentials in proximal dendritic segments (0-200  $\mu\text{m}$  from soma), and action potential-generated calcium transients to monitor activity in distal dendritic segments (200-600  $\mu\text{m}$  from soma). Somatically-elicited action potentials were attenuated in proximal lateral dendrites. The attenuation was not due to impaired access resistance in dendrites or to basal synaptic activity. However, a single somatically-elicited action potential was sufficient to evoke a calcium transient throughout the lateral dendrite, suggesting that action potentials reach distal dendritic compartments. Block of A-type potassium channels ( $I_A$ ) with 4-aminopyridine (4-AP) (10 mM) prevented action potential attenuation in direct recordings and significantly increased dendritic calcium transients, particularly in distal dendritic compartments. Our results suggest that  $I_A$  may regulate inhibition in the olfactory bulb by controlling action potential amplitudes in lateral dendrites.

## Introduction

Odorant-specific projections to olfactory bulb glomeruli determine the functional units by which olfactory stimuli are encoded (Buck 1996; Mori 1995; Mori et al. 1999). In the rat, each such unit includes  $\approx 1000$  odorant-specific receptor neurons, 20-25 mitral cells and the glomerular neuropil to which they both project. Inhibition between these functional units, mediated by the arrangement of mitral cells and bulb interneurons, is thought to enhance or tune the code (Wilson and Leon 1987; Yokoi et al. 1995). Mitral cells within a single glomerular unit influence mitral cells of adjacent glomerular units by an extensive system of dendrodendritic synapses that are distributed along mitral cell lateral dendrites. Dendritic propagation of action potentials in mitral cells is necessary to drive transmission at these synapses, and thus inhibition depends on action potential backpropagation. Action potentials propagate in apical dendrites without changes in waveform (Bischofberger and Jonas 1997; Chen et al. 1997). In lateral dendrites, attenuation of action potentials has been reported (Lowe 2002; Margrie et al, 2001), although others (Xiong and Chen 2002) have argued that action potentials propagate with full somatic fidelity. Regulation of action potential propagation in lateral dendrites could provide insight into the role of inhibition in odorant coding.

The efficacy of action potential propagation in dendrites varies widely between cell types. In substantia nigra neurons and hippocampal oriens-alveus interneurons, axo-somatically initiated action potentials are conserved throughout the dendritic arbor (Hausser et al. 1995; Martina et al. 2000). However action potentials decrement along dendrites in cerebellar Purkinje cells, CA1 hippocampal pyramidal cells and cortical pyramidal cells (Llinas and Sugimori 1980; Spruston et al. 1995; Stuart and Hausser 1994; Stuart and Sakmann 1994). These differences presumably reflect the relative densities of voltage-gated ion channels in



dendrites (Hausser et al. 2000). For example, in hippocampal CA1 apical dendrites, the density of TTX-sensitive sodium channels appears uniform (Magee and Johnston 1995), but the density of A-type potassium channels ( $I_A$ ) steadily increases with distance from the soma (Hoffman et al. 1997).  $I_A$  thus can regulate action potential amplitudes in CA1 neurons by shunting voltage-dependent sodium current in distal dendrites (Hoffman et al. 1997). We examined action potential propagation in mitral cell dendrites in olfactory bulb slices. Action potentials were attenuated in lateral dendrites based on somatic and dendritic paired recordings as well as imaging of dendritic calcium transients. The attenuation was prevented by block of A-type potassium channels. These results suggest that the extent of lateral inhibition could be shaped by the incomplete propagation of full amplitude action potentials.

## **Materials and Methods**

We prepared horizontal slices of main olfactory bulb (300  $\mu\text{M}$ ) from Sprague-Dawley rat pups (PND 11-15). Briefly, slices were cut and incubated in an oxygenated solution containing 125 mM NaCl, 25 mM NaHCO<sub>3</sub>, 25 mM glucose, 2.5 mM KCl, 1.25 mM NaH<sub>2</sub>PO<sub>4</sub>, 2 mM MgCl<sub>2</sub>, and 1 mM CaCl<sub>2</sub> (pH 7.3). For whole-cell current and voltage clamp recordings from mitral cells, we used the same solution except MgCl<sub>2</sub> was 1 mM and CaCl<sub>2</sub> was 2 mM. The bath temperature was maintained at 33-35°C.

Infrared/DIC optics were used to identify mitral cell bodies and dendrites. Patch pipettes (soma 4-5 M $\Omega$ ; dendrites 10-12 M $\Omega$ ) contained 125 mM K-gluconate, 2 mM MgCl<sub>2</sub>, 2 mM CaCl<sub>2</sub>, 10 mM EGTA, 2 mM Na-ATP, 0.5 mM Na-GTP, and 10 mM HEPES (pH 7.3). For some experiments, synaptic currents were blocked with 100  $\mu\text{M}$  AP5, 10  $\mu\text{M}$  NBQX and 10  $\mu\text{M}$  GABAzine (Tocris Cookson, Bristol England). To counteract recording errors, we used

capacitance neutralization and bridge balance compensation. If  $V_m$  was more positive than  $-50$  mV, or bridge balance compensation was greater than  $15\text{ M}\Omega$  (soma) and  $40\text{ M}\Omega$  (dendrites), we terminated the experiment. Mitral cells were held at a slightly hyperpolarized membrane potential (ca.  $-60$  -  $-65$  mV) in order to prevent random spiking. Potassium currents were measured in nucleated patches with pipettes ( $4\text{-}5\text{ M}\Omega$ ) that contained  $140\text{ mM KMeSO}_4$ ,  $7\text{ mM NaCl}$ ,  $5\text{ mM EGTA}$ ,  $2\text{ mM Mg-ATP}$ , and  $10\text{ mM HEPES}$  (pH 7.3). TTX ( $0.5\text{ }\mu\text{M}$ ) eliminated sodium conductances. Online subtraction protocols removed linear leak and capacitance currents; series resistance compensation was used to minimize steady-state voltage errors ( $>80\%$ ). For calcium imaging, mitral cells were filled with the low affinity ( $K_d=20\text{ mM}$ ) calcium indicator Oregon Green BAPTA-5N ( $100\text{ }\mu\text{M}$ , Molecular Probes, Eugene, OR) via the recording pipette. The pipette also contained  $135\text{ mM K-gluconate}$ ,  $6\text{ mM KCl}$ ,  $4\text{ mM MgATP}$ ,  $0.5\text{ mM Na-GTP}$  and  $10\text{ mM HEPES}$  (pH 7.3). After allowing the dye to equilibrate for  $>20$  minutes, action potential-evoked changes in fluorescence were recorded in the presence of synaptic receptor blockers (AP5, NBQX, and GABAazine). The fluorescence ( $DF/F$ ) evoked by short train of three action potentials in lateral dendrites ( $DF/F = 113.2 \pm 15.5\%$ ) was comparable to three times the fluorescence evoked by the first action potential ( $DF/F = 122.9 \pm 21.5\%$ ,  $n=6$ ), confirming that the dye was not saturated.

Current and voltage signals were recorded with Axopatch 1B and 1D amplifiers (Axon Instruments, Foster City, CA). Signals were filtered with the built-in 4-pole Bessel filter ( $2\text{-}10\text{ kHz}$ ) and digitized ( $20\text{-}50\text{ kHz}$ ). Data were acquired and analyzed using Axon Instruments software (pCLAMP 8.2 and AXOGRAPH 4.5). A confocal microscope (Odyssey XL, Noran Instruments, Middleton, WI), equipped with  $40\times$  and  $63\times$  objectives, was used for calcium imaging. Fluorescence was displayed as  $DF/F$ . We determined statistical significance using

standard Student's t-tests or repeated measures ANOVA as appropriate (Microsoft Excel, Redmond, WA).

## **Results**

### *Action potential backpropagation in mitral cell dendrites*

We used paired somatic and dendritic current clamp recordings to determine the origin and extent of action potential propagation in mitral cell apical and lateral dendrites.

Depolarizing current injections (range 200-1000 pA, 100 ms) in either the soma or dendrites were used to generate action potentials. Regardless of the current injection location, action potentials were initiated in the soma/axon hillock and backpropagated into the dendrites (Fig. 1A). Consistent with previous reports (Bischofberger and Jonas, 1997; Chen et al. 1997; Margrie et al. 2001), apical dendritic and somatic action potential amplitudes were equivalent (dendritic amplitude was  $97.0 \pm 0.7\%$  of somatic amplitude,  $n=9$ ) (Fig. 1A). However, we found that action potentials recorded in proximal lateral dendritic segments (90-225  $\mu\text{m}$ ) were significantly attenuated (Fig. 1A) ( $76.4 \pm 5.1\%$  of somatic amplitude,  $n=12$ ).

The attenuation was not due to granule cell-mediated synaptic inhibition because action potential amplitudes were unchanged when synaptic conductances were blocked with AP5 (100  $\mu\text{M}$ ), NBQX (10  $\mu\text{M}$ ) and GABAzine (10  $\mu\text{M}$ ) (Fig. 2A and 2B). Furthermore, in control conditions, somatic and dendritic action potential amplitudes were unaffected by repetitive firing (range 10-80 Hz) (Fig 1A and 2A); activity thought sufficient for recruitment of recurrent inhibition. Xiong and Chen (2002) observed a similar lack of inhibitory control of action potential propagation under physiological conditions. They reasoned that single cell stimulation was insufficient to overcome magnesium block of NMDA receptors in granule

cells (Isaacson and Strowbridge 1998; Schoppa et al. 1998). However, shunting of lateral dendritic action potentials has been observed with focal GABA applications (Lowe 2002) and by focally evoked granule cell IPSPs (Xiong and Chen 2002).

The reduced amplitude of action potentials in proximal lateral dendrites raised the possibility that action potentials might fail in more distal segments. Direct recordings are not possible along the full extent of lateral dendrites ( $\approx 1000 \mu\text{m}$ , Orona et al. 1984) due to pronounced dendritic tapering. Thus we used optical imaging to assess penetration of voltage signals in distal dendritic segments ( $>200 \mu\text{m}$ ). Mitral cells were loaded individually with the calcium indicator Oregon Green BAPTA-5N ( $100 \mu\text{M}$ ). Experiments were conducted in the absence of synaptic activity ( $100 \mu\text{M}$  AP5,  $10 \mu\text{M}$  NBQX and  $10 \mu\text{M}$  GABA<sub>A</sub>zine). Single, somatically-elicited action potentials (depolarizing current injection  $250\text{-}500 \text{ pA}$ ,  $5.0\text{-}7.5 \text{ ms}$ ) evoked rapidly activating calcium transients in dendrites (peak  $\text{DF}/\text{F}$  range  $8\text{-}48\%$ , time to peak  $2\text{-}4 \text{ ms}$  and half-width range  $60\text{-}220 \text{ ms}$ ). The size and shape of the evoked response was stable during  $30\text{-}60$  minutes of recording, suggesting that the dye concentration was relatively constant. During brief action potential trains, calcium transients added linearly with spike number, indicating that the dye was not saturated (see methods).

Dendritic calcium transients could reflect the active propagation of action potentials or the passive propagation of somatic depolarizations. In order to resolve this question, we used an action potential train waveform ( $25 \text{ Hz}$ ,  $120 \text{ ms}$ ) as a somatic voltage-clamp command (Fig.  $3A_1$ ). Robust calcium transients were generated in the initial dendritic segment ( $3A_2$  left), and in distal dendritic segments (Fig.  $4A_2$  right) when TTX-sensitive sodium conductances were left intact. However, calcium transients were diminished in the initial segment and completely absent in distal dendritic segments ( $3A_2$  and  $3B$ ) when sodium-dependent action potential

propagation was blocked with TTX (0.5  $\mu$ M). Thus dendritic calcium transients reflect local calcium entry mediated by action potentials. The TTX block of calcium transients also indicates that mitral cell dendrites lack regenerative calcium spikes (Charpak et al. 2001; Margrie et al. 2001; Xiong and Chen, 2002).

Action potential-evoked calcium transients were generated in all dendritic segments monitored (Fig. 4A and 4C), suggesting that action potentials penetrate into distal segments. We compared the size of calcium transients evoked in the initial lateral dendritic segment and at distances of 200  $\mu$ m in the same cell. Calcium transients recorded from both sites were similar in size ( $DF/F=22.0 \pm 3.3$  at 0-25  $\mu$ m;  $DF/F=24.1 \pm 2.4$  at 175-225  $\mu$ m; respectively,  $n=4$ ) (Fig. 4B). Consistent with this observation, attenuation of calcium transients was not apparent when data was pooled from all sites (Fig. 4C). The lack of calcium transient attenuation does not exclude attenuation of the underlying voltage signal due to differences in the membrane surface-to-volume ratio. Calcium transients in thin dendrites can appear larger than in thick dendrites as demonstrated in neocortical pyramidal cells (Holthoff et al. 2002). The dendritic tapering in mitral cell lateral dendrites (Mori et al. 1983) would tend to underestimate the calcium signal in proximal dendritic sites as compared to distal dendritic sites. In fact, the low surface-to-volume ration of the soma prevented detection of single action potential-mediated calcium signals (data not shown).

#### *A-type potassium conductances contribute to action potential attenuation*

In hippocampal CA1 apical dendrites, a high density of A-type potassium channels ( $I_A$ ) underlies action potential attenuation (Hoffman et al. 1997). We examined whether a similar mechanism affects action potential amplitude in mitral cell dendrites. A-currents are present in

mitral cells (Wang et al. 1996) as demonstrated by 4-AP (6-10 mM) block of a transient outward current in nucleated outside-out patches (n=6) (Fig. 5A). In paired somatic and dendritic recordings, 4-AP (10 mM) increased the amplitude and half-width of action potentials in the soma, apical and lateral dendrites (Fig. 5B and 5C<sub>1,3</sub>). The increase in peak amplitude was much greater in lateral dendrites (>100  $\mu\text{m}$  from soma), indicating that A-channels ( $I_A$ ) contribute to action potential attenuation in lateral dendrites (Fig. 5C<sub>3</sub>). 4-AP produced similar increases in the action potential half-width in somatic, apical and lateral dendritic sites (Fig. 5C<sub>2</sub>). In addition, 4-AP decreased the firing rate and the time to initiate the first action potential (Figure 5B). In contrast to other cell types (Hoffman et al. 1997) 4-AP did not shift the initiation site of action potentials to dendrites with large dendritic current injections (1000 pA).

Lower concentrations of 4-AP (<100  $\mu\text{M}$ ) inhibit D-type potassium currents (Storm 1988) that, like A-currents, are rapidly activating sub-threshold currents (Storm 1988) and thus could contribute to action potential attenuation. However, the specific D-current antagonist  $\alpha$ -dendrotoxin (1  $\mu\text{M}$ ) did not affect action potential attenuation in lateral dendrites. In direct dendritic recordings,  $\alpha$ -dendrotoxin had no significant effect on the action potential amplitude and increased the half-width marginally ( $102.0 \pm 1.1\%$  and  $111.9 \pm 5.9\%$  of control, respectively; n=3). Thus, the D-current does not have a role in attenuating action potentials in mitral cell lateral dendrites.

We used optical imaging to assess whether A-current block altered action potential propagation in distal dendritic segments. 4-AP (10 mM) increased the peak calcium transient at all dendritic sites (Fig. 6A). The magnitude of the increase varied with location. The increase at 200  $\mu\text{m}$  on lateral dendrites was greater than increases on the initial dendritic segment or sites on apical dendrites. However there was no significant difference between 200  $\mu\text{m}$  and sites

more distal (Fig. 6B), suggesting that action potentials reach an attenuated plateau potential in control conditions. 4-AP also increased the half-width of calcium transients at all sites (Fig. 6B<sub>2</sub>). Differences between sites were not significant.

In proximal segments of lateral dendrites, 4-AP increased the action potential amplitude and half-width by 26% and 60%, respectively (see Figure 5). To determine whether the 4-AP induced changes in action potential shape could account for changes in the calcium transient, we used action potential waveforms in voltage clamped lateral dendrites (>100  $\mu\text{m}$ ) (Fig. 7A). The amplitude or half-width of the action potential waveform were modified to match changes induced by 4-AP. Calcium transients were measured in close proximity to the pipette ( $\leq 20$   $\mu\text{m}$ ) to insure adequate voltage clamp and in the presence of TTX (0.5  $\mu\text{M}$ ) to block active conductances. Action potential waveforms induced robust calcium transients that were comparable to those evoked by unclamped spikes (compare Fig. 7B, Fig. 3 and Fig. 6). Small increases in the half-width of the calcium transient most likely reflect the slow accumulation and dissipation of calcium in the imaged region due to space clamp issues associated with loss of active conductances. Increasing the action potential waveform amplitude or half-width increased the calcium transient (Fig. 7B, 7C). These results indicate that the A-current reduces calcium entry in mitral cell dendrite by controlling the peak and duration of the action potential.

## **Discussion**

### *Attenuation of backpropagating action potentials in lateral dendrites*

Our results indicate that block of A-currents in lateral dendrites prevents attenuation of backpropagating action potentials. We used paired somatic and dendritic recordings to measure

action potential backpropagation. We found that action potentials were attenuated in proximal lateral dendrites. Lowe (2002) and Margrie et al. (2001), also using paired recordings, reported action potential attenuation in lateral dendrites. Xiong and Chen (2002) using a single dendritic recording pipette, observed smaller action potentials in lateral dendrites, but they attributed it to series resistance errors. Series resistance artifacts cannot explain our results. Our recording criteria was similar to Xiong and Chen (2002); dendritic pipette resistances were 10-12 M $\Omega$  and dendritic recordings with a series resistance > 40 M $\Omega$  were excluded. For series resistance in the range considered acceptable in our experiments, some low resistance lateral dendritic recordings showed more attenuation than cells with relatively higher series resistance. Furthermore, 4-AP reversed the attenuation and correspondingly increased the peak calcium transients in distal dendritic segments.

Although action potentials were attenuated in lateral dendrites, attenuation did not lead to propagation failure in distal segments. We used single somatically evoked calcium signals as a measure of propagation in distal lateral dendrites. Margrie et al. (2001) and Xiong and Chen (2002) performed similar experiments. Margrie et al. (2001) concluded that action potentials failed to propagate in distal segments whereas Xiong and Chen (2002) concluded that action potentials traverse the entire dendrite. In terms of the extent of propagation, our results are more in agreement with the Xiong and Chen (2002). Our results suggest that action potential amplitudes reach a plateau level in distal dendrites, similar to that described in CA1 (Spruston et al. 1995) and neocortical pyramidal cells (Stuart and Sakmann 1994). This result is particularly important for mitral cells because glutamate released along the lateral dendrites drives dendrodendritic inhibition. The amplitude and duration of the voltage signals will determine the extent of transmitter release. Because calcium transients in lateral dendrites



required TTX-sensitive action potentials, regulation of backpropagating action potentials may be an important mechanism in shaping the pool of granule cells activated by lateral dendrites.

#### *A-channels in lateral dendrites*

Dendritic excitability depends critically on the density and distribution of voltage-dependent ion channels (Hausser et al. 2000). This is consistent with the role of dendrites in synaptic integration rather than point-to-point transmission of action potentials. Because mitral cell dendrites lack calcium-dependent regenerative potentials (Charpak et al. 2001; Margrie et al. 2001; Xiong and Chen, 2002), the mechanisms governing sodium-dependent action potential backpropagation provide functional control of dendritic excitability. In hippocampal CA1 pyramidal cells, a high density of dendritic A-channels underlies action potential attenuation (Hoffman et al. 1997). Block of A-channels also prevented action potential attenuation in our experiments. We did not make an estimate of A-channel current density in lateral dendrites, thus our results could be explained either by a high density of dendritic A-channels or a non-uniform distribution of dendritic sodium channels. It is likely that sodium/potassium channel ratio is lower in mitral cell lateral dendrites than in the soma/axon initial segment because action potentials were always initiated at the somatic electrode even with large current injections in dendrites in control conditions as well as in the presence of 4-AP.

A-channels are good candidates for control of dendritic excitability because they operate in the subthreshold voltage and their activity can be modulated (Hoffman and Johnston 1998; Mayer and Sugiyama 1988; Villarroel and Schwarz 1996). For example, decreasing the availability of A-channels due to membrane depolarization could increase dendritic action

potential amplitudes. The subthreshold depolarization driven by NMDA autoreceptors (Isaacson 1999; Schoppa and Westbrook 2001) could serve such a role. We did not observe changes in action potential amplitude during repetitive firing ( $< 100$  Hz), suggesting that A channels did not accumulate inactivation. However, this behavior is likely to be strongly influenced by membrane potential. Our results were obtained at resting membrane potentials of  $\approx -65$  mV whereas Margrie et al. (2001) reported a gradual increase in dendritic action potential amplitudes during spike trains for cells with more depolarized membrane potentials.

#### *Functional implications*

The dendritic action potential waveform provides the stimulus necessary for release of glutamate at dendrodendritic synapses. The resulting recurrent and lateral inhibition from synaptically-activated granule cells could thus be determined by the shape of the action potential. In our experiments, calcium transients in proximal dendritic segments were sensitive to the amplitude and duration of action potential waveforms. Although voltage-dependent calcium channels are responsible for dendritic glutamate release (Isaacson and Strowbridge 1998; Xiong and Chen 2002), the calcium sensitivity of glutamate release from this unusual synapse is not known. However, it seems likely that modest changes in action potential amplitude might not markedly affect transmitter release, at least for proximal dendritic segments. For example, 4-AP did not increase the size of granule cell EPSPs evoked by focal mitral cell stimulation although the action potential was broadened (Schoppa and Westbrook 1999). However, given the small dendritic arbor of granule cells ( $\approx 100$   $\mu$ m) (Mori et al. 1983), these experiments were most likely examining release from proximal lateral dendrites and thus may not accurately reflect the behavior at more distal synapses.

Although the baseline synaptic activity in our experiments did not influence backpropagating action potentials, Lowe (2002) recently demonstrated that exogenous GABA application to lateral dendrites could further attenuate backpropagating action potentials. Focal stimulation of granules cells can lead to local action potential failure (Xiong and Chen 2002). Thus the extent and pattern of incoming synaptic inhibition could strongly influence the penetration of action potential into distal dendritic segments. Because attenuated spikes in distal segments would presumably be more influenced by such inhibition, it raises the possibility that proximal and distal segments can be independently regulated. One might expect that this would alter the extent of lateral inhibition.

### **Acknowledgments**

This work was supported by National Institute of Health grant NS26494 (GLW) and 1F31-DC05124-01 (JMC). We thank Nathan E. Schoppa and Didier De Saint Jan for their helpful discussions and Andrew J. Delaney for his assistance.

### **Figure Legends**

#### **Fig. 1.** Action potential attenuation in mitral cell lateral dendrites

(A) Paired somatic and dendritic whole-cell current clamp recordings in apical (*top*) or lateral (*bottom*) dendrites show that action potentials generated by somatic (*left*) or dendritic (*right*) current injection were attenuated in lateral dendrites, but not in apical dendrites. The action potentials enclosed with boxes are enlarged below (1-3). (B) Dendritic action potential amplitudes were plotted as a percentage of the somatic action potential for 27 mitral cell paired

recordings. Action potentials were attenuated in lateral dendrites (filled circles,  $>100 \mu\text{m}$  from soma), but not in apical dendrites (open circles).

**Fig. 2.** Attenuation was not dependent on synaptic activity

(A) Bath application of synaptic receptor antagonists (*right*,  $100 \mu\text{M}$  AP5,  $10 \mu\text{M}$  NBQX and  $10 \mu\text{M}$  GABAzine) did not affect action potential attenuation in lateral dendrites (*top*) or in the soma (*bottom*). The action potential enclosed in boxes are enlarged below (1 and 2). (B) Action potential amplitudes were plotted as a percentage of the somatic action potential. The amplitude of the 4<sup>th</sup> action potential in a train was chosen for comparison because feedback inhibition should be activated by repetitive stimuli.

**Fig. 3.** Dendritic calcium transients require backpropagating action potentials

(A1) We used a 90 ms train of action potentials (33 Hz) recorded in current-clamp as a voltage clamp command. Dendritic calcium transients evoked by this waveform were recorded in either the initial dendritic segment ( $0\text{-}25 \mu\text{m}$ ) or in a more distal dendritic location ( $200 \pm 25 \mu\text{m}$ ). (A2) TTX reduced the calcium transients in the initial dendritic segment ( $0 \mu\text{m}$ ). In a different cell, TTX eliminated calcium transients at distal dendritic locations ( $200 \mu\text{m}$ ). (B) The nearly complete block of calcium transients in distal segments indicates calcium transients can be used as an indication of backpropagating action potentials. Calcium transients are plotted as  $\Delta F/F$ .

**Fig. 4.** Action potential-evoked calcium transients in distal lateral dendrites

(A) Single action potentials evoked a calcium transient (*inset*) in a lateral dendrite distal segment, 625  $\mu\text{m}$  from the soma. Note, the example image is an ensemble composed of several images acquired at low magnification following the experiment. White box denotes imaging area. (B) Action potential-evoked calcium transients had similar amplitudes at 25 and 200  $\mu\text{m}$  in this cell. The calcium transients for each location were stable; compare transients at 25  $\mu\text{m}$  for the beginning (*top*) and end (*bottom*) of the recording period. (C) Data from all cells were binned based on location. The peak amplitudes in each segment were not significantly different.

**Fig. 5.** 4-AP prevented action potential attenuation in lateral dendrites

(A) Potassium currents were evoked in outside-out nucleated patches. Patches were held at  $-50$  mV, stepped briefly (250 ms) to  $-110$  mV to remove resting inactivation and then stepped to a test potential of  $+60$  mV; sodium channels were blocked TTX ( $0.5$   $\mu\text{M}$ ). (A2) Bath application of 4-AP ( $6\text{mM}$ ) blocked a rapidly activating and deactivating component, consistent with an A-type potassium current (see subtracted trace, *right*). (B) In a paired recordings of lateral dendrites (*top*) and soma (*bottom*), 4-AP ( $10$  mM) preferentially increased the amplitude of the dendritic action potential. Action potentials in boxes are enlarged below (1 and 2, respectively). 4-AP also slowed the firing frequency. (C1 and C2) 4-AP increased action potential amplitudes in all segments, but the largest increases were in lateral dendrites. Changes in the half-width were not dependent on location. (C3) 4-AP markedly reduced action potential attenuation in lateral dendrites.

**Fig. 6.** 4-AP increased peak calcium transient in lateral dendrites

(A) The amplitude of calcium transients at varying distances along their lateral dendrite were compared in the presence and absence of 4-AP (10 mM). The data from each location are from separate cells. Calcium transients evoked by single somatically-elicited action potentials were increased by 4-AP. These increases were more prominent in more distal locations (190 and 625  $\mu\text{m}$ ). (B1) The largest increases in calcium transients occurred in distal segments of the lateral dendrites ( $\geq 200 \mu\text{m}$ ). (B2) The effects of 4-AP on the shape of the calcium transient, as measured by half-width, were not location-dependent.

**Fig. 7.** Action potential amplitude and duration can alter the peak calcium transients in lateral dendrites

(A1,A2) In the presence of TTX, simulated action potential voltage clamp commands were applied (*right*) during direct dendritic recordings, 100  $\mu\text{m}$  from soma. The command protocol was varied to match the effects of 4-AP on action potentials. (B) Increasing the test action potential amplitude by 126% or half-width by 160% increased the peak calcium transient peak and its half-width. Data are from the same cell. (C) Histograms summarizing the effects of simulated action potential amplitude and half-width changes on evoked calcium transients.

# Figures

## Fig. 1

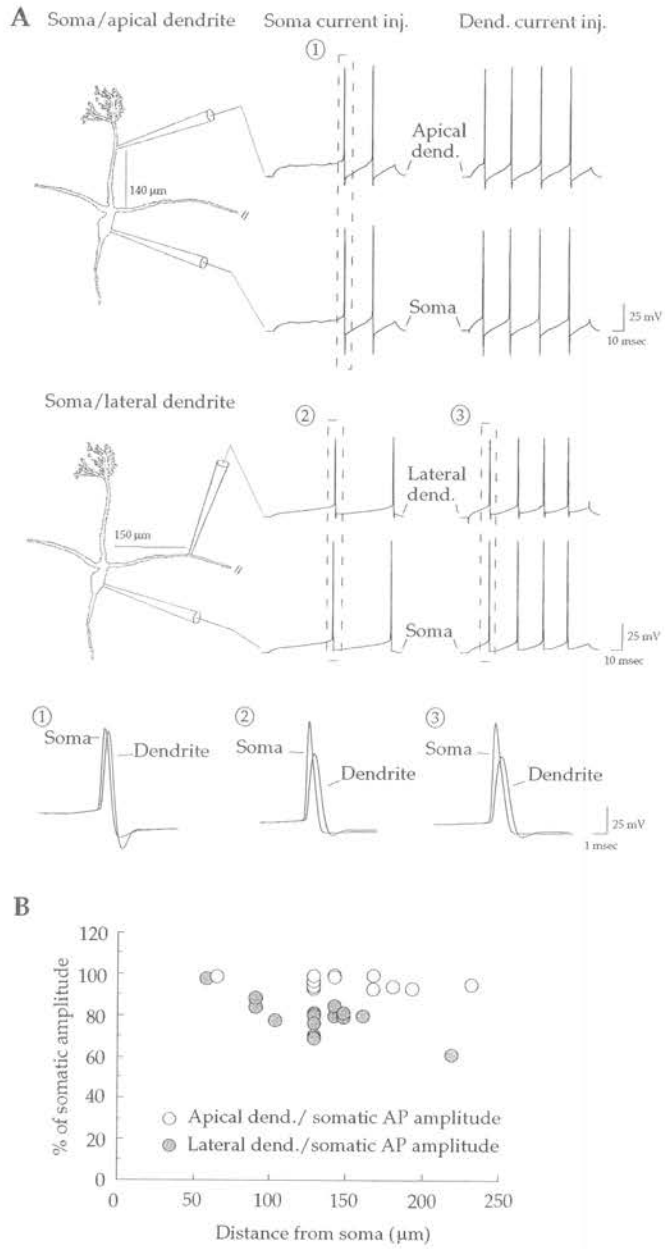


**Fig. 2**

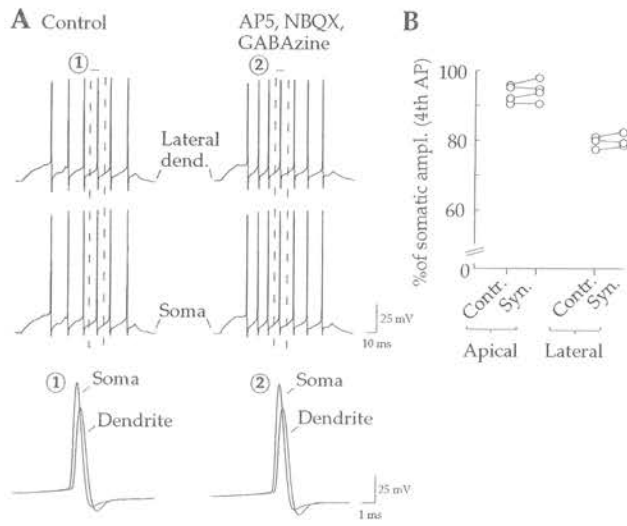




**Fig. 3**

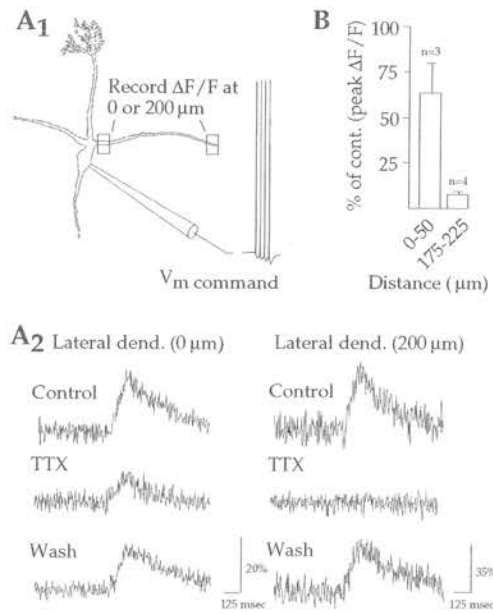


**Fig. 4**

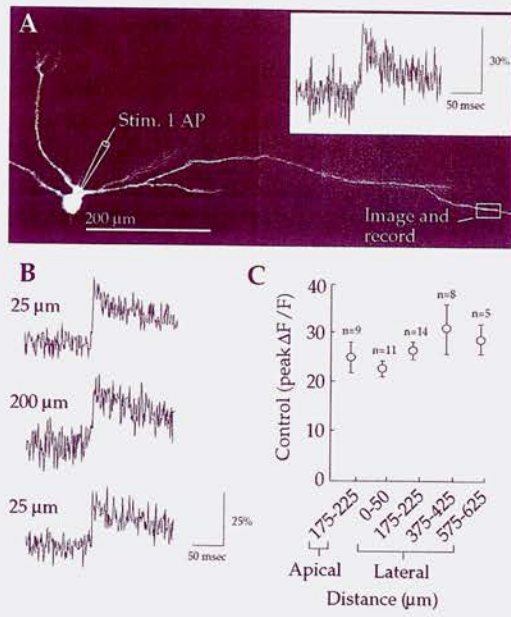


**Fig. 5**

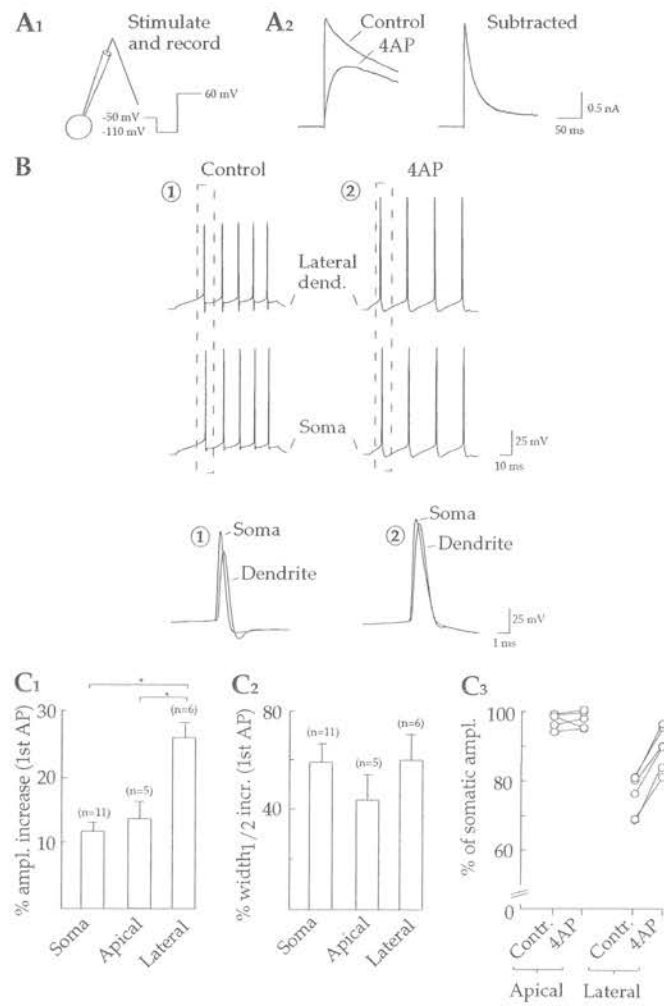


**Fig. 6**

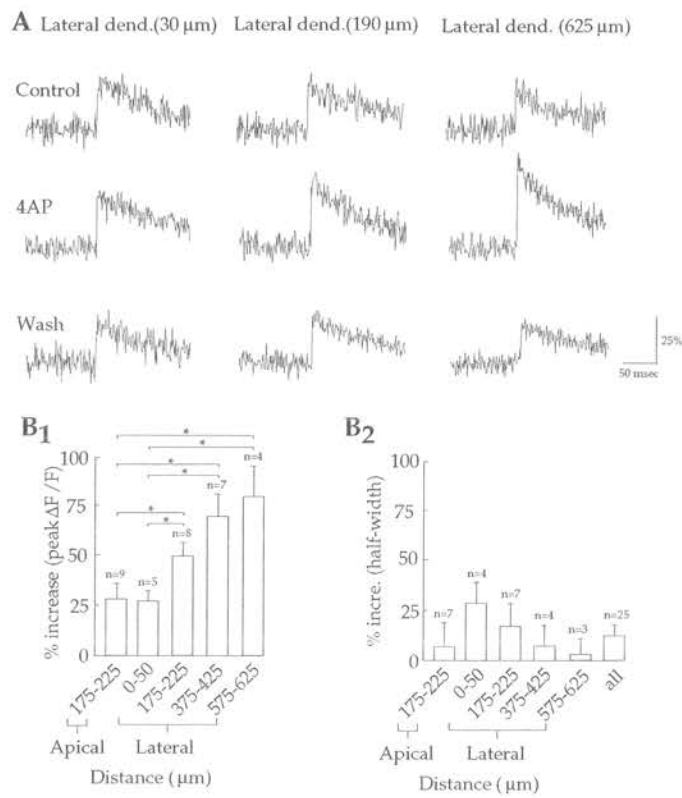
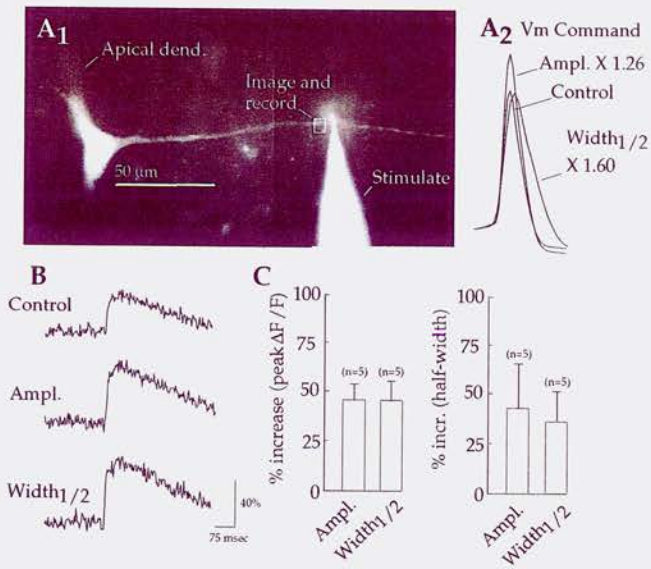


**Fig. 7**



## **CHAPTER 3**

### **Connexin36 mediates spike synchrony in olfactory bulb glomeruli**

Jason M. Christie<sup>1,2,4</sup>, Christine Bark<sup>3,4</sup>, Sheriar G. Hormuzdi<sup>3</sup>, Ingo Helbig<sup>3</sup>, Hanna  
Monyer<sup>3</sup>, and Gary L. Westbrook<sup>1</sup>

<sup>1</sup>Vollum Institute, Oregon Health & Science University

Portland, OR USA

<sup>2</sup>Graduate Neuroscience Program

<sup>3</sup>Department of Clinical Neurobiology, University Hospital of Neurology

Heidelberg, Germany

<sup>4</sup>The first two authors contributed equally to this work

Address for Correspondence:

Jason M. Christie

Vollum Institute

Oregon Health & Science University

3181 SW Sam Jackson Park Road

Portland, OR 97201

phone: (503) 494-5436

fax: (503) 494-1243

email: christij@ohsu.edu

Running title: Disrupted spike synchronization in Cx36 knockout mice

## **Abstract**

Neuronal synchrony is important to network behavior in many brain regions. In the olfactory bulb, principal neurons (mitral cells) project apical dendrites to a common glomerulus where they receive a common input. Synchronized activity within a glomerulus depends on chemical transmission but mitral cells are also electrically coupled. We examined the role of connexin-mediated gap junctions in mitral cell coordinated activity. Electrical coupling between mitral cells projecting to the same glomerulus was entirely absent in connexin36 (Cx36) knockout mice. Ultrastructural analysis of glomeruli confirmed that mitral-mitral cell gap junctions on distal apical dendrites contain Cx36. Correlated spiking as well as coupled AMPA responses between mitral cell pairs were absent in the knockout, confirming that action potential synchrony requires electrical coupling in addition to chemical transmission. Our results indicate that Cx36-mediated gap junctions between mitral cells orchestrate rapid coordinated signaling via a novel form of electro-chemical transmission.

## **Introduction**

Neurons involved in olfactory detection and discrimination show highly correlated spike activity (Laurent et al., 1996; MacLeod et al., 1998; Laurent et al., 2001). The olfactory bulb of mammals, and its equivalent in insects the antennal lobe, also show a striking modular organization with glomeruli long-considered as functional units (Mori et al., 1999). The intersection of this functional activity with the anatomical organization determines how the odorant map is transformed into a sensory code. Olfactory receptor neurons (ORNs) expressing one odorant receptor project their afferents to a single olfactory bulb glomerulus. Mitral cells project an apical dendrite to a single glomerulus so that mitral cells are organized as odorant-specific glomerular units (Mori et al., 1999; Xu et al., 2000; Bozza and Mombaerts, 2001). This organization is important in correlated activity of mitral cells because cells that project to the same glomerulus show synchronized activity on both fast and slow time scales (Carlson et al., 2000; Schoppa and Westbrook, 2001; Schoppa and Westbrook 2002). Thus, mitral cells within a glomerular unit can bundle output in a temporally coherent manner. There is still considerable debate whether the olfactory bulb serves as a simply relay or is involved in more complex feature extractions. Understanding the mechanisms of coordinated activity within glomerular sets of mitral cells provides one approach to this problem.

Spike synchrony in mitral cells is glomerulus-specific and appears to involve both chemical and electrical components (Schoppa and Westbrook, 2002). Electrical neurotransmission, determined by members of the connexin (Cx) family, mediates fast and slow synchrony in cell networks throughout the central nervous system (Bennett and Zukin, 2004; Connors and Long, 2004; Hormuzdi et al. 2004). Gap junctions serve a



variety of functional roles in neurons and astrocytes, yet there are few examples of cooperativity between electrical and chemical transmission. The mixed electro-chemical synapses between goldfish auditory afferents and Mauthner cells provides interesting example where postsynaptic potentials are electrically coupled to the pre-synaptic terminals. The retrograde electrical communication can then influence afferent activity and transmitter release (Pereda et al., 1995; Smith and Pereda, 2003). Although the connexins represent a large family, only Cx36 has been identified between central neurons (Condorelli et al., 1998; Rash et al., 2000; Venance et al., 2000). Cx36 is also expressed in olfactory bulb glomeruli (Condorelli et al., 1998; Belluardo et al., 2000; Parenti et al., 2000; Teubner et al., 2000; Zhang and Restrepo 2003).

We used olfactory bulb slice recordings from control and Cx36 knockout mice to examine the role of gap junctions in glomerular-specific synchronized activity. Electrical coupling between mitral cells within the same glomerulus was absent in Cx36<sup>-/-</sup> mice. Ultrastructural analysis of bulb glomeruli in Cx36-EGFP transgenic mice revealed Cx36 at mitral-mitral dendritic gap junctions. Consistent with the loss of electrical coupling in knockout mice, action potentials were no longer synchronized in mitral cells that project their apical dendrites to the same glomerulus. In contrast, slow coordinated activity within glomerular sets of mitral cells was preserved suggesting that alternative forms of synchrony do not depend on electrical coupling.

Neurons involved in olfactory detection and discrimination show highly correlated spike activity (Laurent et al., 1996; MacLeod et al., 1998; Laurent et al., 2001). The olfactory bulb of mammals, and its equivalent in insects the antennal lobe, also show a striking modular organization with glomeruli long-considered as functional units (Mori

et al., 1999). The intersection of this functional activity with the anatomical organization determines how the odorant map is transformed into a sensory code. Olfactory receptor neurons (ORNs) expressing one odorant receptor project their afferents to a single olfactory bulb glomerulus. In turn, mitral cells project an apical dendrite to a single glomerulus such that mitral cells are organized as odorant-specific glomerular units (Mori et al., 1999; Xu et al., 2000; Bozza and Mombaerts, 2001). This organization is important in correlated activity of mitral cells because cells that project to the same glomerulus show synchronized activity on both fast and slow time scales (Carlson et al., 2000; Schoppa and Westbrook, 2001; Schoppa and Westbrook 2002). Thus, mitral cells within a glomerular unit can bundle output in a temporally coherent manner. There is still considerable debate whether the olfactory bulb serves simply as a relay or performs more complex feature extractions. Understanding the mechanisms of coordinated activity within glomerular sets of mitral cells can provide insight into this issue.

Spike synchrony in mitral cells is glomerulus-specific and may to involve both chemical and electrical components (Schoppa and Westbrook, 2002). Electrical neurotransmission, determined by members of the connexin (Cx) family, mediates fast and slow synchrony in cell networks throughout the central nervous system (Bennett and Zukin, 2004; Connors and Long, 2004; Hormuzdi et al. 2004). Gap junctions serve a variety of functional roles in neurons and astrocytes, yet there are surprisingly few examples of tight cooperativity between electrical and chemical transmission. The mixed electrochemical synapse between goldfish auditory afferents and Mauthner cells provides one interesting example in which postsynaptic potentials are electrically coupled to the presynaptic terminals. This retrograde electrical communication can then directly

influence afferent activity and transmitter release (Pereda et al., 1995; Smith and Pereda, 2003). Until recently, the molecules responsible for neuron-neuron electrical coupling were unknown. Among the large family of the connexins that mediate electrical coupling, Cx36 has been identified in central neurons (Condorelli et al., 1998; Sohl et al. 1998; Rash et al., 2000; Venance et al., 2000), and is also expressed in olfactory bulb glomeruli (Condorelli et al., 1998; Belluardo et al., 2000; Parenti et al., 2000; Teubner et al., 2000; Zhang and Restrepo 2003).

We used olfactory bulb slice recordings from control and Cx36 knockout mice to examine the role of gap junctions in glomerular-specific synchronized activity. Electrical coupling between mitral cells within the same glomerulus was absent in Cx36<sup>-/-</sup> mice. Ultrastructural analysis of bulb glomeruli in Cx36-EGFP transgenic mice identified Cx36 at mitral-mitral dendritic gap junctions. Consistent with the loss of electrical coupling in knockout mice, action potentials were no longer synchronized in mitral cells that project their apical dendrites to the same glomerulus. In contrast, slow coordinated activity within glomerular sets of mitral cells could still be evoked by block of glutamate uptake.

## **Materials and Methods**

### *Mice*

Cx36-EGFP and Cx36 knockout mice were generated as described previously (Hormuzdi et al., 2001; Feigenspan et al., 2004). Electrophysiological data were generated in knockout and wild-type mice. Heterozygous crosses were used to generate knockout pups. Wild-type controls included Cx36<sup>+/+</sup> littermates as well as unrelated C57-

BLK background mice. Differences were not observed between these two groups so all data was pooled.

### *Electrophysiology*

We prepared horizontal slices of main olfactory bulb (250-300  $\mu\text{m}$ ) from mice (PND 14-21). Slices were cut and incubated in an oxygenated solution containing (in mM): 83 NaCl, 26.2 NaHCO<sub>3</sub>, 2.5 KCl, 1 NaH<sub>2</sub>PO<sub>4</sub>, 3.3 MgCl<sub>2</sub>, 0.5 CaCl<sub>2</sub>, 22 glucose, and 72 sucrose (pH 7.3). For recording, we made the following substitutions (in mM): 119 NaCl, 1.3 MgCl<sub>2</sub>, and 2.5 CaCl<sub>2</sub>; sucrose was omitted. The bath perfusion temperature was maintained at 32-35°C.

Whole-cell recordings were obtained under visual control using DIC optics (Carl Zeiss). For paired recordings, mitral cell bodies were typically separated by 5-45  $\mu\text{m}$ . Patch pipettes (4-6 M $\Omega$ ) contained a solution of (in mM): 125 Kgluconate, 2 MgCl<sub>2</sub>, 0.025 CaCl<sub>2</sub>, 1 EGTA, 2 NaATP, 0.5 NaGTP, and 10 HEPES (pH 7.3). Current recordings were made with Axopatch 200A and 200B amplifiers (Axon instruments). The analog signals were filtered at 1-5 kHz with the built in eight-pole Bessel filter and digitized at 0.5-10 kHz. Data were acquired and analyzed using Axograph 4.6 (Axon Instruments). Mitral cells were often held at hyperpolarized potentials to prevent random spiking.

To assess cell morphology, mitral cells were filled with biocytin (0.1%) during whole-cell recordings. Slices were then fixed in PBS (72 mM NaH<sub>2</sub>PO<sub>4</sub> and 28 mM Na<sub>2</sub>HPO<sub>4</sub>, pH 7.2) with formaldehyde (4%) overnight, then permeabilized and labeled in PBS containing 0.3% Triton X-100 and Cy-5-conjugated streptavidin (1:2000, Jackson

Immunoresearch) for 12 hr at 4°C. Propidium Iodide (1:2000, Molecular Probes) was used as a nuclear counterstain. Images were acquired on a confocal microscope (Olympus) equipped with a 20X objective.

### *Analysis*

Correlated spiking was determined as described (Schoppa and Westbrook, 2002). Briefly, a cross-correlogram of spike lag times ( $\Delta t$ ) between each paired cell recording ( $\pm 100$  ms, single cell reference) was generated. Initially,  $\Delta t$  measurements were placed in 20 ms bins and the normalized standard deviation (raw s.d./mean) of bins  $|\Delta t| \geq 40$  ms was determined. The largest normalized s.d. value across 41 paired recordings was 0.31.  $\Delta t$  measurements were then placed in 5 ms bins and a ratio of probability ( $S$ ) that  $|\Delta t| < 10$  ms versus  $30 \leq |\Delta t| \leq 40$  ms was computed (an  $S$  value of 1.00 reflects random spiking). The minimum  $S$  value as a criterion for determining whether cells synchronized spikes was set at twice the largest normalized s.d. value for all recordings ( $S \geq 1.62$ ).

We determined the synchronization of TBOA-induced depolarizations by generating the average cross-correlation of 10s epochs of a continuous recording (total time > 60s) and calculating the cross-correlation at  $t=0$  ( $C_0$ ). Because the glomerular target of mitral cells could not be reliably determined by DIC optics, we used the synchrony of TBOA-induced depolarizations to determine the glomerular specificity of mitral cell pairs (Schoppa and Westbrook, 2001; Schoppa and Westbrook, 2002). As expected, wild-type and knockout pairs of mitral cells that projected to the same glomerulus had highly synchronized depolarizations ( $C_0$  values  $\geq 0.75$ ; confirmed by biocytin fills, wild-type  $n=5$ , knockout  $n=6$ ) whereas cells that projected to different

glomeruli were not synchronized ( $C_0$  values  $\leq 0.50$ , confirmed by cell fills, wild-type n=5) (see Fig. 1C and 6C).

#### *Perfusion and preparation of tissue sections*

Cx36-EGFP mice (n= 3) and wild-type control mice (n= 3) were deeply anesthetized with a mixture of Ketanest, Xylain, and NaCl and perfused through the heart with 0.9% saline followed by fixative containing 4% paraformaldehyde, 0.05% glutaraldehyde (Sigma) in 0.1 M phosphate buffer (PB, pH 7.4). The olfactory bulbs were dissected out and coronal sections of 40-60  $\mu\text{m}$  thickness were cut on a vibratome (VT1000S, Lecia Microsystems).

#### *Pre-embedding immunogold staining*

5% BSA (Sigma) in PBS (pH 7.4) was used for blocking, followed by incubation in 1:10000 dilution of rabbit anti-EGFP primary antibody (Molecular Probes). For immunogold reaction, sections were incubated in a goat anti-rabbit IgG coupled to 1 nm gold particles (Amersham Life Science; diluted 1:30 in 1% NGS, 0.1% IGSS, and 0.8% BSA). The UltraSmall gold particles were silver enhanced by IntenSE<sup>TM</sup>M as described by the manufacturer (Amersham). Sections for electron microscopy were postfixated with 1% OsO<sub>4</sub>, contrasted in 1% uranyl acetate, dehydrated in graded alcohol series and propylene oxide, and embedded flat in epoxy resin (Durcupan ACM, Fluka) on slides. After polymerization of the resin, selected areas were re-embedded in Durcupan blocks for sectioning. Serial 60 nm sections were collected on pioloform-coated copper grids

and contrasted with lead citrate. The electron micrographs were taken on an EM 10 Zeiss CR electron microscope.

### *Statistics*

T-tests were used where appropriate. Significance was considered as  $p \leq 0.05$ .

## **Results**

### *Synchronized spiking in Cx36<sup>-/-</sup> mice*

In paired recordings from wild-type mitral cells that projected to the same glomerulus, injection of depolarizing current (100-400 pA; 2.5 s) elicited irregular trains of action potentials that were highly correlated (Fig. 1A<sub>2</sub>). We compared the spiking of cell pairs by cross-correlating action potential lag times between cells ( $\Delta t$ ), binning the results, and then generating a synchronization parameter  $S$  (see methods). Correlated spiking was apparent as a peak ( $S \gg 1$ ) in spike time lag cross-correlograms near  $\Delta t = 0$  (Fig. 1A<sub>3</sub>).  $S$  values ranged from 1.26 to 7.91 ( $2.99 \pm 0.53$ ,  $n=13$ ). In contrast to wild-type mice, correlated spiking was completely absent in cell pairs from Cx36 knockouts. In paired recordings, current injections elicited action potentials that occurred independent of one another (Fig. 1B<sub>1</sub>) as reflected in flat cross-correlograms (Fig. 1B<sub>2</sub>).  $S$  values for Cx36<sup>-/-</sup> cells projecting to the same glomeruli were  $1.01 \pm 0.07$  ( $n=9$ ). As previously reported (Schoppa and Westbrook, 2002), action potentials were not correlated in mitral cell pairs that projected to different glomeruli (Fig. 1A<sub>4</sub> and 1B<sub>4</sub>;  $S = 1.12 \pm 0.06$  and  $0.99 \pm 0.07$  WT ( $n=12$ ) and KO ( $n=8$ ) pairs, respectively).

The loss of correlated spiking in the absence of Cx36 could not be explained by changes in the projection pattern of mitral cell apical dendrites. Mitral cells, labeled with biocytin during paired recordings (Fig. 1C<sub>1</sub> and 1C<sub>2</sub>), had apical dendrites that projected to a single glomerulus in both wild-type (n=5) and Cx36<sup>-/-</sup> mice (n=6). Apical dendritic tufts with overlapping processes in close apposition were comparable in both lines. The absence of Cx36 also did not affect the gross morphology of cell layers in olfactory bulb slices.

#### *Cx36 expression in olfactory bulb*

In cortical interneurons, Cx36-mediated gap junctions are thought to be preferentially expressed relatively close to the soma (Amitai et al. 2002). However, mitral-mitral cell correlated spiking is glomerulus-specific, and thus the connexin responsible for electrical coupling should be expressed in distal dendrites. To address this issue, we first mapped the distribution of Cx36 in the olfactory bulb using a transgenic mouse in which the C-terminus of Cx36 was tagged with enhanced green fluorescent protein (EGFP) (2A). Cx36 mRNA showed a similar distribution in wild-type and Cx36-EGFP mice (Fig. 2B<sub>1</sub> and 2B<sub>2</sub>) confirming the correct expression of the transgene. In the olfactory bulb, Cx36 mRNA was expressed in mitral cells, juxtglomerular cells, and in granule cells. EGFP fluorescence, an indicator of Cx36 protein expression, revealed a punctate distribution indicating hot-spots of protein localization in glomeruli (Fig. 2C<sub>1</sub>). When Cx36-EGFP was enhanced using an antibody directed against EGFP, signal was also observed in mitral cell soma (Fig. 2C<sub>2</sub>) confirming that mitral cells express Cx36.



To determine whether Cx36 underlies functional coupling between mitral cells, we used paired recording in cells projecting to the same glomerulus. In slices from wild-type mice, hyperpolarizing current injections (100-800 pA, 500 ms) in one cell evoked a hyperpolarization in the other cell indicative of electrical coupling (Fig. 3A). The coupling ratio (*CR*, the ratio of the voltage deflection in the stimulated to that in the test cell) was  $0.039 \pm 0.005$  (n=19) for mitral cells that projected to the same glomerulus. In contrast, Cx36<sup>-/-</sup> mitral cell pairs were not electrically coupled (*CR*=  $0.002 \pm 0.001$ ; Fig. 3C). Coupling was not detectable in mitral cell pairs that projected to different glomeruli in either wild-type (*CR*=  $0.002 \pm 0.001$ , n=12; Fig. 3B) or knockout mice (*CR*=  $0.001 \pm 0.001$ , n=12; Fig. 3D). The input resistance of Cx36<sup>-/-</sup> mitral cells ( $117 \pm 9 \text{ M}\Omega$ , n=28) was significantly larger than that of wild-type cells ( $68 \pm 4 \text{ M}\Omega$ , n=30;  $P < 0.05$ ) consistent with the loss of neuron-neuron gap junctions in Cx36<sup>-/-</sup> glomeruli. In mature mice (PND 42-44), mitral cells projecting to the same glomerulus were also electrically coupled (n= 4), suggesting that electrical coupling is not limited to juvenile animals. These results indicate that mitral cell expression of Cx36 is necessary for glomerulus-specific electrical coupling as well as correlated spiking.

#### *Ultrastructural expression of Cx36 in mitral cell glomerular tufts*

Although Cx36 expression has been previously described in the glomerular layer, the existence of mitral-mitral cell gap junctions has been controversial (Kosaka and Kosaka, 2003). Because the punctate fluorescence observed in the glomeruli of Cx36-EGFP mice could potentially represent gap junctions between cells other than mitral cells (Belluardo et al., 2000; Hormuzdi et al., 2001) we used immunogold electronmicroscopy

to examine the subcellular location of Cx36 within glomeruli. To maximize detection, we visualized the Cx36-EGFP fusion protein by preembedding immunocytochemistry with EGFP antibodies in conjunction with silver-enhanced gold particles (Fig. 4). The distribution of gold particles within glomeruli was evaluated in tissue obtained from 3 transgenic animals. Of the gold particles counted, 82.5% were associated with plasma membranes. Of these, 95% were within dendritic processes. Dendrites were labeled at areas of close membrane apposition in serial sections consistent with the presence of a neuronal gap junction. We more closely examined 19 gap junctions that contained a total of 55 gold particles. The labeled gap junctions had characteristic features such as localization next to punctum adhaerens and a cytoplasmic semi-dense material undercoating the junctional plasma membrane surface (Fig. 4A<sub>1-3</sub>). Mitral cell dendrites were identified based on their pale cytoplasmic matrix, few organelles, spherical vesicles, and asymmetric synapses (Pinching and Powell, 1971). Mitral-mitral cell gap junctions were labeled with silver-enhanced gold particles (Fig. 4B<sub>1-3</sub>). In some cases immunogold particles labeled both sides of mitral-mitral gap junctions indicative of homotypic Cx36 channels. These results indicate that Cx36 is responsible for gap junctions between distal dendrites of mitral cells in olfactory bulb glomeruli. As expected, the labeling was not exclusively limited to mitral cells, consistent with the expression pattern of Cx36 mRNA and protein. However, non-mitral gap junctions were not investigated in detail.

#### *AMPA auto receptor mediated excitation in Cx36<sup>-/-</sup> mice*

Our results indicate that mitral cell correlated spiking requires Cx36-containing gap junctions. However, correlated spiking also depends on AMPA receptor responses in

distal mitral cell dendrites (Schoppa and Westbrook 2002). This implies that both electrical and chemical transmission must contribute to action potential synchronization in distal dendrites. Action potentials in mitral cells evoke dendritic glutamate release that activates AMPA receptors on apical tufts of the same dendrite (autoreceptors, Salin et al., 2001, Schoppa and Westbrook, 2001). Electrical coupling of the evoked AMPA autoreceptor potential between mitral cells ( $D_{AMPA}$ ) could drive correlated firing by bringing the coupled cells to spike threshold (Schoppa and Westbrook, 2001). Alternatively, glutamate released from one mitral cell could spill over and directly excite AMPA receptors on neighboring mitral cells within a glomerulus (Urban and Sakmann, 2002). We examined these possibilities in  $Cx36^{-/-}$  mice.

In recordings from wild-type mitral cells projecting to the same glomerulus, single action potentials elicited in one cell evoked a two-component depolarization in the unstimulated adjacent mitral cell (Fig. 5A<sub>1</sub>). The first component was a rapid spikelet that was time-locked to the action potential in the stimulated cell. The second component was larger and slower ( $0.82 \pm 0.29$  mV,  $W_{1/2} = 12.75$  msec) and was eliminated by NBQX (20  $\mu$ M;  $12 \pm 6\%$  of control,  $n=4$ ) consistent with the previously described  $D_{AMPA}$  (Schoppa and Westbrook, 2002). In two additional cases it was difficult to resolve an action potential evoked response. In contrast to wild-type mice, we were unable to evoke either component in  $Cx36^{-/-}$  cell pairs that projected to the same glomerulus ( $n= 6$ ) (Fig. 5B<sub>1</sub>).

Despite the lack of the electrically coupled  $D_{AMPA}$  depolarization, AMPA autoexcitatory potentials were present in  $Cx36^{-/-}$  mice. In wild-type ( $n= 6$ ) and  $Cx36^{-/-}$  ( $n= 5$ ) mice, AMPA autoreceptor potentials generated by action potentials had similar amplitude and shape to  $D_{AMPA}$  (Fig. 5A<sub>2</sub>, 5B<sub>2</sub>, and Fig. 5C). These results indicate that

$D_{\text{AMPA}}$  is mediated by electrical coupling of AMPA autoreceptor potentials. Thus Cx36-mediated gap junctions combine with dendritic glutamate release to create a novel form of electro-chemical transmission.

### *Slow synchronization and electrical junctions*

Electrical coupling can mediate both fast and slow synchrony in neuronal networks (Bennett and Zukin, 2004; Connors and Long, 2004; Hormuzdi et al., 2004). Our results indicate that fast synchronization of action potentials is dependent on Cx36 electrical coupling. However, mitral cells also have slow synchronized oscillations (Isaacson, 1999; Puopolo and Belluzzi, 2001) that are glomerulus-specific (Carlson et al., 2000; Schoppa and Westbrook, 2000). Other cell types can generate slow synchronized oscillations that involve electrical coupling, including neocortical interneurons, inferior olivary neurons, thalamic reticular nucleus interneurons, and locus coeruleus neurons (Beierlein et al., 2000; Alvarez et al., 2002; Long et al., 2002; De Zeeuw et al., 2003; Long et al., 2004).

To examine whether electrical coupling mediates slow oscillations in mitral cells we evoked periodic slow depolarizations with the glutamate uptake blocker TBOA (50  $\mu\text{M}$ , Isaacson, 1999). Depolarizations alternated with silent interburst periods (not shown), but often the depolarizations oscillated at a regular frequency ( $\approx 0.5$  Hz, Fig. 6A<sub>1</sub>). In wild-type mice, pairs of mitral cells that projected to the same glomerulus had highly synchronized depolarizations ( $C_o$  values  $\geq 0.75$ ,  $n=5$ ) consistent with previous reports (Carlson et al., 2000; Schoppa and Westbrook, 2000). When mitral cells were held near the resting membrane potential, action potential bursts were often evoked at the

peaks of the depolarizations (Fig. 6A<sub>2</sub>). Although the slow depolarizations provided rhythmicity in action potential bursts, spiking within each burst was too fast to allow an assessment of high fidelity spike synchronization. Slow depolarizations in mitral cell pairs that projected to different glomeruli were not synchronized (Fig. 6C, n=5).

Electrical coupling was not required for the slow oscillations evoked by glutamate uptake block. Specifically, mitral cells that projected to the same glomerulus in Cx36<sup>-/-</sup> mice had periodic depolarizations that were synchronized ( $C_0$  values  $\geq 0.75$ , n= 6; 6B<sub>1</sub>). As in wild-type mice, action potential bursts were temporally correlated when the membrane potential was held near rest (6B<sub>2</sub>). These results support the observations that spillover, at least under conditions of glutamate uptake block, can drive slow correlated activity in a glomerulus even in the absence of electrical coupling (Isaacson, 1999; Schoppa and Westbrook, 2001).

## **Discussion**

### *Cx36 in the olfactory bulb*

Although gap junctions are widespread throughout the mammalian brain, the evidence for electrical synaptic transmission has been limited. Early studies of the connexins, the molecular mediators of electrical junctions, were largely directed at non-neuronal cells (Nagy and Rash, 2000). The identification of a neuronal-specific connexin (Cx36) (Condorelli et al., 1998; Sohl et al. 1998) changed that focus. Cx36-mediated gap junctions have been identified in neocortex, hippocampus, and thalamus (Deans et al., 2001; Hormuzdi et al., 2001; Landisman et al., 2002; Blatow et al., 2003). However, these Cx36-mediated junctions are primarily between interneurons (Connors and Long,

2004) with the exception of inferior olive projection neurons (Long et al., 2002). Our results indicate that projection cells of the olfactory bulb, mitral cells, are coupled by Cx36-mediated gap junctions thus extending the role of these junctions to a new class of neuron. Mitral cells may express at least two additional connexins (Cx43 and Cx45) (Paternostro et al., 1995; Miragall et al., 1996; Zhang and Restrepo, 2002). Although the functional significance of these connexins is not known, they could participate in coupling mitral cells to local inhibitory interneurons (both granule and periglomerular cells) (Paternostro et al. 1995; Kosaka and Kosaka, 2003).

Before connexins were identified, dye coupling was considered a required feature of a functional gap junction. We did not observe dye coupling between mitral cells in wild-type mice, presumably because of their small single channel conductance (Srinivas et al., 1999) and distal dendritic location. In the thalamic reticular nucleus and neocortex, where Cx36 also mediates gap junctions between neurons, dye coupling is rarely observed (Gibson et al., 1999; Landisman et al., 2002). In contrast, Cx36-mediated dye transfer does occur between the strongly coupled AII amacrine cells in the retina (Deans et al. 2002).

Unlike prior reports of Cx36-mediated gap junctions in other neurons, both our physiological and immunolocalization studies indicate a distal dendritic location in mitral cells. The predominant distribution of Cx36 in bulb glomeruli, identified using a Cx36-EGFP fusion protein, is in agreement with immunocytochemical studies targeting Cx36 directly (Belluardo et al., 2000; Teubner et al., 2000; Zhang and Restrepo, 2003). Ultrastructural studies have revealed an extensive gap junctional network in the glomerular layer (Kosaka and Kosaka, 2003). Although Cx36 is expressed in several cell

types in the glomerulus, our immunoelectronmicroscopy clearly demonstrates expression in mitral cell dendritic tufts. Our search for mitral-mitral cell gap junctions was made easier because we could focus on gold-labeled Cx36 in unambiguously identified mitral cell dendrites. Kosaka and Kosaka (2003) did not report mitral-mitral cell gap junctions, most likely because of the processes containing gap junctions were unidentified. On further examination, however, they also identified mitral-mitral cell gap junctions (Kosaka and Kosaka, 2004).

#### *Role of Cx36 in electrical coupling and synchronous spiking*

The AMPA receptor dependence of correlated spiking is a distinct feature of mitral-mitral cell synchrony. An AMPA receptor-mediated potential ( $D_{\text{AMPA}}$ ) is necessary for correlated spiking in mitral cells and could originate from electrical coupling of the AMPA autoreceptor response (Schoppa and Westbrook, 2002). Although a glomerulus-specific AMPA-mediated potential with identical kinetics has been attributed to glutamate spillover (Urban and Sakmann, 2002),  $D_{\text{AMPA}}$  could not be elicited in mice lacking Cx36. Our data supports the idea that  $D_{\text{AMPA}}$  propagates electrically, and furthermore, single action potentials do not produce glutamate spillover in glomeruli. Thus the distal dendrites of mitral cells generate a unique electro-chemical form of transmission. The glomerular localization of Cx36 and AMPA receptors and the large size of the coupled potential (Schoppa and Westbrook, 2002) make it likely that these proteins form a structural complex. Although the protein-protein interactions of connexins are only now being explored, it is apparent that C-termini of connexins can interact with anchoring proteins such as the MAGUK family (Herve et al. 2004). A close

association of Cx35 and glutamate receptors has been recently reported at the goldfish Mauthner cell synapse (Pereda et al., 2003).

The coupled potential had two components with the chemical component,  $D_{\text{AMPA}}$ , acting as a booster or amplifier of depolarizations in the distal dendrites of the glomerular tuft. The second component, the spikelet of the coupled response, is not sufficient to ensure action potential synchronization (Schoppa and Westbrook, 2002). This arrangement places constraints on the frequency response of the network. The time course  $D_{\text{AMPA}}$  is measured in tens of milliseconds whereas purely electrical connections can transmit instantaneously. Electrical coupling occurs at dendrodendritic sites in hippocampal and neocortical interneurons where they are known to enhance  $\gamma$  oscillations (25-70 Hz, Traub et al., 2003). Likewise, axo-axonal electrical coupling can be very fast allowing action potentials to cross from one axon to the next (Schmitz et al., 2001; Traub et al., 2003). The impact of the frequency response characteristics of the glomerular network will depend on the odor-evoked frequency of action potentials in mitral cells. In our experiments we used long depolarizing current injections to elicit action potentials. Although this stimulation does not precisely reflect natural odor stimuli, ORN stimulation evokes slow synchronized depolarizations (Schoppa and Westbrook, 2001) on which action potentials may be superimposed.

#### *Spillover and electrical coupling as distinct mechanisms of synchrony*

Although our data demonstrate that gap junctions are required for spike synchronization, the loss of Cx36 did not eliminate all rhythmic activity. In particular, TBOA-induced depolarizing oscillations persisted in the Cx36<sup>-/-</sup> mice. This situation



bears some resemblance to the inferior olive where neurons normally show slow synchronous activity. The synchrony is lost in Cx36<sup>-/-</sup> mice, but subthreshold rhythmic activity persists (Long et al., 2002; De Zeeuw et al., 2003). In the olfactory bulb, glial-encapsulated glomerular subcompartments (Chao et al., 1997; Kasowski et al., 1999) may promote rhythmic activity by glutamate pooling and spillover. In fact, large depolarizing stimuli can generate spillover potentials between pairs of mitral cells (Isaacson, 1999; Schoppa and Westbrook, 2001). This spillover is thought to synchronize slow oscillations evoked by olfactory nerve stimulation (Schoppa and Westbrook, 2001). Glomeruli in Cx36<sup>-/-</sup> mice showed apparently normal morphology thus spillover between mitral cells could provide an additional mechanism for synchronizing activity.

Slow oscillations can drive synchronized patterns of mitral cell firing (Schoppa and Westbrook, 2001; Schoppa and Urban, 2003). Bursts of action potentials mediated by TBOA-induced depolarizing oscillations are sufficient to at least coarsely organize coherent mitral cell firing in the absence of electrical coupling. Because spillover potentials are large and slow compared to the rapid D<sub>AMPA</sub> potential, TBOA-induced depolarization are less effective in precisely synchronizing spikes.

### *Functional Implications*

Correlated spiking is widespread in the central nervous system, although the relationship to information processing in circuits is still not obvious in all cases. In the olfactory system, odor inhalation evokes prominent high frequency oscillations of local field potentials suggesting that groups of output cells synchronize activity (Adrian, 1950). Synchronized single-unit activity, induced by odor inhalation, has been reported in the

rabbit olfactory bulb. However, the glomerular specificity of the paired units was not determined (Kashiwadani et al., 1999). In insects, network oscillations that presumably reflect precise timing relationships among output neurons also occur (Laurent et al., 1996; Wehr and Laurent, 1996, Stopfer et al., 1997). A critical issue is whether precise timing of action potentials is necessary or important. Our results indicate that Cx36-mediated coupling is necessary for rapid spike synchronization but not for clustering of spikes on slow synchronous oscillations. At first pass this implies that Cx36-gap junctions are necessary only for rapid synchrony. However we measured slow synchrony under extreme conditions, i.e. glutamate uptake block. Given the amplification generated by the hybrid Cx36-AMPA coupling mechanism, it seems likely that this coupling will also enhance intraglomerular excitability evoked by natural stimuli.

Functional studies indicate that an odorant elicits a specific map of glomerular activation (Xu et al., 2000; Korsching, 2002). Spillover-mediated excitation and electrical coupling, working in concert, could provide a mechanism of maintaining the fidelity of the map by synchronizing mitral cells projecting to the same glomerulus. Ultimately, olfactory information from the bulb is conveyed to high order processing centers via action potentials in mitral cell axons. If axons of mitral cells from the same glomerulus converge on common target neurons in the olfactory cortex, then olfactory cortical neurons will receive odorant-coded spike trains. Spike-timing dependent plasticity might be one mechanism for these neurons to discriminate between odors.

## Acknowledgments

This work was supported by National Institute of Health grant NS26494 (GLW), 1F31-DC051224-01 (JMC), and DFG grant SFB 488 (HM). We thank members of the Westbrook and Monyer labs for their helpful discussions including Linda Overstreet for her comments on the manuscript. In addition, we thank Aesoon Benson for her assistance.

## Figure Legends

**Fig. 1.** Glomerulus-specific mitral cell synchronous spiking is absent in  $Cx36^{-/-}$  mice. (A<sub>1</sub> and A<sub>2</sub>) Simultaneous depolarizing current injections ( $M_A$  and  $M_B$ , 250 pA, 2 s) elicited correlated action potentials in a pair of mitral cells that projected to the same glomerulus in a wild-type mouse. Paired action potentials that occurred together within a brief temporal window (time lag or  $\Delta t < 10$  ms; reference cell  $M_A$ ) are denoted with asterisks. (A<sub>3</sub>) Cross-correlogram, generated by binning  $\Delta t$  measurements ( $n = 614$ ), shows a prominent peak centered near  $\Delta t = 0$  indicative of highly synchronized action potentials. The synchronization value  $S$  (see methods) for this cell pair was 4.17. (A<sub>4</sub>) Summary histograms from wild-type mice show that 12 of 13 pairs projecting to the same glomerulus had synchronized action potentials (significant  $S$  value  $> 1.62$ ) whereas pairs projecting to different glomeruli did not. (B<sub>1</sub>) Depolarizing current injections ( $M_A$  and  $M_B$  100 and 200 pA respectively) elicited action potentials in a pair of mitral cells that projected to the same glomerulus in a  $Cx36^{-/-}$  mouse. In contrast to wild-type mice, action potentials occurred independently in the two test cells. (B<sub>2</sub>) Cross-correlogram of spike

lag times lacked a prominent peak with an  $S$  value of 1.29 ( $n= 467$ ). (B<sub>3</sub>) Correlated spiking did not occur in pairs of mitral cells projecting to the same glomerulus in Cx36<sup>-/-</sup> mice. (C<sub>1</sub> and C<sub>2</sub>) Pairs of mitral cells filled with biocytin (*red*) show normal mitral cell morphology in both a wild-type (C<sub>1</sub>) and a knockout mouse (C<sub>2</sub>). Note the extensive network of lateral dendrites and glomerulus specific projection pattern of apical dendrites. Cell body layers are demarcated with a nuclear stain (propidium iodide, *green*). Glom., glomeruli; MCL, mitral cell layer; GCL, granule cell layer. Scale bars: C<sub>1</sub> and C<sub>2</sub>= 50  $\mu$ m.

**Fig. 2.** Distribution of Cx36-EGFP in the olfactory bulb.

(A) The diagram shows translation initiation and termination codons, sequences in the two exons encoding the Cx36 protein (black boxes), the location of the EGFP coding sequence (grey box), and the approximate lengths of the BAC genomic sequence 5' and 3' of the Cx36 coding segment. (B<sub>1,2</sub>) *In situ* hybridization of brain slices derived from wild-type (B<sub>1</sub>) or transgenic Cx36<sup>Cx36-EGFP</sup> (B<sub>2</sub>) mice with oligonucleotide probes derived from the Cx36 (B<sub>1</sub>) or EGFP (B<sub>2</sub>) coding sequences share expression of the wild-type and modified Cx36 transcripts. The distribution of the EGFP transcript in the transgenic Cx36<sup>Cx36-EGFP</sup> line suggests that Cx36-EGFP is expressed only in Cx36-containing neurons. Some deviations in signal intensity between probes were noted, for example in the cerebellum. (C<sub>1</sub>) At the protein level, EGFP fluorescence was present as punctate labeling of glomeruli in transgenic mice. (C<sub>2</sub>) The Cx36-EGFP fusion protein, as determined by anti-EGFP immunoreactivity, was present within glomeruli and in mitral cells. Scale bars: B= 2.5 mm; C= 50  $\mu$ m, inset= 200  $\mu$ m; D= 200  $\mu$ m. OB, olfactory bulb;

RT, reticular thalamic nucleus; H, hippocampus; C, cerebellum; Glom., glomeruli; MCL, mitral cell layer.

**Fig. 3.** Glomerulus-specific electrical coupling is eliminated in  $Cx36^{-/-}$  mice.

(A, *left*) In a wild-type mouse paired recording from mitral cells that projected to the same glomerulus, a hyperpolarizing current injection (500 pA, 500 ms) in one mitral cell ( $M_A$ ) elicited a large hyperpolarization in that cell as well as an electrically-coupled smaller hyperpolarization in an adjacent test mitral cell ( $M_B$ ). (A, *right*) Likewise, current injection (500 pA, 500 ms) in  $M_B$  revealed a coupled potential in  $M_A$  indicating a symmetrical junction. A coupling ratio ( $CR$ , ratio of the voltage deflection in the stimulated versus the test cell) was computed for this cell pair ( $M_A \rightarrow M_B$   $CR= 0.062$ ;  $M_B \rightarrow M_A$   $CR= 0.080$ ; pair average= 0.071). (B) Summary histogram from wild-type mice shows that 19 of 19 mitral cell pairs projecting to the same glomerulus had  $CR \geq 0.005$  (reciprocal measurements were averaged and thus reflect a single point). Cells projecting to different glomeruli were not electrically coupled ( $CR < 0.005$ ). (C, *left*) In a  $Cx36^{-/-}$  mouse, paired recording from mitral cells projecting to the same glomerulus, a hyperpolarization (500 pA, 500 ms) in one mitral cell failed to generate an electrically coupled potential in the adjacent test cell ( $M_A \rightarrow M_B$   $CR= 0.001$ ). (C, *right*) The reciprocal recording configuration also failed to generate a coupled current ( $M_B \rightarrow M_A$   $CR= 0.004$ ; pair average 0.003). (D) Summary histograms show that electrical coupling did not occur in pairs of mitral cells projecting to the same glomerulus in  $Cx36^{-/-}$  mice.

**Fig. 4.** Cx36 mediates mitral-mitral cell glomerular gap junctions.

(A<sub>1</sub>, A<sub>2</sub>, and A<sub>3</sub>) Serial sections reveal gap junctions in the glomerular layer of Cx36<sup>Cx36-EGFP</sup> mouse olfactory bulb. Sections were labeled by pre-embedding immunogold electronmicroscopy with an anti-EGFP antibody. At punctum adhaerens (pa), Cx36-EGFP immunoreactivity (black dot) was found adjacent. Note the cytoplasmic semi-dense material undercoating the entire length of the inner surface of the junctional plasma membrane. Scale bars: 50 nm. (B<sub>1</sub> and B<sub>2</sub>) Two silver enhanced gold particles are located at a morphologically-identified gap junction (gj) (arrows) between two dendrites (d1 and d2) of mitral cells in this glomerulus. Note the pale cytoplasmic matrix of the mitral cell dendrites containing spherical synaptic vesicles and the electron dense granular cytoplasm of the olfactory nerve (ON) terminals. (B<sub>3</sub>) The neuronal gap junction of B<sub>2</sub> is shown at higher magnification. The extracellular space is narrowed to a small gap of 2-3 nm. Note the characteristic laminar appearance of the membranes. Scale bars: B<sub>1</sub> and B<sub>2</sub> 100 nm; B<sub>3</sub> 50 nm.

**Fig. 5.** AMPA autoreceptor-mediated potentials are no longer coupled in Cx36<sup>-/-</sup> mice.

(A<sub>1</sub>) In a wild-type mouse, a brief current injection (800 pA, 4 ms) elicited an action potential in one cell (M<sub>B</sub>) of a paired mitral cell recording and evoked a synaptic potential in the adjacent test cell (M<sub>A</sub>). The potential was blocked by NBQX (20 μM) confirming that it was AMPA receptor-mediated. AP5 and GABAzine, 100 μM and 5 μM respectively, were present throughout the experiment. The coupled action potential waveform or spikelet (*inset*) was insensitive to NBQX. (A<sub>2</sub>) An isolated AMPA autoexcitatory potential evoked by an action potential in a wild-type mouse single cell

recording. A subtraction protocol ( $\pm$ NBQX) was used to remove the action potential waveform and after-hyperpolarization (*inset*) and thus reveal the underlying AMPA autoexcitatory potential. (B<sub>1</sub>) In a paired recording from a Cx36<sup>-/-</sup> mouse, an evoked action potential in one cell failed to evoke an AMPA autoreceptor-mediated potential in the adjacent test mitral cell. (B<sub>2</sub>) In a single cell recording from a Cx36<sup>-/-</sup> mouse, an NBQX subtraction protocol revealed a prominent AMPA autoreceptor-mediated potential. (C) Shown in the summary histograms are the AMPA autoreceptor kinetics. The AMPA autoexcitatory potentials in Cx36<sup>-/-</sup> mice were comparable in size and shape as to wild-type mice (WT AP-sub. and KO AP-sub.). The electrically coupled AMPA potential in wild-type mice (WT-Paired) tended to be smaller in size and shape when compared to the autoexcitatory potential. Asterisk denotes statistical significance ( $p < 0.05$ ).

**Fig. 6.** TBOA-evoked slow synchronized depolarizations in Cx36<sup>-/-</sup> mice.

(A<sub>1</sub>) In a wild-type mouse, a pair of mitral cells projecting to the same glomerulus exhibited large synchronized slow depolarizations (*inset*) in the presence of TBOA (50  $\mu$ m). Hyperpolarizing current injections were used to prevent cells from spiking. The peak of the cross-correlogram ( $\Delta t = 0$ ;  $C_0$ ) for this pair was 0.84, indicative of a high degree of synchrony. (A<sub>2</sub>) When the holding potentials of the mitral cells were held near rest TBOA-induced depolarizations evoked closely-spaced bursts of action potentials. (B<sub>1</sub>) In a paired recording from a Cx36<sup>-/-</sup> mouse in which mitral cells projected to the same glomerulus, TBOA induced highly synchronized depolarizations ( $C_0 = 0.75$ ) demonstrating that slow correlated oscillations can be evoked without electrical coupling.

(B<sub>2</sub>) When mitral cells were held near rest, the TBOA-induced depolarizations organized temporally similar bursts of action potentials. (C) Summary data shows that slow depolarizations were well synchronized in wild-type and Cx36<sup>-/-</sup> mice. Biocytin cell fills (data not shown) confirmed the apical dendritic projection patterns.



# Figures

## Fig. 1

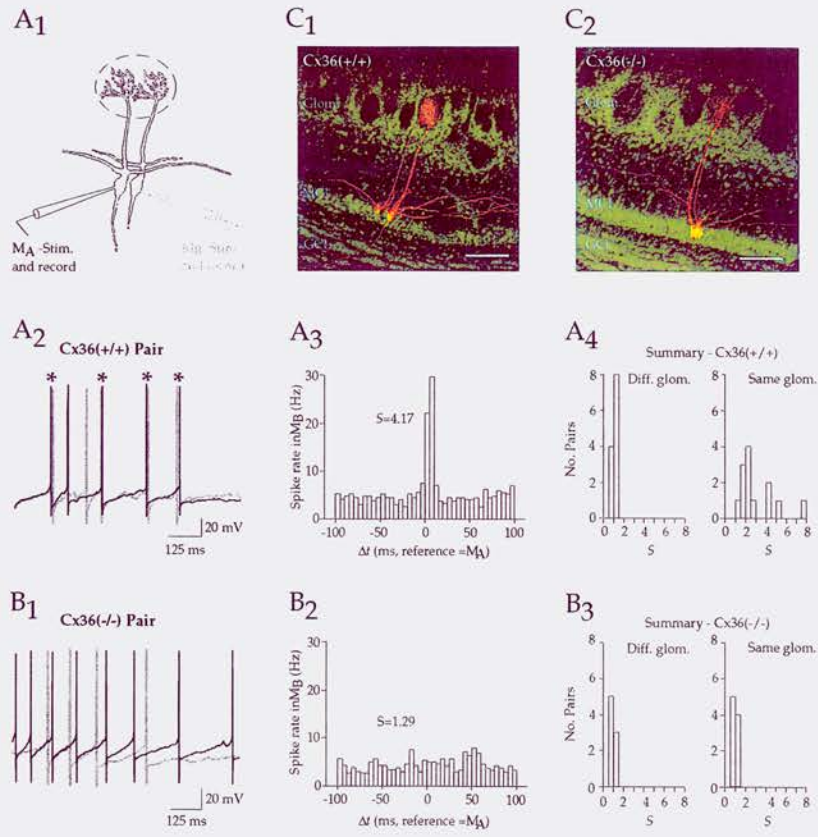


**Fig. 2**

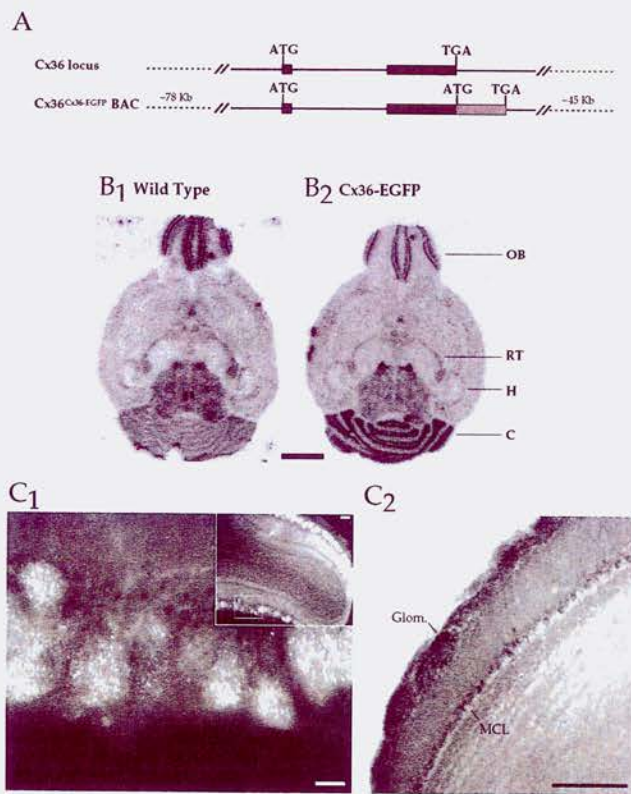


**Fig. 3**

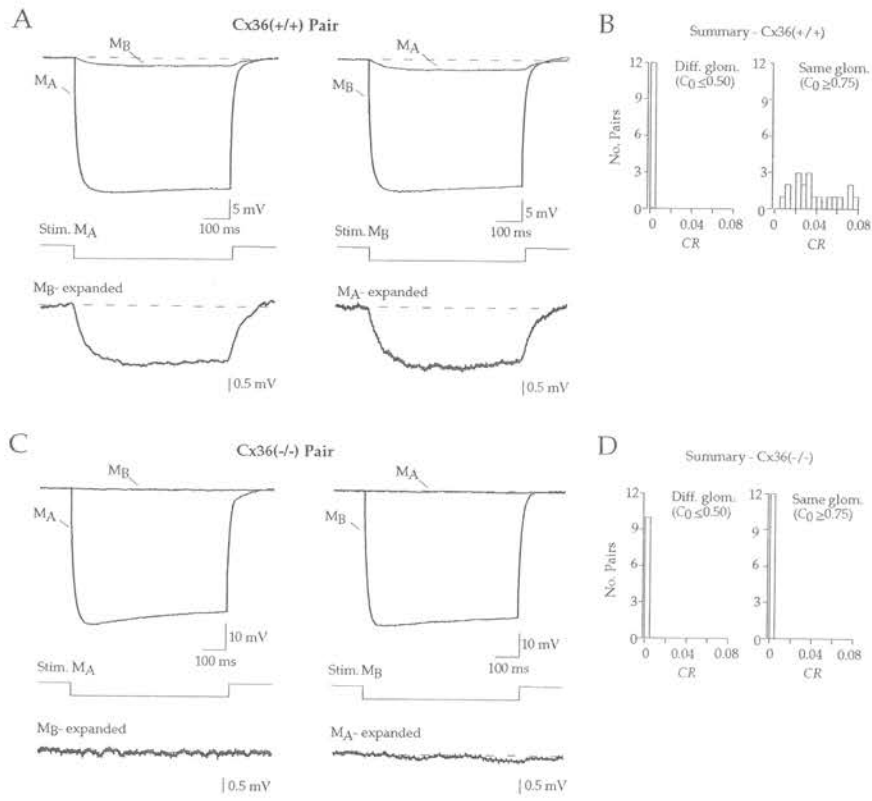


**Fig. 4**

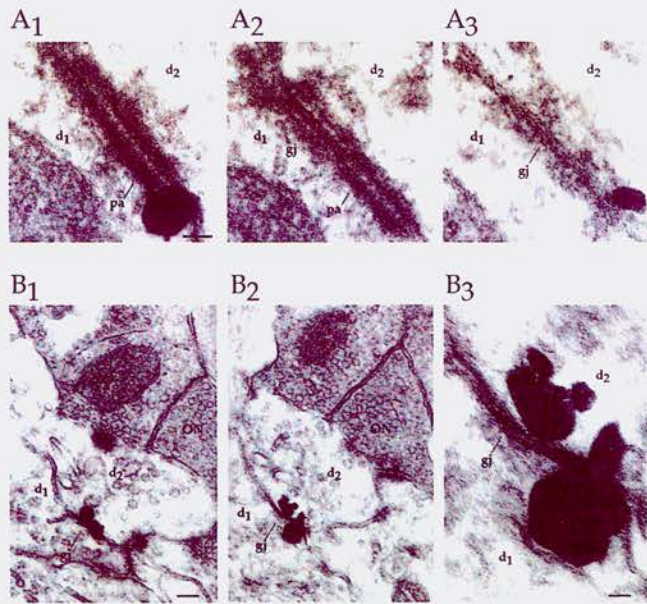
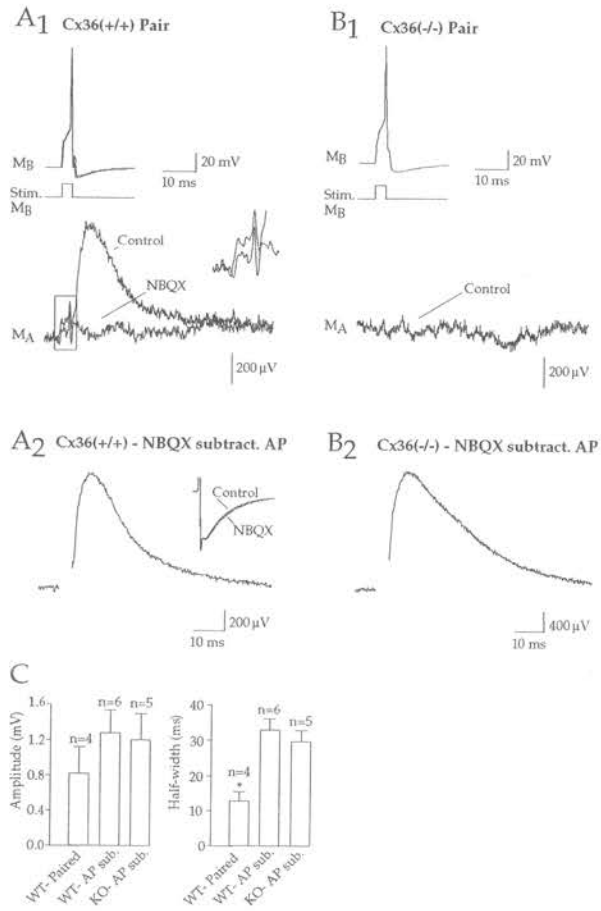
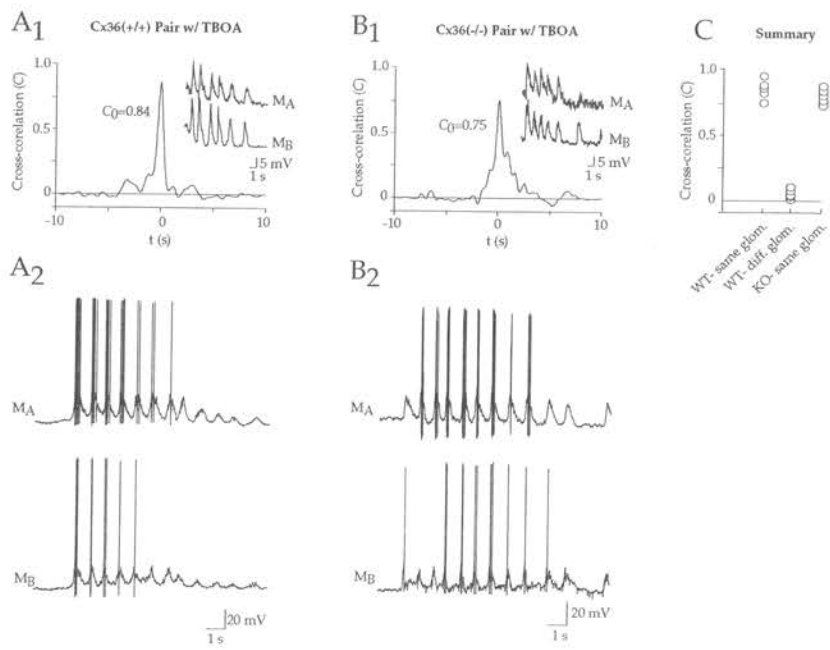


Fig. 5



**Fig. 6**



## **CHAPTER 4**

### **Connexin36-mediated interglomerular mitral cell excitation in the olfactory bulb**

Jason M. Christie<sup>1,2</sup> and Gary L. Westbrook<sup>1</sup>

<sup>1</sup>Vollum Institute, Oregon Health & Science University

Portland, OR USA

<sup>2</sup>Graduate Neuroscience Program

Address for Correspondence:

Jason M. Christie

Vollum Institute

Oregon Health & Science University

3181 SW Sam Jackson Park Road

Portland, OR 97201

phone: (503) 494-5436

fax: (503) 494-1243

email: christij@ohsu.edu

Running title: Interglomerular mitral cell excitation

## **Abstract**

In olfactory bulb mitral cells, glutamate spillover is thought to mediate autoexcitation as well as cross-excitation of neighboring cells. However, electrical communication via gap junctions between mitral cells may mimic spillover and thus provide an alternative means to excite surrounding cells. We examined mitral cell cross-excitation in paired recordings with particular interest in the role of electrical coupling. We found that putative mitral cell spillover between cells projecting to the same glomerulus was dependent on electrical coupling as cross-excitation elicited by an AP burst was absent in mice lacking mitral cell electrical junctions. However, spillover could be evoked in several conditions. Spillover induced from single cell activity could be evoked during glutamate uptake block, was mediated by AMPA receptors, and was localized within a glomerulus. Spillover could also occur, without glutamate uptake, during concerted mitral cell excitation. Finally, lateral dendritic (non-glomerular) NMDA receptor-mediated spillover could be induced in conditions that favor NMDA receptor activation. Our results indicate that Cx36-mediated electrical junctions enhance excitability within a same-glomerulus mitral cell network and mediate synchronous activity.



## **Introduction**

At central synapses, glutamate release directly activates post-synaptic receptors expressed immediately across the cleft. At some synapses, diffusion of transmitter from the cleft can activate distant synaptic or extrasynaptic receptors thereby exciting neighboring cells. Mitral cells, the principal neurons of the olfactory bulb, release glutamate from apical and lateral dendrites at specialized dendrodendritic synapses formed with inhibitory interneurons (Shepherd and Greer, 1998). Mitral cell glutamate release not only excites postsynaptic interneuronal targets, but can also lead to autoexcitation mediated by both NMDA and AMPA autoreceptors (Nicoll and Jahr, 1982; Aroniadou-Anderjaska et al., 1999; Isaacson, 1999; Freidman and Strowbridge, 2000; Salin et al., 2001; Schoppa and Westbrook, 2001). In addition, several studies have reported that the release of glutamate from one mitral cell may also directly excite neighboring mitral cells (Isaacson, 1999; Schoppa and Westbrook, 2001; Urban and Sakmann 2002). Because mitral cells lack direct synaptic contact with other mitral cells (Price and Powell, 1970; Pinching and Powell, 1971) this cross-excitation has been attributed to extrasynaptic glutamate transmission (spillover).

Mitral cell spillover-excitation, mediated by NMDA receptors (Isaacson, 1999; Schoppa and Westbrook, 2001) or both NMDA and AMPA receptors (Urban and Sakmann, 2002) is thought to occur between mitral cells sharing the same dendritic glomerular projection (Schoppa and Westbrook, 2001; Urban and Sakmann 2002). Consistent with this localization of spillover, the glomerulus is a highly compartmentalized structure (Chao et al., 1997; Kasowski et al., 1999) where glial ensheathed bundles of primary dendrites may provide a chemical compartment for

glutamate accumulation (Carlson et al., 2000; Schoppa and Westbrook, 2002).

Considering that mitral cells project a single apical dendrite to a single glomerulus, and that there are approximately 2000 glomeruli per bulb (Shepherd and Greer, 1998), spillover could be considered a highly specific mitral cell phenomenon. However, the notion of mitral cell cross-excitation may be more complicated. For example, mitral cells projecting to the same glomerulus are also electrically coupled via Connexin36 (Cx36)-mediated gap junctions expressed on apical dendritic tufts (Schoppa and Westbrook, 2002; Christie et al., 2004). Gap junctional coupling allows the rapid propagation of currents throughout a same-glomerulus electrical syncytium (Bennett and Zukin, 2004; Hormuzdi et al., 2004; Schoppa and Westbrook, 2002; Christie et al., 2004). In mitral cells, an AMPAergic potential attributed to spillover (Urban and Sakmann, 2002) in fact reflects an electrically coupled AMPA autoexcitatory potential (Schoppa and Westbrook, 2002; Christie et al., 2004).

We used paired mitral cell recordings from both wildtype and Cx36 KO mice in order to examine mitral cell cross-excitation. We found that putative intraglomerular spillover evoked by single mitral cell activity is initiated and/or entirely mediated by gap junctional coupling of autoreceptor responses in stimulated cells. However, glomerulus-specific spillover potentials, mediated entirely by AMPA receptors, could be elicited in Cx36 KO mice during uptake block. In addition, in conditions favoring NMDA receptor activation, promiscuous spillover responses evoked along lateral dendrites could be elicited by single mitral cell activity. Electrical coupling is thus shown to promote and enhance excitability in same-glomerulus mitral cell circuits by coupling depolarizing autoreceptor responses and thereby provide coincident excitation.

## Materials and Methods

Horizontal slices of main olfactory bulb (250-300  $\mu\text{m}$ ) were prepared from mice with and without a null mutation to Cx36 (PND 14-21) (Hormuzdi et al., 2001). Following halothane anesthesia, mice were decapitated and olfactory bulbs were removed. Slices were cut in an ice-cold oxygenated solution containing (in mM): 83 NaCl, 26.2 NaHCO<sub>3</sub>, 2.5 KCl, 1 NaH<sub>2</sub>PO<sub>4</sub>, 3.3 MgCl<sub>2</sub>, 0.5 CaCl<sub>2</sub>, 22 glucose, and 72 sucrose (pH 7.3). Slices were transferred a warmed bath (35°C) of the same solution for 30 min, following, slices were allowed to incubate at room temperature.

Whole-cell recordings were obtained under visual control using DIC optics (Carl Zeiss) in a base solution (32-35°C) containing (in mM) 119 NaCl, 26.2 NaHCO<sub>3</sub>, 2.5 KCl, 1 NaH<sub>2</sub>PO<sub>4</sub>, 1.3 MgCl<sub>2</sub>, 2.5 CaCl<sub>2</sub>, and 22 glucose (pH 7.3). For some voltage-clamp experiments, MgCl<sub>2</sub> was omitted and TTX (0.5-1  $\mu\text{M}$ ) was added. All experiments were performed in the presence of the GABA<sub>A</sub> antagonist SR 95531 hydrobromide (2-5  $\mu\text{M}$ ). For paired recordings, mitral cell bodies were typically separated by <45  $\mu\text{m}$  (edge-to-edge). Patch pipettes (4-6 M $\Omega$ ) in current clamp recordings contained a solution of (in mM): 125 Kgluconate, 2 MgCl<sub>2</sub>, 0.025 CaCl<sub>2</sub>, 1 EGTA, 2 NaATP, 0.5 NaGTP, and 10 HEPES (pH 7.3). A similar internal solution was used during voltage clamp experiments (in mM): 125 Cs gluconate, 2 MgCl<sub>2</sub>, 0.025 CaCl<sub>2</sub>, 1 EGTA, 2 NaATP, 0.5 NaGTP, 10 HEPES, 10 4-Aminopyridine, and 15 Tetraethylammonium chloride (pH 7.3).

Electrophysiological recordings were made with Axopatch 200A and 200B amplifiers (Axon instruments). The analog signals were filtered at 1-5 kHz with the built in eight-pole Bessel filter and digitized at 0.5-10 kHz. For presentation purposes, a 10

point sliding boxcar filter was applied to voltage-clamp traces of  $I_{\text{small}}$ . Data were acquired and analyzed using Axograph 4.6 (Axon Instruments). In current-clamp experiments, mitral cells were often held at hyperpolarized potentials compared to rest to prevent random spiking. Unless indicated otherwise, cells were held at  $-60$  mV during voltage-clamp experiments.

Some mitral cells were excited via antidromic stimulation of the lateral olfactory tract, the tight bundle of mitral cell axons exiting the olfactory bulb. The LOT is an anatomically distinct fiber tract running caudal to the main olfactory bulb and can be easily imaged with DIC optics. The LOT was preserved in slices by positioning the dissected olfactory bulb and proximal portion of cortex ( $\approx 5$  mm) in horizontal register with the basal part of the brain (Aroniadou-Anderjaska et al., 1999). For stimulation, a bipolar electrode was positioned above the LOT 75-150  $\mu\text{m}$  from the test mitral cell. Brief pulses (100 ms, 10-100 V), triggered by a stimulation isolation unit (Digitimer), were elicited every 20 seconds. For olfactory nerve stimulation, a bipolar electrode was placed above visually identified bundles of afferents near the presumed glomerulus to which the test mitral cell(s) projected. Brief pulses (100  $\mu\text{s}$ , 50-100 V), triggered by the same stimulation isolation unit, were elicited every 20 seconds.

Because the apical dendritic projection of mitral cells could not be determined by DIC optics we used a variety of methods either alone or in combination to determine the glomerular relationship of cells. Same-glomerulus projections could be confirmed in wildtype mice by the presence of direct electrical coupling (Schoppa and Westbrook, 2002; Christie et al., 2004). In addition, the glomerular relationship of mitral cells in both wildtype and Cx36 KO mice could be confirmed by filling cells with fluorescent

indicators (see below) or deducing the synchrony of TBOA-induced spontaneous depolarizations (Christie et al., 2004). Briefly, in wildtype and Cx36 KO mice, pairs of mitral cells that project to the same glomerulus have highly synchronized depolarizations ( $C_0$  values  $\geq 0.75$ ) while cells that project to different glomeruli are not well synchronized ( $C_0$  values  $\leq 0.50$ ). Since TBOA induced depolarizations occur intermittently during the time course of its application, experiments examining TBOA-induced spillover required higher rates of episode averaging.

The coupling ratio of cell pairs was determined as described (Schoppa and Westbrook, 2002; Christie et al., 2004). Briefly, hyperpolarizing current injections (100-500 pA, 500 ms) in one cell of paired recordings elicited large voltage deflections in the stimulated cells (15-30 mV), and if the adjacent test cells projected to the same glomerulus in a wildtype mouse, small voltage deflections were also recorded reflecting electrical coupling. The coupling ratio ( $CR$ ) reflects the size of the voltage deflection in the stimulated cell divided by the deflection in the test cell.

For morphological characterization of mitral cell pairs biocytin (0.1%) or lucifer yellow (KCl- for Kgluconate based internal /LithiumCl for Csgluconate based internal) were added to the pipette solutions. When recordings were completed slices were fixed in a PBS based (72 mM  $\text{NaH}_2\text{PO}_4$  and 28 mM  $\text{Na}_2\text{HPO}_4$ , pH 7.2) formaldehyde solution (4%) overnight and were then permeabilized and labeled in the same PBS based solution (no formaldehyde) with the addition of 0.4% Triton X-100. Cy-5-conjugated streptavidin (1:2000, Jackson ImmunoResearch) was reacted against biocytin (12 hr at 4°C) in the same PBS/Triton X-100 solution. Slices were washed in Triton-free PBS (X3 10 min) then incubated (30 min) in a blocking PBS-based solution with 5% goat serum and 0.4%

Triton X-100. In the same blocking solution, anti-lucifer yellow IgG (1:1000, Molecular Probes) was reacted against lucifer yellow (12 hr at 4°C). Slices were washed in PBS (3X, 10 min) and labeled with a secondary antibody (goat anti-rabbit Alexa 488, 1:500, Molecular Probes). After washing in PBS (3X, 10 min), propidium Iodide (1:2000, Molecular Probes) was used as a nuclear counterstain. Slices were mounted on slides with ProLong Antifade (Molecular Probes) and imaged on a confocal microscope (Olympus) equipped with a 20X objective.

## Results

### *Putative intraglomerular mitral cell spillover*

High frequency action potential bursts (120-360 Hz) elicited by current injection (500-1750 pA, 50 ms) were used to excite mitral cells and evoke glutamate release. In excited cells, a clear depolarizing potential following the spike burst was often recorded (Fig 1B<sub>1</sub> *top*- M<sub>A</sub>) and was sensitive to glutamate receptor antagonists consistent with glutamatergic autoexcitation (Nicoll and Jahr, 1982; Aroniadou-Anderjaska et al., 1999; Isaacson, 1999; Freidman and Strowbridge, 2000; Salin et al., 2001; Schoppa and Westbrook, 2001). The size and shape of the autoexcitatory potential was difficult to quantify as the current injection used to elicit the response also evoked a prominent after-hyperpolarization. Interestingly, in 16 of 16 paired recordings from mitral cells projecting to the same glomerulus, the action potential burst in stimulated cells also resulted in a time-locked cross-excitation of neighboring unstimulated cells (Fig 1B<sub>1</sub> *bottom*- M<sub>B</sub>). This potential (D<sub>cross-excite</sub>) was also sensitive to glutamate receptor antagonists (see below) and thus is consistent with glutamatergic spillover. Paired recordings from mitral cells

that projected to different glomeruli failed to generate  $D_{\text{cross-excite}}$  (10 of 10 cell pairs, average integral  $0.010 \pm 0.005$  mV/s) (Fig 1C) suggesting that cross-excitation is glomerular dependent.

The size and shape of  $D_{\text{cross-excite}}$  was variable across cells (Fig 1D) (average integral  $0.314 \pm 0.047$  mV/s), however, it often persisted for hundreds of milliseconds ( $w_{1/2} = 99.8 \pm 8.4$  ms,  $n = 16$ ) (Fig 1B<sub>1</sub> bottom-  $M_B$ ). Application of the NMDA-receptor antagonist *D,L*-AP5 (100 mM) reduced  $D_{\text{cross-excite}}$  ( $62.4 \pm 6.0\%$  of control,  $n = 8$ ) and eliminated any long-lasting component (Fig 1B<sub>1</sub> and 1B<sub>2</sub>). The additional application of the AMPA-receptor antagonist NBQX (20 mM) further reduced the potential ( $22.4 \pm 6.5\%$  of control,  $n = 4$ ) suggesting that both NMDA and AMPA receptors mediate  $D_{\text{cross-excite}}$ . NBQX applied alone nearly abolished  $D_{\text{cross-excite}}$  ( $30.7 \pm 8.0\%$  of control,  $n = 9$ ) (Fig 1B<sub>1</sub>) indicating that NMDA-receptor activity requires the co-activation of AMPA receptors.

A small depolarization persisted in the presence of NBQX in unstimulated cells. This potential was not dependent on evoked release as increasing the resting potential of the stimulated cell to  $-100$  mV, such that the excitatory current injection was well below spike threshold, continued to evoke a potential that was similar in size to that evoked by an action potential burst (integral APs  $0.074 \pm 0.018$  mV/s; integral no APs  $0.081 \pm 0.018$  mV/s,  $p = 0.78$ ). Same glomerulus mitral cells are electrically coupled via Cx36-mediated gap junctions located on apical dendritic tufts allowing current flow through all mitral cells in the same-glomerulus electrical syncytium (Schoppa and Westbrook, 2002; Christie et al., 2004). Therefore, the NBQX-insensitive potential most likely reflects the electrical coupling of the excitatory current injection in the stimulated mitral cell.

Consistent with this hypothesis, the size of NBQX-insensitive potential was highly correlated ( $r= 0.82$ ,  $p= <0.001$ ,  $n= 13$ ) with the electrical coupling ratio determined for each same-glomerulus mitral cell pair (see methods) (same glomerulus coupling ratio  $0.042 \pm 0.005$ ,  $n=26$ ; different glomerulus coupling ratio  $0.002 \pm 0.001$ ,  $n=10$ ).

The observation that a component of  $D_{\text{cross-excite}}$  is composed of an electrically coupled current injection from the stimulated cell suggests that electrical coupling of the autoexcitatory potential may also contribute to  $D_{\text{cross-excite}}$ . Electrically coupled events occur concurrently in connected cells (Bennett and Zukin, 2004; Hormuzdi et al., 2004) whereas spillover events occur with some delay due to the diffusion of glutamate. The lack of any measurable delay between the peak of the autoexcitatory potential in the stimulated cell and the peak of  $D_{\text{cross-excite}}$  in the unstimulated cell (difference Peak- $D_{\text{spillWT}}$  and Peak-autoexcitation  $-9.3 \pm 6.2$  ms,  $n= 8$ ) (Fig 1B<sub>3</sub>) further supports this hypothesis. Additionally, the size of  $D_{\text{cross-excite}}$  in each cell pair was correlated with the coupling ratio (Fig 1D) suggesting that there is a relationship between gap junctional coupling and the putative spillover potential recorded in unstimulated cells.

#### *Intraglomerular glutamate spillover in Cx36 KO mice*

Electrical coupling could complicate the interpretation and analysis of mitral cell cross-excitation. Therefore, we used mice lacking Cx36 and thus direct electrical coupling (Christie et al., 2004) to examine spillover. Surprisingly, in paired recordings from same-glomerulus mitral cells, high frequency action potential bursts failed to evoke mitral cell cross-excitation (8 of 8 pairs, average integral  $0.009 \pm 0.004$  mV/s) (Fig 2A). Robust autoexcitatory potentials evoked in stimulated cells discounted the possibility that



Cx36 gene deletion disrupted mitral cell glutamate release or receptor expression (Fig 2A). This result suggests that electrical coupling plays a critical role in the genesis and/or mediation of  $D_{\text{cross-excite}}$ .

If glutamate neurotransmission between mitral cells occurs at a distance, the diffuse action of glutamate may be highly susceptible to uptake (Diamond, 2001); blocking uptake may then induce spillover potentials. Consistent with this hypothesis, action potential bursts in the presence of the specific glutamate transporter blocker TBOA (50  $\mu\text{M}$ ) induced a depolarizing potential ( $D_{\text{spillKO}}$ ) in 7 of 8 unstimulated cells from same-glomerulus mitral cell pairs (average integral  $0.362 \pm 0.108$  mV/s,  $n=7$ ) (Fig 2A and 2D). The clear difference in the peak timing of the autoexcitatory potential and  $D_{\text{spillKO}}$  (Fig 2B *top*) (difference Peak- $D_{\text{spillWT}}$  and Peak-autoexcitation  $56.6 \pm 7.9$  ms,  $n=5$ ) is indicative of the diffuse action of glutamatergic spillover. In the presence of TBOA,  $D_{\text{spillKO}}$  was not detected in mitral cell pairs projecting to different glomeruli (Fig 2D) (5 of 5 cells, average integral  $-0.015 \pm 0.025$  mV/s,  $n=5$ ) suggesting that spillover is glomerular dependent.

Spillover-mediated glutamatergic responses in many other cell types are mediated solely NMDA receptors owing to their low affinity for glutamate binding or location (Asztely et al., 1997; Diamond, 2001; Chen and Diamond, 2002; Clark and Cull-Candy, 2002). In contrast to these cell types, *D,L*-AP5 (100  $\mu\text{M}$ ) had no effect on the mitral cell  $D_{\text{spillKO}}$ , however, application of NBQX (20  $\mu\text{M}$ ) completely abolished the potential (Fig 2B *bottom* and 2E). These results provide a stark contrast to the activation and receptor complement mediating  $D_{\text{spillWT}}$  where NMDA receptors contribute to the cross-excitatory response (Fig 2D). In summary, AMPA receptors alone mediate  $D_{\text{spillKO}}$  and the glutamate

concentration is only sufficiently high enough during transporter block to activate these relatively low affinity receptors.

#### *Glomerular morphology in Cx36 KO mice*

The exquisite intercalation and close contact of mitral cell dendritic processes in glomeruli may provide a physical basis for spillover communication between mitral cells. Therefore, mitral cell morphological deficits in Cx36 KO mice could confound physiological comparisons to wildtypes. In an earlier study, cursory examination revealed no obvious morphological abnormalities (Christie et al., 2004). Because our results suggest that cross-excitation is glomerular dependent and considering the finely ordered structure of mitral cell dendrites in glomeruli, we examined the morphological relationship of wildtype and Cx36 KO dendritic tufts in greater detail.

Pairs of same-glomerulus mitral cells were labeled concomitantly with either biocytin or lucifer yellow, were fixed, processed, and then evaluated. Mitral cells from both wildtype and Cx36 KO mice were similar both possessing several lateral dendrites as well as single apical dendrites ending in glomerular tufts of processes (Fig. 3A<sub>1</sub> and 3B<sub>1</sub>). Extensive overlapping of dendritic tuft processes was apparent in both lines (Fig. 3A<sub>2</sub> and 3B<sub>2</sub>). Z-stack images of glomerular tufts (100X) were analyzed for areas of putative membrane contact by an investigator blind to slice genotypic conditions. Significant differences were not found in the number of putative contacts (3C). The validity of putative contact points is confirmed by the strong correlation with the coupling ratio determined for each pair (3D). In addition, the average per z-slice overlap of labeled processes was not significantly different (WT=  $1.58 \pm 0.23\%$ , KO=  $1.94 \pm$

0.40%, n= 9 and 10, respectively). Because morphological deficits were not observed between the two lines of mice, our paired-recording results are best explained by differences in physiology.

#### *NMDA receptor-mediated spillover*

Our results thus far indicate that cross-excitation of mitral cells is highly specific, only occurring between same-glomerulus mitral cells, and is mediated by a potential either partly (Fig 1 WT) or entirely (Fig 2 KO) composed of AMPA receptors. A previous study has described a mitral cell spillover current mediated entirely by NMDA receptors that occurs in a majority of cell pairs (Isaacson, 1999). In order to rectify these differences, we examined cross-excitation in conditions that favor NMDA receptor activation (Isaacson, 1999). Cells were voltage-clamped at  $-60$  mV in  $Mg^{+2}$  free solution-containing TTX ( $1 \mu\text{M}$ ). Brief voltage steps ( $-60$  mV to  $+10$  mV, 35 ms) were used to excite mitral cells and evoke glutamate release.

In wildtype mice, mitral cell depolarization elicited autoexcitatory currents that were sensitive to *D,L*-AP5 ( $100 \mu\text{M}$ ) (Fig 4A<sub>1</sub> *top*) (Isaacson, 1999; Freidman and Strowbridge, 2000). Large cross-excitatory currents ( $I_{\text{cross-excite}}$ ) were also elicited in 11 of 11 same-glomerulus paired recordings (Fig 4A<sub>1</sub> *middle*). The subsequent addition of *D,L*-AP5 ( $100 \mu\text{M}$ ) highly reduced  $I_{\text{cross-excite}}$  confirming that this current is NMDA receptor-mediated ( $17.7 \pm 2.4\%$  of control, n=9). Small *D,L*-AP5-resistant currents persisted in unstimulated cells reflecting electrically coupled voltage steps from stimulated cells. Similar to  $D_{\text{cross-excite}}$ , evidence indicates that  $I_{\text{cross-excite}}$  does not entirely reflect a direct action of glutamate binding onto neighboring mitral cells. Changing the holding potential

of unstimulated cells, and thereby the electrochemical gradient for NMDA receptors, had no effect on the current-voltage relationship of  $I_{\text{cross-excite}}$  (Fig 4A<sub>1</sub> *bottom* and 4A<sub>2</sub>). The lack of voltage-dependence implies that this current is beyond unstimulated cell clamp and is therefore occurring in coupled stimulated cells (Schoppa and Westbrook, 2002). Inadequate voltage-clamp of test mitral cells can be ruled out as apical dendritic clamp and reversal of NMDA autoexcitatory currents have been demonstrated previously (Friedman and Strowbridge, 1999; Schoppa and Westbrook, 2002). In addition, the size of  $I_{\text{cross-excite}}$  was well correlated with the coupling ratio determined for each cell pair ( $r=0.93$ ,  $p < 0.001$ ,  $n=16$ ).

In Cx36 KO mice, mitral cell depolarization also elicited *D,L*-AP5-sensitive autoexcitatory currents (Fig 4B *top*), albeit on average, were slightly smaller than those generated in WT mice (4D *left*). This result confirms NMDA receptor expression in Cx36 KO mitral cells and indicates that the absence of an NMDA-receptor potential in  $D_{\text{cross-excite}}$  (Fig 2) is not due to the lack of functioning receptors. Large cross-excitatory currents could not be evoked in same-glomerulus mitral cell paired recordings further supporting that same-glomerulus cross-excitation in WT mice is dominated by electrically coupled autoexcitation. However, in some Cx36 KO same-glomerulus cell pairs (3 of 7), small excitatory currents ( $I_{\text{small}}$ ) were generated (Fig 4B *bottom* and *inset*). Similar sized excitatory currents were also evoked in 5 of 10 different-glomerulus mitral cell recordings from WT mice (Fig 4D *right*).  $I_{\text{small}}$  was evoked in cell pairs lacking direct electrical junctions due to either gene deletion (Cx36 KO) or apical dendritic location (different-glomeruli); therefore  $I_{\text{small}}$  does not reflect an electrically coupled event.

Glutamate release occurs along lateral dendrites at dendrodendritic synapses (Shepherd and Greer, 1998). As illustrated in the different-glomerulus cell pair in Fig 5A<sub>1</sub>, the projection pattern of lateral dendrites can repeatedly bring the processes into close register. In light of these observations,  $I_{\text{small}}$  could reflect glutamate release and spillover-excitation along lateral dendrites. Blocking glutamate transport (TBOA 50  $\mu\text{M}$ ) caused an enhancement of  $I_{\text{small}}$  in both WT different-glomerulus cell pairs (Fig 5A<sub>2</sub> and 5A<sub>3</sub>) and Cx36 KO same-glomerulus cell pairs (5B<sub>1</sub> and 5B<sub>2</sub>) consistent with a diffuse action of glutamate. In several pairs ( $n=4$ ),  $I_{\text{small}}$  was undetectable in control conditions but was robustly generated during transporter block (Fig 5B<sub>1</sub>, 5B<sub>2</sub> and 5C). TBOA also enhanced both WT and Cx36 KO autoexcitation ( $133.5 \pm 9.1\%$  of control,  $n=11$ ) suggesting that not all receptors were saturated or some processes were insufficiently excited (but see Isaacson, 1999).

Application of *D,L*-AP5 (100  $\mu\text{M}$ ) completely blocked  $I_{\text{small}}$  in both WT and Cx36 mitral cell pairs confirming that the current is NMDA-receptor mediated (Fig 5A<sub>3</sub>, 5B<sub>2</sub> and 5C). The similarity of  $I_{\text{small}}$  in WT different-glomerulus cell pairs and Cx36 KO same-glomerulus cell pairs suggests a common localization and mechanism. The physical limitation of non-overlapping tufts in WT mice and the lack of any detectable AMPA component in Cx36 KO pairs strongly argues that the  $I_{\text{small}}$  is generated between lateral dendrites. Due to space clamp errors, the depolarizing voltage step is most likely insufficient to excite distal dendritic compartments, including the glomerular tuft where AMPAergic spillover excitation occurs (Fig 2). However, proximal portions of lateral dendrites would presumably be within clamp range for excitation.

### *Glutamate spillover evoked by LOT stimulation*

The striking results of uptake block uncovering or enhancing spillover responses (Fig 2 and 5) imply that transporters in the olfactory bulb tightly sequester glutamate. Thus far, spillover responses were evoked by the excitatory activity of single mitral cells. Perhaps the coincident release activity of multiple cells can overcome transporter buffering of glutamate and excite neighboring cells. In normal bath conditions, stimulation of the lateral olfactory tract (LOT) with a bipolar electrode (100 ms, 10-100 V) was used to antidromically excite mitral cells en mass. In mitral cell current-clamp recordings from wildtype mice, stimulation evoked prolonged depolarizing potentials (Fig 6A<sub>2</sub>) (Aroniadou-Anderjaska et al., 1999). The prolonged depolarizing potential was not dependent on activity from the test cell itself. Robust depolarizations continued to be evoked in test mitral cells during single-cell antidromic spike failures (data not shown). In addition, single action potentials evoked by brief current injection (700-1250 pA, 3-5 ms) in the test mitral cell also failed to evoke after-depolarizations (Fig 6A<sub>1</sub>). Bath application of *D,L*-AP5 (100 mM) highly reduced the long lasting depolarization (Fig 6A<sub>3</sub> and 6D) leaving a brief AMPA-receptor mediated potential. Following washout, application of NBQX (20 mM) completely abolished the potential (Fig 6A<sub>3</sub> and 6D *left*) indicating that NMDA receptor activity requires the co-activation of AMPA receptors. Imaging of biocytin-filled cells revealed that the long-lasting depolarizations, at least in part, were not necessarily generated in the glomerulus. Long lasting depolarizations could be evoked in mitral cells with severed apical dendrites, although the potentials were reduced in size as compared to responses generated in mitral cell with intact dendritic projections (not shown). These results clearly demonstrate that the prolonged

depolarization is dependent on the activity of surrounding cells and imply that spillover potentials can be generated in near physiological conditions (normal  $Mg^{2+}$  and no uptake block).

LOT stimulation could infrequently evoke after-depolarizing potentials in mitral cells from Cx36 KO mice (4 of 12) that were blocked by glutamatergic antagonists. However, the potentials were much more brief and highly reduced as compared to depolarizations evoked in wildtype mice (6D *right*). LOT-induced potentials in Cx36 KO mice reflect the coordinated action of surrounding cells as action potential excitation (500-1000 pA, 3-5 ms) in the test mitral cells also failed to generate similar after-depolarizations. These results imply that spillover potentials can be generated in control conditions by increasing the density of active synapses beyond that of single mitral cells. Also importantly, the excitability of mitral cell ensembles is compromised in the absence of electrical coupling.

#### *ORN-evoked activity in same-glomerulus mitral cell ensembles*

Olfactory receptor neuron (ORN) stimulation results in a synchronous pattern of oscillatory depolarizations in all mitral cells that project to the same glomerulus. These oscillations are thought to reflect the coordinated activity of mitral cells that results in regenerative bursts of glutamate release followed by AMPA and NMDA receptor activation (Schoppa and Westbrook, 2001). Because glomerular spillover has been proposed to mediate synchronization, we sought to determine the influence of electrical coupling on this circuit response.

In mitral cells from wildtype mice, bipolar electrode stimulation (100 ms, 10-100 V) of the ORN nerve layer evoked a complex series of oscillations superimposed on a persistent depolarization (7 of 9 mitral cells) (Fig 7A<sub>1</sub>), similar to results previously reported (Schoppa and Westbrook, 2001). In paired recordings from same glomerulus mitral cells (6 of 6), oscillating depolarizations were highly synchronized ( $C_0$  values  $\geq 0.75$ ) (Fig 7A<sub>2</sub> and 7A<sub>3</sub>). In contrast, ORN stimulation failed to evoke patterned responses in mitral cell recordings from Cx36 KO mice (5 of 5 mitral cells) (Fig 7B<sub>1</sub>). However, oscillating depolarizations time locked to ORN stimulation were evoked in conditions of uptake block (50  $\mu$ M TBOA) (Fig 7B<sub>1</sub>). As expected, these oscillations were highly synchronized ( $C_0$  values  $\geq 0.75$ ) in same-glomerulus mitral cell paired recordings (4 of 4) (Fig 7B<sub>2</sub> and 7B<sub>3</sub>). These results suggest that the electrical coupling enhances the excitability of same-glomerulus mitral cells and initiates and/or mediates the synchronous activity necessary for patterned ensemble responses.

## Discussion

We found that mitral cells excite neighboring mitral cells via electrical junctions and in some cases glutamatergic spillover. Within a glomerulus, mitral cell cross-excitation evoked by single-cell activity, previously attributed to glutamate spillover (Schoppa and Westbrook, 2001; Urban and Sakmann, 2002) is driven by Cx36-electrical junctions. However, intraglomerular mitral cell spillover could be evoked in conditions of uptake block and surprisingly was mediated by AMPA receptors. In addition, small NMDA-spillover responses could be evoked in conditions that favor NMDA-receptor activation and were not glomerular-specific suggesting a lateral dendritic localization.



Our results indicate that electrically coupled cross-excitation has a profound influence on the excitability of mitral cell circuits enhancing mitral cell responses to both LOT and ORN stimulation.

### *Spillover at central synapses*

At some conventional central synapses, transmitter can escape the synaptic cleft and activate neighboring synaptic or extrasynaptic receptors. The ability of transmitter to act at distant receptors depends on several factors including the biophysical properties of the receptor, the intersite distance and geometry, as well as the kinetics and location of transporters (Barbour and Hausser, 1997). In the CA1 hippocampal neuropil where synaptic connections between Shaffer-collaterals and pyramidal cells are densely packed, glutamate, perhaps from a single release site, can spillover and activate receptors at adjacent synapses (Kullmann et al., 1996; Asztely et al., 1997; Diamond, 2001). Glutamate outside of the cleft quickly dissipates in the large extrasynaptic volume thereby limiting its action. Glutamate transporters also tightly regulate extrasynaptic transmitter diffusion and therefore receptor activation at adjacent synapses (Bergles and Jahr, 1998; Diamond, 2001). Thus glutamate spillover at this synapse, as well as others, preferentially activates synaptic or extrasynaptic NMDA receptors because of their localization and/or high affinity for glutamate binding (Asztely et al., 1997; Diamond, 2001; Chen and Diamond, 2002; Clark and Cull-Candy, 2002).

Some central synapses have specialized morphology that presents a conducive environment for glutamate spillover, for example calyceal synapses in the brainstem (Otis and Trussel, 1996; Otis et al., 1996) and synapses in cerebellar glomeruli (Silver et al.,

1996; Kinney et al., 1997; Overstreet et al., 1999; DiGregorio et al., 2002). At these synapses, closely clustered release sites and a constrained extrasynaptic space promote transmitter accumulation and pooling as well as spillover. Interestingly, these glutamatergic-spillover responses include a component mediated by AMPA receptors. Because of the relatively high affinity of AMPA receptors for glutamate binding (Patneau and Mayer, 1990), high concentrations of glutamate must reach adjacent receptors, a processes facilitated by the unique glomerular ultrastructure. AMPA-receptor mediated spillover responses can also occur at non-specialized synapses such as the parallel fiber-stellate cell synapse, however, intense pre-synaptic stimulation is required to generate spillover responses (Carter and Regehr, 2000).

#### *Spillover in the olfactory bulb*

The arrangement of glutamate release sites and receptors on olfactory bulb mitral cells is unusual. Glutamate release occurs at both apical dendritic tufts and along extensive lateral dendrites at dendrodendritic synapses with local inhibitory interneurons (Shepherd and Greer, 1998). Mitral cell glutamate release not only excites the postsynaptic complement of receptors on interneurons but also activates both AMPA and NMDA autoreceptors expressed on the mitral cell itself (Nicoll and Jahr, 1982; Isaacson, 1999; Friedman and Strowbridge, 2000; Salin et al., 2001; Schoppa and Westbrook, 2001; Schoppa and Westbrook 2002). In addition to autoexcitation, mitral cell glutamate release can also lead to cross-excitation of adjacent mitral cells. These cross-excitatory responses are mediated by NMDA receptors (Isaacson, 1999; Schoppa and Westbrook, 2001) or AMPA and NMDA receptors (Urban and Sakmann, 2002) and occur between

mitral cells projecting to the same glomerulus (Schoppa and Westbrook, 2001; Urban and Sakmann, 2002). Anatomical investigations have not identified synaptic connections between mitral cells (Price and Powell, 1970; Pinching and Powell, 1971). Therefore, release of glutamate onto adjacent extrasynaptic autoreceptors (spillover) provided the best explanation for cross-excitation mediated between pairs of mitral cells.

However, we found that Cx36-mediated electrical coupling of autoexcitation, and not glutamate spillover, governs the initiation and mediation of cross-excitation. Closely opposed apical dendritic processes are electrically coupled via Cx36-mediated gap junctions (Schoppa and Westbrook, 2002) that allow the rapid conduction of electrical signals between neurons (Bennett and Zukin, 2004; Long and Connors, 2004; Hormuzdi et al., 2004). Single-cell induced cross-excitation, but not autoexcitation, was absent in mice lacking mitral-mitral cell electrical coupling. Consistent with the glomerular distribution of Cx36 in mitral cells (Christie et al., 2004), cross-excitation was limited to cells projecting to the same glomerulus.

Spillover excitation could be evoked in mitral cell pairs, however, only during glutamate uptake block and between same-glomerulus mitral cells. This result strongly argues that spillover is mediated in the glomerulus between apical dendritic tufts and that glutamate in the extrasynaptic space is highly regulated and sequestered by transporters (Bergles and Jahr, 1998). Intraglomerular mitral cell spillover is mediated by AMPA receptors, a striking result given the relatively low affinity for AMPA-receptor glutamate binding. However, akin to other specialized synapses (Otis and Trussel, 1996; Otis et al., 1996; Silver et al., 1996; Kinney et al., 1997; Overstreet et al., 1999; DiGregorio et al., 2002), glial encapsulated dendrodendritic subcompartments (Chao et al., 1997; Kasowski

et al., 1999) may contribute to the accumulation and pooling of glutamate (Carlson et al., 2000; Schoppa and Westbrook, 2001) and therefore lead to the high concentrations of transmitter required for AMPA receptor activation.

Our experiments do not rule out the possibility that glutamate spillover occurs during bouts of synchronized mitral cell activity, a response common to mitral cells that project to the same glomerulus (Carlson et al., 2000; Schoppa and Westbrook, 2001; Schoppa and Westbrook, 2002; Christie et al., 2004). In fact, synchronized mitral cell excitation elicited by LOT stimulation evoked mitral cell spillover responses in wildtype and Cx36 knock mice. In addition, recordings from periglomerular cells during periods of synchronized mitral cell output indicate that glutamate accumulation and spillover occurs in the glomerulus (Schoppa and Westbrook, 2001). Synchronized activity mediated by electrical coupling (Schoppa and Westbrook, 2002; Christie et al., 2004) may promote coincident release in same-glomerulus mitral cells. This process could lead to spatial overlap of extrasynaptic glutamate in the glomerular neuropil thereby initiating cross-excitatory responses via adjacent receptor activation. Similar cooperation between synapses is known to aid spillover responses in CA1 hippocampal pyramidal cells (Arnth-Jensen et al., 2002). In addition, we observed an NMDA-receptor component in cross-excitatory responses in wildtype mice. This component, absent in Cx36 KO responses, may not reflect autoexcitation in the stimulated cell because of the hyperpolarized resting potential (-60 mV) and more likely reflects activation of adjacent mitral cells not being held at hyperpolarizing membrane potentials. Coincident activation of these cells may generate a coupled NMDA-receptor autoexcitatory response or evoke an en mass spillover response mediated by NMDA receptors.

Small NMDA spillover responses could also be evoked in paired mitral cell recordings, however, only in conditions favoring NMDA receptor activation (no extracellular  $Mg^{2+}$ ) similar to previously published reports (Isaacson, 1999). These responses did not depend on electrical coupling as they occurred in both wildtype and Cx36 KO mitral cell pairs lacking direct gap junctional coupling. Interestingly, these NMDA-spillover responses were localized along lateral dendrites. NMDA-receptor mediated spillover responses could also be evoked following LOT stimulation, however, in normal  $Mg^{2+}$  this response required the co-activation of AMPA receptors. These results provide conclusive evidence that direct NMDA-receptor mediated spillover responses can be generated in the olfactory bulb and imply that coincident depolarization in adjacent cells is required to relieve  $Mg^{2+}$  in order to activate the receptors. Because spillover currents in paired recordings were recorded under conditions that facilitate activation of NMDA receptors it is questionable whether this effect is relevant for synaptic communication in the olfactory bulb.

#### *Receptors mediating inter- and intraglomerular mitral cell spillover*

Autoexcitation in lateral dendrites is mediated primarily by NMDA receptors (Salin et al., 2001) and NMDA receptors mediate long-lasting depolarizations along lateral dendrites (Aroniadou-Anderjaska et al., 1999; Carlson et al., 2001). In contrast, autoexcitation in apical dendrites includes a prominent AMPA receptor component (Salin et al., 2001; Schoppa and Westbrook, 2002). Supporting these findings immunohistochemical studies indicate that mitral cell lateral dendrites express NMDA receptors, albeit at low density (Sassoe-Pognetto et al., 2003). Although apical dendrites

express both NMDA and AMPA receptors (Giustetto et al., 1997; Montague and Greer, 1999), the distribution of autoreceptors in this region is not well known.

Following single cell stimulation, lateral and apical dendritic spillover responses could be evoked between pairs of mitral cells. Interestingly, different sets of glutamatergic receptors located on different dendrites mediated these responses. The relative contribution of AMPA and NMDA receptors to these spillover responses probably reflects not only their different biophysical properties (including voltage-dependent block of NMDA receptors by  $Mg^{2+}$ ) but could also reflect differences in receptor density, affinity, and localization. For example, intraglomerular spillover could be solely mediated by AMPA receptors because glutamate release does not reach NMDA receptors, NMDA receptors may not be expressed on apical dendrites, or because  $Mg^{+2}$  block is not sufficiently relieved.

#### *Functional implications of an electrically coupled mitral cell network*

Gap junctions are well known mediators of rapid oscillations and spike synchrony in neuronal ensembles in neocortex, hippocampus, and inferior olive (Bennett and Zukin, 2004; Long and Connors, 2004; Hormuzdi et al., 2004). In mitral cells, Cx36-mediated electrical coupling underlies correlated firing in mitral cells that project to the same glomerulus (Schoppa and Westbrook, 2001; Christie et al., 2004). Here, we report that gap junctional coupling has a more general effect to enhance excitability between same-glomerulus mitral cells. Coupled autoexcitation may promote oscillatory behavior and long lasting glutamate release following afferent stimulation (Schoppa and Westbrook, 2001; Carlson et al., 2000). Because same-glomerulus mitral cells receive input from

afferents expressing the same olfactory receptors, gap junctional coupling of autoexcitation in same-glomerulus mitral cell ensembles may therefore amplify ORN input by spreading excitation to each mitral cell in the ensemble.

The interplay of electrical coupling, autoexcitation, and glutamate spillover could provide a potent mechanism leading to the glomerulus-specific synchronization of mitral cells. Slow intrinsic oscillations in mitral cells, induced by ORN stimulation, provide a synchronized patterned response in all cells projecting to the same glomerulus (Schoppa and Westbrook, 2001). Entrained mitral cell ensembles may provide for temporally coherent network activity thought necessary for processing of olfactory information (Laurent et al., 2001).

### **Acknowledgments**

This work was supported by National Institute of Health grant NS26494 (GLW) and 1F31-DC051224-01 (JMC). We thank members of the Westbrook labs for their helpful discussions. In addition, we thank Aesoon Benson for her assistance.

### **Figure Legends**

**Fig. 1** Putative intraglomerular glutamatergic spillover between pairs of mitral cells in wildtype mice.

(A and B<sub>1</sub>) In a mitral cell paired recording from a wildtype mouse, an action potential burst (400 pA, 50 ms current injection) evoked an autoexcitatory potential in the stimulated cell (M<sub>A</sub>) (*inset* enlarged averaged trace showing pharmacology) as well as a cross-excitatory potential (D<sub>cross-excite</sub>) in an adjacent unstimulated cell (M<sub>B</sub>) projecting to

the same glomerulus.  $D_{\text{cross-excite}}$  was partly reduced by the NMDA-receptor antagonist *D,L*-AP5 (100 mM; *left*) and nearly abolished by the AMPA-receptor antagonist NBQX (20 mM). A small potential, reflecting the electrical coupling of the excitatory current injection in the stimulated cell, persisted in NBQX. ( $B_2$ ) (*top*) Digital subtraction of the AP5-resistive potential from the control potential revealed a prolonged NMDA-receptor mediated component. (*bottom*) Digital subtraction of the NBQX-resistive potential from the AP5-resistive potential revealed a relatively brief AMPA-receptor mediated component. ( $B_3$ ) Normalization of the autoexcitatory potential and  $D_{\text{cross-excite}}$  (wash condition) shows no clear delay in the peaks of the potentials; (*inset*) expanded view. (C) An action potential burst in a paired recording from mitral cells projecting to different glomeruli failed to evoke cross-excitation. (D) Summary data from all wildtype paired recordings shows a correlation between the electrical coupling ratio determined for each pair (data not shown) and the size of  $D_{\text{cross-excite}}$ . Note: all representative traces reflect averaged responses from many sweeps except those of action potentials bursts.

**Fig. 2** Intraglomerular glutamatergic spillover between pairs of mitral cells in Cx36 KO mice.

( $A_1$ ) In a mitral cell paired recording from a Cx36<sup>-/-</sup> mouse, an action potential burst (325 pA, 50 ms current injection) evoked an autoexcitatory potential in the stimulated cell ( $M_A$ ) (*inset* enlarged averaged trace); however, a cross-excitatory potential was not generated in an adjacent same-glomerulus mitral cell ( $M_B$ ). Subsequent addition of the glutamate transporter blocker TBOA (50 mM) enhanced the autoexcitatory potential in the stimulated cell and uncovered a spillover potential ( $D_{\text{spillKO}}$ ) in the unstimulated cell.



(B) (*top*) Normalization of the autoexcitatory potential and  $D_{\text{spillKO}}$  shows a clear temporal delay in the peaks of the potentials; (*inset*) expanded view. (*bottom*)  $D_{\text{spillKO}}$  was unaffected by *D,L*-AP5, however, NBQX (20 mM) completely abolished the potential. (C) Mitral cell pairs with same-glomerulus projections generated  $D_{\text{spillKO}}$  whereas cross-excitation did not occur in cells projecting to different glomeruli. (D) Summary data shows that the cross-excitatory potential in WT mice is both NMDA and AMPA receptor mediated. Histogram includes the absolute sensitivity of  $D_{\text{crossexcite}}$  to glutamate receptor antagonists as well as the corrected sensitivity (electrically coupled current injection subtracted). In contrast, the cross-excitatory potential in  $\text{Cx36}^{-/-}$  mice is mediated entirely by AMPA receptors. Note: all representative traces reflect averaged responses from many sweeps except action potential burst.

**Fig. 3** Mitral cell dendritic morphology is similar in both wildtype and  $\text{Cx36}^{-/-}$  mice.

(A<sub>1</sub> and B<sub>1</sub>) Pairs of mitral cells filled with biocytin (*red*) and lucifer yellow (*green*) show normal mitral cell morphology in both a wildtype (A<sub>1</sub>) and a  $\text{Cx36}^{-/-}$  mouse (B<sub>1</sub>) Cell body layers are demarcated with a propidium iodide label (*blue*). (A<sub>2</sub> and B<sub>2</sub>) High magnification (100X objective), confocal z-stack images of mitral cell dendritic tufts from A<sub>1</sub> and B<sub>1</sub>. Both pairs have highly intercalated processes and extensive areas of overlap. (C) The number of putative contacts, defined by close membrane opposition or direct overlap, is the same in wildtype and knockout mice. (D) The number of putative contacts was well correlated with the coupling ratio determined for each pair demonstrating the validity of the method. Glom., glomeruli; MCL, mitral cell layer;

GCL, granule cell layer. Scale bars 40  $\mu$ m, 7  $\mu$ m, 50  $\mu$ m, and 7  $\mu$ m in A<sub>1</sub>, A<sub>2</sub>, B<sub>1</sub>, and B<sub>2</sub>, respectively.

**Fig. 4.** Mitral cell cross-excitation in voltage-clamped mitral cells.

(A<sub>1</sub>) In a paired mitral cell voltage-clamp recording (0 Mg<sup>+2</sup> and 1 mM TTX), a brief voltage-step (stimulation artifact removed; -60 to +10 mV, 35 ms) elicited an autoexcitatory current in the stimulated cell (M<sub>A</sub>) as well as a cross-excitatory current in an adjacent mitral cell projecting to the same glomerulus (M<sub>B</sub>). Both the auto- and cross-excitatory currents were blocked by D,L-AP5 (100  $\mu$ M). (*bottom*) Changing the holding potential (V<sub>h</sub>) of the unstimulated mitral cell had no effect on the amplitude of the cross-excitatory current. (A<sub>2</sub>) Current-voltage relationship of the cross-excitatory current does not reflect the predicted relationship based on the electrochemical gradient of NMDA receptors. Instead, the current-voltage relationship is consistent with an electrically coupled event. The data points in the graph reflect cross-excitatory current comparisons to normalized current measurements recorded at V<sub>h</sub> -60 mV. (B) Although a robust autoexcitatory current was generated following a voltage step (-60 to +10 mV, 35 ms) in a Cx36<sup>-/-</sup> mitral cell, the cross-excitatory current (I<sub>small</sub>) recorded in the unstimulated cell was extremely small; (*inset*) expanded view of cross-excitatory current. (D) (*left*) Summary histograms showing that both autoexcitatory currents were evoked in both wild-type and Cx36<sup>-/-</sup> mitral cells, although, currents were slightly smaller on average in Cx36<sup>-/-</sup> mice. (*right*) Summary histograms show that cross-excitatory currents in same-glomerulus mitral cell pairs were relatively large. In some cell same-glomerulus mitral cell pairs from knockout mice, small currents were evoked that were significantly larger

than the standard deviation of the unstimulated cell response (indicated by solid line).  
Note scaling on y-axis.

**Fig. 5.** NMDA receptor mediated spillover currents evoked along lateral dendrites.

(A<sub>1</sub>) A pair of wildtype mouse mitral cells filled with biocytin (*red*) and lucifer yellow (*green*) project to different glomeruli. The lack of apical tuft overlap does not limit putative sites of close dendritic opposition; note that lateral dendrites repeatedly intersect. Glom., glomeruli; and MCL, mitral cell layer; GCL. Scale bar 40  $\mu$ m. (A<sub>2</sub> and A<sub>3</sub> *top*) Mitral cell excitation (M<sub>A</sub>) (-60 to +10 mV, 35 ms) evoked a small cross-excitatory current (I<sub>small</sub>) in an unstimulated mitral cell (M<sub>B</sub>) projecting to a different glomerulus (same pair illustrated in A<sub>1</sub>). Following uptake block (TBOA, 50  $\mu$ M), I<sub>small</sub> is greatly enhanced. In this example, TBOA had no effect on the autoexcitatory current. (A<sub>3</sub> *bottom*) Addition of *D,L*-AP5 (100  $\mu$ M) completely eliminated the I<sub>small</sub>. (B<sub>1</sub> and B<sub>2</sub>) In a Cx36<sup>-/-</sup> mouse, mitral cell excitation did not evoke a cross-excitatory current in control conditions. After TBOA (50  $\mu$ M) application, however, a pronounced I<sub>small</sub> current was recorded that was completely blocked by *D,L*-AP5 (100  $\mu$ M). The autoexcitatory current in M<sub>A</sub>, in this cell pair, was enhanced by TBOA. (C) Summary data shows that TBOA enhanced or uncovered similarly sized NMDA receptor mediated cross-excitatory currents in some wild-type different-glomerulus and Cx36<sup>-/-</sup> same-glomerulus cell pairs. The pharmacology and lack of electrical coupling between either of these types of mitral cell pairings suggest that I<sub>small</sub> reflects glutamate spillover along proximal portions of lateral dendrites.

**Fig. 6.** Spillover potentials generated in the absence of uptake block.

(A<sub>1</sub> and A<sub>2</sub>) Antidromic stimulation of mitral cell axons via the lateral olfactory tract (LOT) evoked an action potential (truncated) followed by a long lasting depolarization in a test mitral cell from a wild-type mouse (*right*). An action potential (truncated) elicited by a brief current injection (1200 pA, 4 ms) in the same test mitral failed to evoke a similar after-depolarization (*left*). (A<sub>3</sub>) The LOT-evoked potential (expanded) was highly reduced by D,L-AP5 (100 mM) and completely abolished by NBQX (20 mM). (B<sub>1</sub> and B<sub>2</sub>) LOT stimulation in a test mitral cell from a Cx36<sup>-/-</sup> mouse also evoked an after-depolarization sensitive to glutamatergic antagonists (D,L-AP5 100 mM, NBQX 20 mM). Single action potentials elicited by current injection in the test mitral cell again failed to evoke similar LOT-evoked after-depolarizations. (C) Comparison of the pharmacology (*right*) and magnitude (*right*) of the LOT-evoked potential in wildtype and Cx36<sup>-/-</sup> mice. The depolarization in wildtype mice was many times larger than that evoked in Cx36<sup>-/-</sup> mice. Interestingly, prolonged depolarizations could be evoked in several mitral cells with a severed apical dendrite (determined by cell fills, not shown). These potentials had similar pharmacology to that of mitral cells with intact apical dendrites but were smaller in size. Note scaling on y-axis.

**Fig. 7.** ORN-evoked oscillatory responses in mitral cells are absent in Cx36 KO mice.

(A<sub>1</sub>) Orthodromic stimulation of olfactory receptor neuron (ORN) afferents evoked a complex patterned response of oscillating depolarizations in a mitral cell recording from a wildtype mouse. (A<sub>2</sub> and A<sub>3</sub>) In a same-glomerulus paired recording, the depolarizing oscillations were well synchronized as indicated by the peak of the cross-correlogram (Dt= 0; C<sub>0</sub>). (B<sub>1</sub>) In a

mitral cell recording from a Cx36 KO mouse, ORN stimulation failed to evoke oscillating depolarizations. However, oscillations were uncovered following uptake block (TBOA 20 mM). (B<sub>2</sub> and B<sub>3</sub>) These depolarizations were also highly synchronized in same-glomerulus paired recordings.

# Figures

## Fig. 1

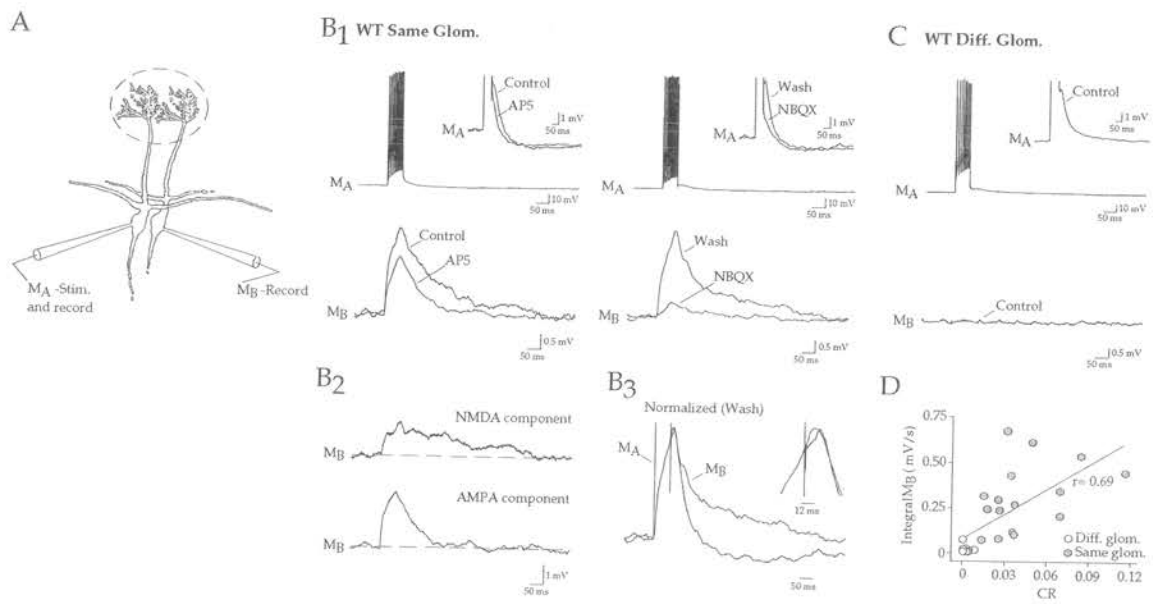
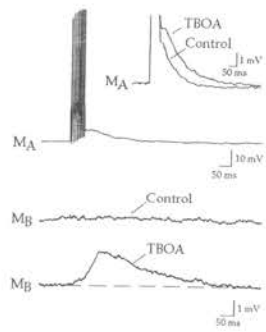
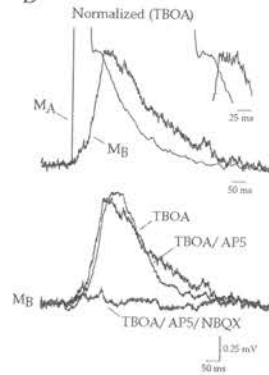


**Fig. 2**

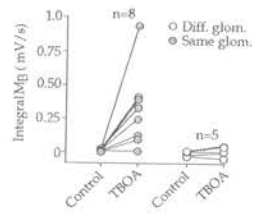
**A** Cx36(-/-) Same Glom.



**B**



**C**



**D**

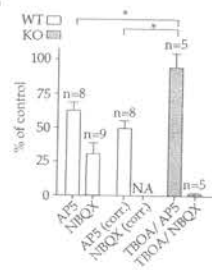


**Fig. 3**

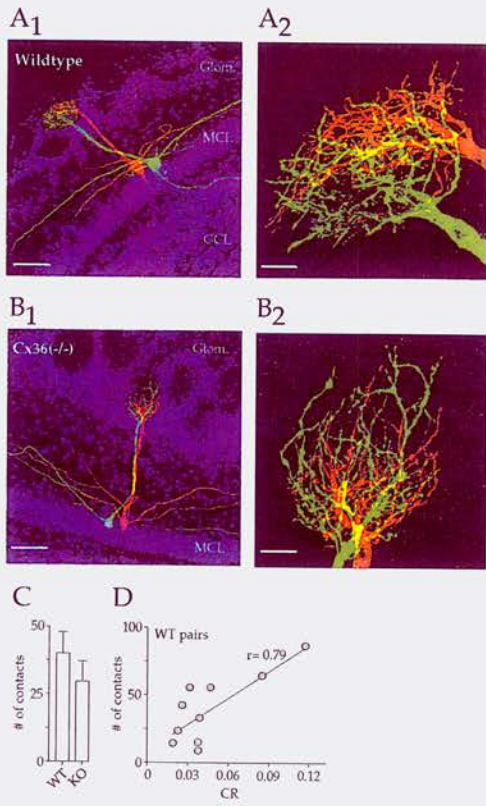




**Fig. 4**

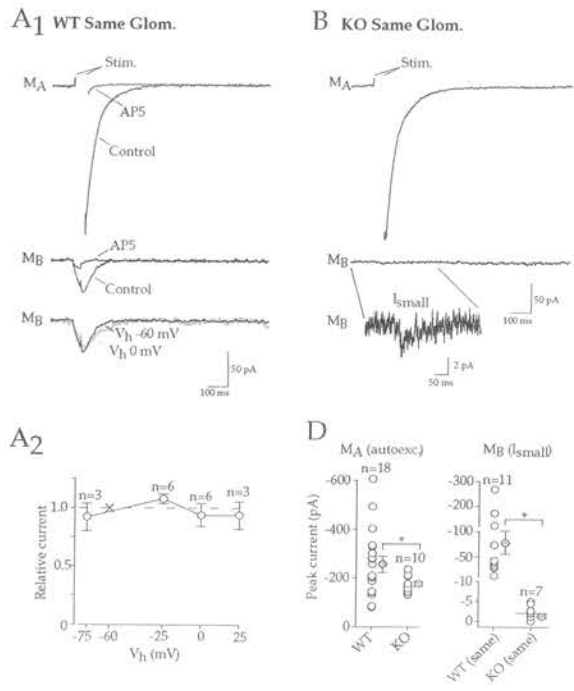


**Fig. 5**

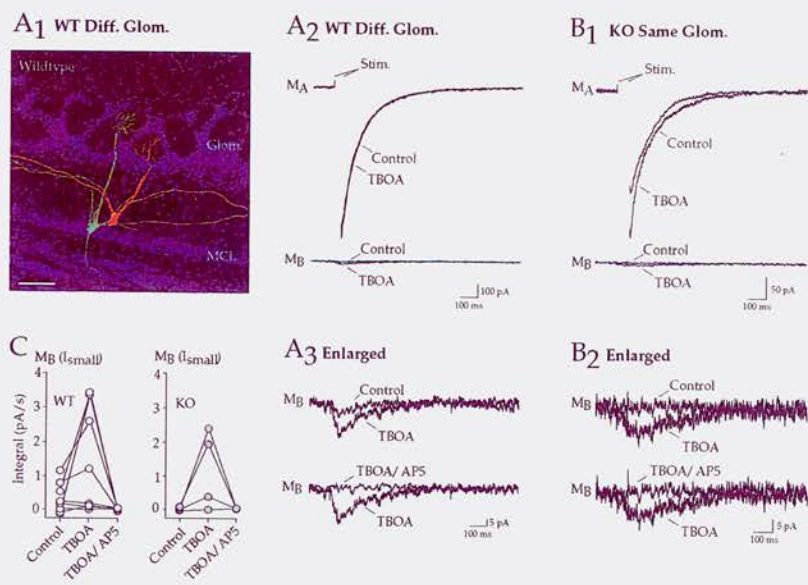


**Fig. 6**

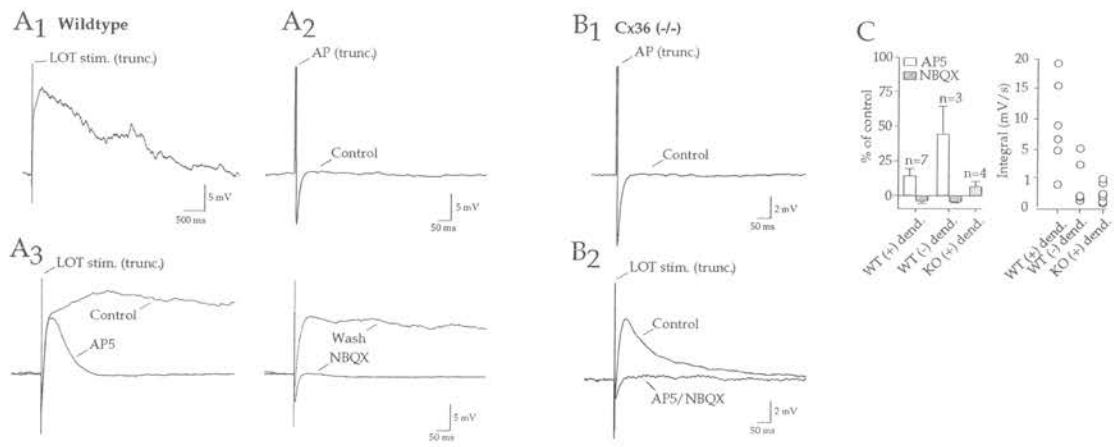
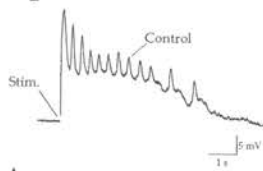
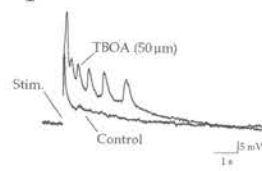


**Fig. 7**

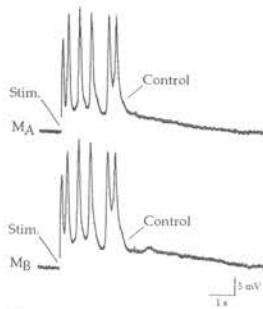
**A<sub>1</sub> WT Same Glom.**



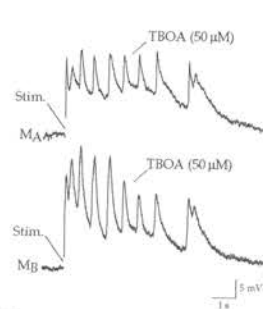
**B<sub>1</sub> KO Same Glom.**



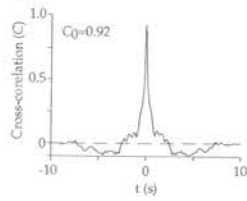
**A<sub>2</sub> Paired Recording**



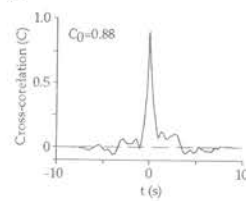
**B<sub>2</sub> Paired Recording**



**A<sub>3</sub>**



**B<sub>3</sub>**



## **CONCLUSIONS**

My thesis examined cellular mechanisms that influence dendritic excitability and shape mitral-mitral cell interactions. I used olfactory bulb slices from wildtype and mutant mice and rats in conjunction with whole-cell voltage and current-clamp recordings. I found that the physiology and circuits of apical and lateral dendrites influence the excitability of mitral cells from which these dendrites project as well as the excitability of neighboring mitral cells. Consequently, these interactions could impact olfactory information coding.

### **The extent of lateral inhibition**

In investigations of mitral cell lateral dendritic processing, I found that the extent of the lateral dendritic arbor determines the spread of inhibition throughout the bulb. In comparisons to tufted cells, whose dendrodendritic circuits are identical to those of mitral cells, the extent of lateral inhibition of tufted cells was much reduced. This is best explained by the more confined dendritic arbor of tufted cells. The amplitudes of backpropagating action potentials were attenuated in mitral cell lateral dendrites. The attenuation of action potentials depended on A-type potassium channels ( $I_A$ ) similar to that described in the apical dendrites of CA1 pyramidal cells (Hoffman et al. 1997). The expression of  $I_A$  can therefore controls the excitability of the lateral dendrite. A current could have a profound consequence on dendrodendritic inhibition because mitral cell glutamate release presumably depends on local calcium entry evoked by backpropagating action potentials. In addition, incoming lateral inhibition may be more effective in preventing the penetration of action potentials into distal dendritic segments due to the attenuation of spikes. This raises the possibility that proximal and

distal segments can be independently regulated. This process may add a dynamic component to mitral cell interactions and thus have important consequences for odorant coding.

*Future directions:* The attenuation of action potentials in lateral dendrites could have a profound impact on lateral inhibition; however, this question was not directly addressed in my work. It would be worth investigating a link between these phenomenon. For example, there are reasons to believe that distal dendritic release may not be compromised. The attenuated action potential may be as effective as a full-blown spike in evoking release or an enhanced expression of calcium channels may compensate for reduced dendritic excitability.

### **Electrical coupling in mitral cells**

I have shown that Cx36 mediates electrical coupling between mitral cells projecting to the same glomerulus. Electrical coupling plays an important role in organizing mitral cell output in a temporally coordinated manner. Without electrical coupling, spike synchronization in same-glomerulus mitral cells is lost. Gap junctional coupling also plays a critical role propagating excitation throughout the electrical syncytium. Glutamatergic autoexcitation electrically coupled to other mitral cells in the glomerular unit provides a strong excitatory drive in all connected mitral cells thereby multiplying mitral cell excitability. This amplification step could increase the sensitivity of mitral cell units to a particular odorant.

Some central synapses have specialized morphology that present a conducive environment for glutamate spillover such as calyceal synapses (Otis and Trussell 1996, Otis et al. 1996) and synapses in the cerebellar glomeruli (Silver et al. 1996, Kinney et al. 1997, Overstreet et al. 1999, DiGregorio et al. 2002). At these synapses, closely clustered release

sites and a constrained extra synaptic space can promote transmitter accumulation and pooling as well as spillover. The olfactory bulb glomerulus shares many of these features. However, it is debatable whether glutamate spillover occurs in this structure. Single-cell excitatory activity in mitral cell lacking electrical coupling was insufficient to generate spillover potentials in physiological conditions. In fact, I found that potentials previously attributed to spillover (Schoppa and Westbrook 2001, Urban and Sakmann 2002) were actually attributed to electrical coupling of autoexcitatory potentials. However, spillover potentials could be evoked by the coordinated activity of many mitral cells. This condition could potentially be replicated by strong ORN input, thereby providing the drive necessary for glutamate accumulation and spillover.

Mitral cell cross-excitation provides a mechanism of maintaining the fidelity of the glomerular-OR map by synchronizing mitral cells projecting to the same glomerulus. This modular organization may facilitate coding downstream from the olfactory bulb such that mitral cells lose their individual coding identity and instead respond as a glomerular unit. In insects, output neurons that project to the same glomerulus exhibit a similar axonal topography in the protocerebrum (Marin et al. 2002, Wong et al. 2002). Mitral cell axonal projections are also stereotyped in the olfactory cortex (Zou et al. 2001). The targeting of axonal projections to specific clusters of cortical neurons raises the possibility that glomerular units converge on the same target neuron. Therefore, synchronization of action potentials between mitral cells may greatly enhance the probability of driving a target cortical neuron in olfactory cortex to spike because of the temporal summation of synaptic inputs from the two same-glomerulus mitral cells (Mori et al. 1999).

*Future directions:* Based on mRNA and protein expression studies, neurons and interneurons in the olfactory bulb are extensively electrically coupled (Paternostro 1995, Miragall 1996, Parenti et al. 2000, Teubner et al. 2000, Zhang and Restrepo 2002, Zhang and Restrepo 2003). Functional studies will be required to understand the role and physiological impact of these electrical circuits. In addition, it is unclear whether spillover occurs in the glomerulus following ORN input although evidence suggests that during induced bouts of concerted mitral cell activity glutamate accumulation and spillover can occur (Schoppa and Westbrook 2001). Large oscillating depolarizations occur simultaneously in all mitral cells projecting to a given glomerulus following ORN stimulation (Schoppa and Westbrook 2001). Although these oscillations are dependent on electrical coupling, they could provide the concerted drive necessary for glutamate spillover. Additional work is also required to understand how mitral cell units integrate excitation and inhibition. These inputs are critical determinates of bulb information transformation and understanding how mitral cells balance these properties will provide insight into odorant coding.



## REFERENCES

### **Introduction**

Bennett, M.V., and Zukin R.S. Electrical coupling and neuronal synchronization in the mammalian brain. *Neuron* 41: 495-511. 2004.

Bozza, T.C., and Mombaerts, P. Olfactory coding: revealing intrinsic representations of odors. *Curr. Biol.* 11: R687-R690. 2001.

Buck, L. and Axel, R. A novel multigene family may encode odorant receptors: a molecular basis for odor recognition. *Cell.* 65: 175-187, 1991.

Carlson, G.C., Shipley, M.T., and Keller, A. Long-lasting depolarizations in mitral cells of the rat olfactory bulb. *J. Neurosci.* 20, 2011-2021. 2000.

Chao, T.I., Kasa, P., and Wolff, J.R. Distribution of astroglia in glomeruli of the rat main olfactory bulb: exclusion from the sensory subcompartment of neuropil. *J. Comp. Neurol.* 388: 191-210. 1997.

Chen, W.R., Xiong, W., and Shepherd, G.M. Analysis of relations between NMDA receptors and GABA release at olfactory bulb reciprocal synapses. *Neuron.* 25: 625-633. 2000.

Didier, A., Carleton, A., Bjaalie, J.G., Vincent, J.D., Ottersen, O.P., Storm-Mathisen, J., and Lledo, P.M. A dendrodendritic reciprocal synapse provides a recurrent excitatory connection in the olfactory bulb. *Proc. Natl. Acad. USA*. 98: 6441-6226. 2001.

Duchamp-Viret, P., Chaput, M.A., and Duchamp, A. Odor response properties of rat olfactory receptor neurons. *Science*. 284: 2171-2174. 1999.

Firestein, S. How the olfactory system makes sense of scents. *Nature*. 413: 211-218. 2001.

Fried, H.U., Fuss, S.H., and Korsching, S.I. Selective imaging of presynaptic activity in the mouse olfactory bulb shows concentration and structure dependence of odor responses in identified glomeruli. *Proc. Natl. Acad. Sci. USA*. 99: 3222-3227. 2002.

Friedman, D. and Strowbridge, B.W. Functional role of NMDA autoreceptors in olfactory bulb mitral cells. *J. Neurophysiol.* 84: 39-50. 2000.

Halabisky, B., Friedman, D., Radojicic, M., and Strowbridge, B.W. Calcium influx through NMDA receptors directly evokes GABA release in olfactory bulb granule cells. *J. Neurosci.* 20: 5124-5134. 2000.

Hayar, A., Karnup, S., Shipley, M.T., and Ennis, M. Olfactory bulb glomeruli: external tufted cells intrinsically burst at theta frequency and are entrained by patterned olfactory input. *J. Neurosci.* 24: 1190-1199. 2004.

Hormuzdi, S.G., Filippov, M.A., Mitropoulou, G., Monyer, H., and Bruzzone, R. Electrical synapses: a dynamic signaling system that shapes the activity of neuronal networks. *Biochim. Biophys. Acta.* 1662: 113-137. 2004.

Isaacson, J.S. Glutamate spillover mediates excitatory transmission in the rat olfactory bulb. *Neuron.* 23: 377-384. 1999.

Isaacson, J.S. Mechanisms governing dendritic gamma-aminobutyric acid (GABA) release in the rat olfactory bulb. *Proc. Natl. Acad. Sci. U.S.A.* 98: 337-342. 2001.

Isaacson, J.S. and Strowbridge, B.W. Olfactory reciprocal synapses: dendritic signaling in the CNS. *Neuron.* 20: 749-761. 1998.

Jahr, C.E. and Nicoll, R.A. An intracellular analysis of dendrodendritic inhibition in the turtle in vitro olfactory bulb. *J. Physiol.* 26: 213-234. 1982.

Johnson, B.A., Woo, C.C., and Leon, M. Spatial coding of odorant features in the glomerular layer of the olfactory bulb. *J. Comp. Neurol.* 393: 457-471. 1998.

Kajiya, K., Inaki, K., Tanaka, M., Haga, T., Kataoka, H., and Touhara, K. Molecular bases of odor discrimination: reconstitution of olfactory receptors that recognize overlapping sets of odorants. *J. Neurosci.* 21: 6018-6025. 2001.

Kashiwadani, H., Sasaki, Y.F., Uchida, N., and Mori, K. Synchronized oscillatory discharges of mitral/tufted with different molecular receptive ranges in the rabbit olfactory bulb. *J. Neurophysiol.* 82: 1786-1792. 1999.

Kasowski, H.J., Kim, H., and Greer, C.A. Compartmental organization of the olfactory bulb glomerulus. *J. Comp. Neurol.* 407: 261-274. 1999.

Korsching, S. Olfactory maps and odor images. *Current Opin. in Neurobiol.* 12: 387-392. 2002.

Kosaka, K., Aika, Y., and Kosaka, T. Structure of the intraglomerular dendritic tufts of mitral cells and their contacts with olfactory nerve terminals and calbindin-immunoreactive type-2 periglomerular neurons. *J. Comp. Neurol.* 440: 219-235. 2001.

Kosaka, K., Toida, K., Aika, Y., Kosaka, T. How simple is the organization of the olfactory glomerulus?: the heterogeneity of so-called periglomerular cells. *Neurosci. Res.* 30: 101-110. 1998.

Kuffler, S.W. Discharge patterns and functional organization of mammalian retina. *J. Neurophysiol.* 16: 37-46. 1953.

Laurent, G., Stopfer, M., Friedrich, R.W., Rabinovich, M.I., Volkovskii, A., and Abarbanel, H.D.I. Odor encoding as an active, dynamical process: experiments, computation, and theory. *Annu. Rev. Neurosci.* 24: 263-297. 2001.

Luo, M. and Katz, L.C. Response correlation maps of neurons in the mammalian olfactory bulb. *Neuron.* 32: 1165-1179. 2001.

Malnic, B., Hirono, J., Sato, T., and Buck, L.B. Combinatorial receptor codes for odors. *Cell.* 96: 713-723, 1999.

Miragall, F., Simburger, E., and Dernietzel, R. Mitral and tufted cells of the mouse olfactory bulb possess gap junctions and express connexin43 mRNA. *Neurosci. Letters* 216: 199-202. 1996.

Mombaerts, P., Wang, P., Dulac, C., Chao, S.K., Nemes, A., Mendelsohn, M. Edmondson, J., and Axel, R. Visualizing an olfactory sensory map. *Cell.* 87: 675-686. 1996.

Montague, A.A. and Greer, C.A. Differential distribution of ionotropic glutamate receptor subunits in the rat olfactory bulb. *J. Comp. Neurol.* 405: 233-246. 1999.

Mori, K. Membrane and synaptic properties of identified neurons in the olfactory. *Prog. In Neurobiology* 29: 275-320, 1987.

Mori, K., Kishi, K., and Ojima, H. Distributions of dendrites of mitral, displaced mitral, tufted, and granule cells in the rabbit olfactory bulb. *J. Comp. Neur.* 219: 339-355, 1983.

Mori K, Nagao H, and Yoshihara Y. The olfactory bulb: coding and processing of odor molecule information. *Science.* 286: 711-715, 1999.

Orona, E., Rainer, E.C., and Scott, J.W. Dendritic and axonal organization of mitral and tufted cells in the rat olfactory bulb. *J. Comp. Neurol.* 226: 346-56, 1984.

Nicoll, R.A. and Jahr, C.E. Self-excitation of olfactory bulb neurons. *Nature.* 296: 441-444. 1982.

Parenti R, Gulisano M, Zappala A, and Cicirata F. Expression of connexin36 mRNA in adult rodent brain. *Neuroreport.* 7: 1497-1502. 2000.

Paternostro, M.A., Reyher, C.K.H., and Brunjes, P.C. Intracellular injections of Lucifer Yellow into lightly fixed mitral cells reveal neuronal dye-coupling in the developing rat olfactory bulb. *Develop. Brain Research.* 84: 1-10. 1995.

Pinching, A.J. and Powell, T.P.S. The neuron types of the glomerular layer of the olfactory bulb. *J. Cell Sci.* 9: 305-345. 1971a.

Pinching, A.J. and Powell, T.P.S. The neuropil of the glomeruli of the olfactory bulb. *J. Cell Sci.* 9: 347-377. 1971b.

Price J.L. and Powell, T.P.S. The morphology of granule cells within the olfactory bulb. *J. Cell. Sci.* 7: 5-155. 1970.

Rubin, B.D. and Katz, L.C. Optical imaging of odorant representations in the mammalian olfactory bulb. *Neuron.* 23: 499-511. 1999.

Salin, P.A., Lledo, P.M., Vincent, J.D., and Charpak, S. Dendritic glutamate autoreceptors modulate signal processing in rat mitral cells. *J Neurophysiol.* 85: 1275-1282. 2001.

Sashse, S. and Galizia, C.G. Role of inhibition for temporal and spatial odor representation in olfactory output neurons: a calcium imaging study. *J. Neurophysiol.* 87: 1106-1117. 2002.

Sassoe-Pognetto, M. and Ottersen, O.P. Organization of ionotropic glutamate receptors at dendrodendritic synapses in the rat olfactory bulb. *J. Neurosci.* 20: 2192-2201. 2000.

Sassoe-Pognetto, M., Utvik, J.K., Camoletto, P., Watanabe, M., Stephenson, F.A., Brecht, D.S., and Otterson, O.P. Organization of postsynaptic density proteins and glutamate receptors in axodendritic and dendrodendritic synapses of the rat olfactory bulb. *J. Comp. Neurol.* 463: 237-248. 2003.

Schoppa, N.E., Kinzie, J.M., Sahara, Y., Segerson, T.P., and Westbrook, G.L. Dendrodendritic inhibition in the olfactory bulb is driven by NMDA receptors. *J. Neurosci.* 18: 6790-6802. 1998.

Schoppa, N.E. and Westbrook, G.L. Regulation of synaptic timing in the olfactory bulb by an A-type potassium current. *Nat. Neurosci.* 2: 1106-1113. 1999.

Schoppa, N.E., and Westbrook, G.L. Glomerulus-specific synchronization of mitral cells in the olfactory bulb. *Neuron.* 31: 639-651. 2001.

Schoppa, N.E., and Westbrook, G.L. AMPA autoreceptors drive correlated spiking in olfactory bulb glomeruli. *Nat. Neurosci.* 5: 1194-1202. 2002.

Scott, J.W. and Harrison, T.A. *Neurobiology of Taste and Smell*; Malabar, FL. Krieger Publishing Company. 1991.

Shepherd, G.L. and Greer, C.A. *The Synaptic Organization of the Brain*. New York, NY. Oxford University Press. 1998.



Teubner, B., Degen, J., Sohl, G., Guldenagel, M., Bukauskas, F.F., Trexler, E.B., Verselis, V.K., De Zeeuw, C.I., Lee, C.G., Kozak, C.A., Petrasch-Parwez, E., Dermietzel, R., and Willecke, K. Functional expression of the murine connexin 36 gene coding for a neuron-specific gap junctional protein. *Membrane Biology*. 176: 249-262. 2000.

Tsuboi, A., Yoshihara, S., Yamazaki, N., Kasai, H., Asai-Tsuboi, H., Komatsu, M., Serizawa, S., Ishii, T., Matsuda, Y., Nagawa, F., and Sakano, H. Olfactory neurons expressing closely linked and homologous odorant receptor genes tend to project their axons to neighboring glomeruli on the olfactory bulb. *J. Neurosci*. 19: 8409-18. 1999.

Urban, N.N., and Sakmann, B. Reciprocal intraglomerular excitation and intra- and interglomerular lateral inhibition between mouse olfactory bulb mitral cells. *J. Physiol*. 542: 355-367. 2002.

Vassar, R., Chao, S.K., Sitcheran, R., Nunez, J.M., Vosshal, L.B., and Axel R. Topographical organization of sensory projections to the olfactory bulb. *Cell*. 79: 981-991. 1994.

Wachowiak, M. and Cohen, L.B. Representation of odorants by receptor neuron input to the mouse olfactory bulb. *Neuron*. 32: 723-735. 2001.

Wellis, D.P. and Kauer, J.S. GABA<sub>A</sub> and glutamate receptor involvement in dendrodendritic synaptic interactions from salamander olfactory bulb. *J. Physiol.* 469: 315-339. 1993.

Wellis, D.P. and Kauer, J.S. GABAergic and glutamatergic synaptic input to identified granule cells in salamander olfactory bulb. *J. Physiol.* 475: 419-430. 1994.

Wilson, D.A. and Leon, M. Evidence of lateral synaptic interactions in olfactory bulb output cell responses to odors. *Brain Res.* 417: 175-180, 1987.

Wilson, R.I., Turner, G.C., and Laurent, G. Transformation of olfactory representations in the *Drosophila* antennal lobe. *Science.* 303: 366-370. 2004.

Xu, F., Greer, C.A., and Shepherd, G.M. Odor maps in the olfactory bulb. *J. Comp. Neurol.* 422: 489-495. 2000.

Yokoi, M., Mori, K., and Nakanishi, S. Refinement of odor molecule tuning by dendrodendritic synaptic inhibition in the olfactory bulb. *Proc. Natl. Acad. Sci. U.S.A.* 92: 3371-3375, 1995.

Zhang, C., and Restrepo, D. Expression of connexin 45 in the olfactory system. *Brain Research.* 929: 37-47. 2002.

Zhang, C., and Restrepo, D. Heterogenous expression of connexin 36 in the olfactory epithelium and glomerular layer of the olfactory bulb. *J. Comp. Neurol.* 459, 426-439. 2003.

## **Chapter 1**

Cajal, R.S. Histologie du Système Nerveux de l'Homme et des Vertébrés. *Tome 2*. Madrid: Instituto Ramón y Cajal. 1911.

Chen, W.R., Xiong, W., and Shepherd, G.M. Analysis of relations between NMDA receptors and GABA release at olfactory bulb reciprocal synapses. *Neuron.* 25: 625-633. 2000.

Ezeh, P.I., Wellis, D.P., and Scott, J.W. Organization of inhibition in the rat olfactory bulb external plexiform layer. *J. Neurophysiol.* 70: 263-74. 1993.

Giustetto, M., Bovolin, P., Fasolo, A., Bonino, M., Cantino, D., and Sassoe-Pognetto, M. Glutamate receptors in the olfactory bulb synaptic circuitry: heterogeneity and synaptic localization of N-methyl-D-aspartate receptor subunit 1 and AMPA receptor subunit 1. *Neuroscience.* 76: 787-798. 1997.

Halabisky, B., Friedman, D., Radojicic, M., and Strowbridge, B.W. Calcium influx through NMDA receptors directly evokes GABA release in olfactory bulb granule cells. *J. Neurosci.* 20: 5124-5134. 2000.

Isaacson, J.S. Glutamate spillover mediates excitatory transmission in the rat olfactory bulb. *Neuron*. 23: 77-84. 1999.

Isaacson, J.S., and Strowbridge, B.W. Olfactory reciprocal synapses: dendritic signaling in the CNS. *Neuron*. 20: 749-761. 1998.

Kosaka, K., Toida, K., Aika, Y., and Kosaka, T. How simple is the organization of the olfactory glomerulus?: the heterogeneity of so-called periglomerular cells. *Neurosci Res*. 30: 101-110. 1998.

Macrides, F. and Schneider, S.P. Laminar organization of mitral and tufted cells in the main olfactory bulb of the adult hamster. *J. Comp. Neurol*. 208: 419-430. 1982.

Malnic, B., Hirono, J., Sato, T., and Buck, L.B. Combinatorial receptor codes for odors. *Cell*. 96: 713-723. 1999.

Mori, K., Kishi, K., and Ojima, H. Distributions of dendrites of mitral, displaced mitral, tufted, and granule cells in the rabbit olfactory bulb. *J. Comp. Neur*. 219: 339-355. 1983.

Mori, K., Nagao, H., and Yoshihara, Y. The olfactory bulb: coding and processing of odor molecule information. *Science*. 286: 711-715. 1999.

Mori, K. and Takagi, S.F. An intracellular study of dendrodendritic inhibitory synapses on mitral cells in the rabbit olfactory bulb. *J. Physiol.* 279: 569-588. 1978.

Nicoll, R.A. and Jahr, C.E. Self-excitation of olfactory bulb neurones. *Nature.* 296: 441-444. 1982.

Orona, E., Rainer, E.C., and Scott, J.W. Dendritic and axonal organization of mitral and tufted cells in the rat olfactory bulb. *J. Comp. Neurol.* 226: 346-56. 1984.

Orona, E., Scott, J.W., and Rainer, E.C. Different granule cell populations innervate superficial and deep regions of the external plexiform layer in rat olfactory bulb. *J. Comp. Neurol.* 217: 227-37. 1983.

Pinching, A.J. and Powell, T.P.S. The neuron types of the glomerular layer of the olfactory bulb. *J. Cell Sci.* 9: 305-345. 1971a.

Pinching, A.J. and Powell, T.P.S. The neuropil of the glomeruli of the olfactory bulb. *J. Cell Sci.* 9: 347-377. 1971b.

Price J.L. and Powell, T.P.S. The morphology of granule cells within the olfactory bulb. *J. Cell. Sci.* 7: 5-155. 1970.

Rubin, B.D. and Katz, L.C. Optical imaging of odorant representations in the mammalian olfactory bulb. *Neuron*. 23: 499-511. 1999.

Schoppa, N.E., Kinzie, J.M., Sahara, Y., Segerson, T.P., and Westbrook, G.L. Dendrodendritic inhibition in the olfactory bulb is driven by NMDA receptors. *J. Neurosci*. 18: 6790-6802. 1998.

Schoppa, N.E. and Westbrook, G.L. Regulation of synaptic timing in the olfactory bulb by an A-type potassium current. *Nature Neurosci*. 2: 1106-1113. 1999.

Scott, J.W. and Harrison, T.A. *Neurobiology of Taste and Smell*; Malabar, FL. Krieger Publishing Company, 1991.

Tsuboi, A., Yoshihara, S., Yamazaki, N., Kasai, H., Asai-Tsuboi, H., Komatsu, M., Serizawa, S., Ishii, T., Matsuda, Y., Nagawa, F., and Sakano, H. Olfactory neurons expressing closely linked and homologous odorant receptor genes tend to project their axons to neighboring glomeruli on the olfactory bulb. *J. Neurosci*. 19: 8409-18. 1999.

Vassar, R., Chao, S.K., Sitcheran, R., Nunez, J.M., Vosshall, L.B., and Axel, R. Topographic organization of sensory projections to the olfactory bulb. *Cell*. 79: 981-991. 1994.

Yokoi, M., Mori, K., and Nakanishi, S. Refinement of odor molecule tuning by dendrodendritic synaptic inhibition in the olfactory bulb. *Proc. Natl. Acad. Sci. U.S.A.* 92: 3371-3375. 1995.

## **Chapter 2**

Bischofberger, J. and Jonas, P. Action potential propagation into the presynaptic dendrites of rat mitral cells. *J. Physiol.* 504: 359-65. 1997.

Buck, L.B. Information coding in the vertebrate olfactory system. *Annu. Rev. Neurosci.* 19: 517-544. 1996.

Charpak, S., Mertz, J., Beaupaire, E., Moreaux, L., and Delaney, K. Odor-evoked calcium signals in dendrites of rat mitral cells. *Proc. Natl. Acad. Sci. USA.* 98: 1230-1234. 2001.

Chen, W.R., Midtgaard, J., and Shepherd, G.M. Forward and backward propagation of dendritic impulses and their synaptic control in mitral cells. *Science.* 278: 463-467. 1997.

Hausser, M., Stuart, G., Racca, C., and Sakmann B. Axonal initiation and active dendritic propagation of action potentials in substantia nigra neurons. *Neuron.* 15: 637-647. 1995.

Hausser, M., Spruston, N., Stuart, G.J. Diversity and dynamics of dendritic signaling. *Science.* 290: 739-744, 2000.

Hoffman, D.A. and Johnston, D. Downregulation of transient K<sup>+</sup> channels in dendrites of hippocampal CA1 pyramidal neurons by activation of PKA and PKC. *J. Neurosci.* 18: 3521-3528. 1998.

Hoffman, D.A., Magee, J.C., Colbert, C.M., and Johnston, D. K<sup>+</sup> channel regulation of signal propagation in dendrites of hippocampal pyramidal neurons. *Nature.* 387: 869-875. 1997.

Holthoff, K., Tsay, D., and Yuste, R. Calcium dynamics of spines depend on their dendritic location. *Neuron.* 33: 425-437. 2002.

Isaacson, J.S. Glutamate spillover mediates excitatory transmission in the rat olfactory bulb. *Neuron.* 23: 377-384. 1999.

Isaacson, J.S. and Strowbridge, B.W. Olfactory reciprocal synapses: dendritic signaling in the CNS. *Neuron.* 20: 749-761. 1998.

Llinas, R. and Sugimori, M. Electrophysiological properties of in vitro Purkinje cell dendrites in mammalian cerebellar slices. *J. Physiol.* 305: 197-213. 1980.

Lowe, G. Inhibition of backpropagating action potentials in mitral cell secondary dendrites. *J. Neurophysiol.* 88: 64-85. 2002.



Magee, J.C. and Johnston, D. Characterization of single voltage-gated Na<sup>+</sup> and Ca<sup>2+</sup> channels in apical dendrites of rat CA1 pyramidal neurons. *J. Physiol.* 487: 67-90. 1995.

Margrie, T.W., Sakmann, B., and Urban, N.N. Action potential propagation in mitral cell lateral dendrites is decremental and controls recurrent and lateral inhibition in the mammalian olfactory bulb. *Proc. Natl. Acad. Sci. USA.* 98: 319-324. 2001.

Martina, M., Vida, I., and Jonas, P. Distal initiation and active propagation of action potentials in interneuron dendrites. *Science.* 287: 295-300. 2000.

Mayer, M.L. and Sugiyama, K. A modulatory action of divalent cations on transient outward current in cultured rat sensory neurones. *J. Physiol.* 196: 417-433. 1988.

Mori, K. Relation of chemical structure to specificity of response in the olfactory glomeruli. *Curr. Opin. Neurobiol.* 5: 467-474. 1995

Mori, K., Kishi, K., and Ojima, H. Distribution of mitral, displaced mitral, tufted, and granule cells in the rabbit olfactory bulb. *J. Comp. Neurol.* 219: 339-355. 1983.

Mori, K, Nagao, H., and Yoshihara, Y. The olfactory bulb: coding and processing of odor molecule information. *Science.* 286: 711-715. 1999.

Orona, E., Rainer, E.C., and Scott, J.W. Dendritic and axonal organization of mitral and tufted cells in the rat olfactory bulb. *J. Comp. Neurol.* 226: 346-356. 1984.

Schoppa, N.E., Kinzie, J.M., Sahara, Y., Segerson, T.P., and Westbrook, G.L. Dendrodendritic inhibition in the olfactory bulb is driven by NMDA receptors. *J. Neurosci.* 18: 6790-6802. 1998.

Schoppa, N.E. and Westbrook, G.L. Regulation of synaptic timing in the olfactory bulb by an A-type potassium current. *Nat. Neurosci.* 2: 1106-1113. 1999.

Schoppa, N.E. and Westbrook, G.L. Glomerulus-specific synchronization of mitral cells in the olfactory bulb. *Neuron.* 31: 639-651. 2001.

Spruston, N., Schiller, Y., Stuart, G., and Sakmann, B. Activity-dependent action potential invasion and calcium influx into hippocampal CA1 dendrites. *Science.* 268: 297-300. 1995.

Storm, JF. Temporal integration by a slowly inactivating K<sup>+</sup> current in hippocampal neurons. *Nature.* 336: 379-381. 1988.

Stuart, G. and Hausser, M. Initiation and spread of sodium action potentials in cerebellar Purkinje cells. *Neuron.* 13: 703-712. 1994.

Stuart, G.J. and Sakmann, B. Active propagation of somatic action potentials into neocortical pyramidal cell dendrites. *Nature*. 367: 69-72. 1994.

Villarroel, A. and Schwarz, T.L. Inhibition of the Kv4 (Shal) family of transient K<sup>+</sup> currents by arachidonic acid. *J. Neurosci*. 16: 2522-2532. 1996.

Wang, X.Y., McKenzie, J.S., and Kemm, R.E. Whole-cell K<sup>+</sup> currents in identified olfactory bulb output neurones of rats. *J. Physiol*. 490: 63-77. 1996.

Wilson, D.A. and Leon, M. Evidence of lateral synaptic interactions in olfactory bulb output cell responses to odors. *Brain Res*. 417: 175-180. 1987.

Xiong, W. and Chen, W.R. Dynamic gating of spike propagation in the mitral cell lateral dendrites. *Neuron*. 34: 115-126. 2002.

Yokoi, M., Mori, K., and Nakanishi, S. Refinement of odor molecule tuning by dendrodendritic synaptic inhibition in the olfactory bulb. *Proc. Natl. Acad. Sci. USA*. 92: 3371-3375. 1995.

### **Chapter 3**

Adrian, E.D. The electrical activity of the mammalian olfactory bulb. *Electroencephalogr. Clin. Neurophysiol*. 2: 377-388. 1950.

Alvarez, V.A., Chow, C.C., Van Bockstaele, E.J., and Williams, J.T. Frequency dependent synchrony in the locus ceruleus: Role of electrotonic coupling. *Proc. Nat. Acad. Sci. USA.* 99: 4032-4036. 2002.

Amatai, Y., Gibson, J.R., Beierlein, M., Patrick, S.L., Ho, A.M., Connors, B.W., and Golomb, D. The spatial dimensions of electrically coupled networks of interneurons in the neocortex. *J. Neurosci.* 22: 4142-4152. 2002.

Beierlein, M., Gibson, J.R., and Connors, B.W. A network of electrically coupled interneurons drives synchronized inhibition in neocortex. *Nat. Neurosci.* 3: 904-910. 2000.

Belluardo, N., Mudo, G., Trovato-Salinaro, A., Le Gurun, S., Charollais, A., Serre-Beinier, V., Amato, G., Haefliger, J.A., Meda, P., and Condorelli, D. Expression of connexin36 in the adult and developing rat brain. *Brain Research.* 865: 121-138. 2000.

Bennett, M.V., and Zukin R.S. Electrical coupling and neuronal synchronization in the mammalian brain. *Neuron.* 41: 495-511. 2004.

Blatow, M., Rozov, A., Katona, I., Hormuzdi, S.G., Meyer, A.H., Whittington, M.A., Caputi, A., and Monyer, H. A novel network of multipolar bursting interneurons generates theta frequency oscillations in neocortex. *Neuron.* 38: 805-817. 2003.

Bozza, T.C., and Mombaerts, P. Olfactory coding: revealing intrinsic representations of odors. *Curr. Biol.* 11: R687-R690. 2001.

Carlson, G.C., Shipley, M.T., and Keller, A. Long-lasting depolarizations in mitral cells of the rat olfactory bulb. *J. Neurosci.* 20: 2011-2021. 2000.

Chao, T.I., Kasa, P., and Wolff, J.R. Distribution of astroglia in glomeruli of the rat main olfactory bulb: exclusion from the sensory subcompartment of neuropil. *J. Comp. Neurol.* 388: 191-210. 1997

Condorelli, D.L., Parenti, R., Spinella, F., Trovato-Salinaro, A., Belluardo, N., Cardile, V., and Cicirata, F. Cloning of a new gap junction gene (Cx36) highly expressed in mammalian brain neurons. *Eur. J. Neurosci.* 10: 1202-1208. 1998.

Connors, B.W., and Long, M.A. Electrical synapses in the mammalian brain. *Annu. Rev. Neurosci.* 27: 393-418. 2004.

Deans, M.R., Gibson, J.R., Sellitto, C., Connors, B.W., and Paul, D.L. Synchronous activity of inhibitory networks in neocortex requires electrical synapses containing connexin36. *Neuron.* 31: 477-485. 2001.

De Zeeuw, C.I., Chorev, E., Devor, A., Manor, Y., Van Der Giessen, R.S., De Jeu, M.T., Hoogenraad, C.C., Bijman, J., Ruigrok, T.J., French, P., Jaarsma, D., Kistler, W.M.,

Meier, C., Petrasch-Parwez, E., Dermietzel, R., Sohl, G., Gueldenagel, M., Willecke, K., and Yarom, Y. (2003). Deformation of network connectivity in the inferior olive of connexin 36-deficient mice is compensated by morphological and electrophysiological changes at the single neuron level. *J. Neurosci.* 23: 4700-4711.

Felgenspan, A., Janssen-Blenhold, U., Hormuzdi, S., Monyer, H., Degen, J., Sohl, G., Willecke, K., Ammermuller, J., and Weller, R. Expression of connexin36 in cone pedicles and off-cone bipolar cells of the mouse retina. *J. Neurosci.* 24: 3325-3334. 2004.

Fukuda, T., and Kosaka, T. Gap junctions linking the dendritic network of GABAergic interneurons in the hippocampus. *J. Neurosci.* 20: 1519-1528. 2000.

Fukuda, T., and Kosaka, T. Ultrastructural study of gap junctions between dendrites of parvalbumin-containing GABAergic neurons in various neocortical areas of the adult rat. *Neuroscience.* 120: 5-20. 2003.

Gibson, J.R., Beierlein, M., and Connors, B.W. Two networks of electrically coupled inhibitory neurons in neocortex. *Nature.* 402: 75-79. 1999.

Hormuzdi, S.G., Filippov, M.A., Mitropoulou, G., Monyer, H., and Bruzzone, R. Electrical synapses: a dynamic signaling system that shapes the activity of neuronal networks. *Biochim. Biophys. Acta.* 1662: 113-137. 2004.

Hormuzdi, S.G., Pais, I., LeBeau, F.E.N., Towers, S.K., Rozov, A., Buhl, E.H., Whittington, M.A., and Monyer, H. Impaired electrical signaling disrupts gamma frequency oscillations in connexin 36-deficient mice. *Neuron*. 31: 487-495. 2001.

Isaacson, J.S. Glutamate spillover mediates excitatory transmission in the rat olfactory bulb. *Neuron*. 23: 377-384. 1999.

Kashiwadani, H., Sasaki, Y.F., Uchida, N., and Mori, K. Synchronized oscillatory discharges of mitral/tufted with different molecular receptive ranges in the rabbit olfactory bulb. *J. Neurophysiol.* 82: 1786-1792. 1999.

Kasowski, H.J., Kim, H., and Greer, C.A. Compartmental organization of the olfactory bulb glomerulus. *J. Comp. Neurol.* 407: 261-274. 1999.

Kosaka, T., and Kosaka, K. Neuronal gap junctions in the rat main olfactory bulb, with special reference to intraglomerular gap junctions. *Neurosci. Res.* 45: 189-209. 2003.

Kosaka, T., and Kosaka, K. Neuronal gap junctions between intraglomerular mitral/tufted cell dendrites in the mouse main olfactory bulb. *Neurosci. Res.* 49: 373-378. 2004.

Korsching S. Olfactory maps and odor images. *Curr. Opin. Neurobiol.* 12: 387-392. . 2002.

Landisman, C.E., Long, M.A., Beierlein, M., Deans, M.R., Paul, D.L., and Connors, B.W. Electrical synapses in the thalamic reticular nucleus. *J. Neurosci.* 22: 1002-1009. 2002.

Laurent, G., Stopfer, M., Friedrich, R.W., Rabinovich, M.I., Volkovskii, A., and Abarbanel, H.D.I. Odor encoding as an active, dynamical process: experiments, computation, and theory. *Annu. Rev. Neurosci.* 24: 263-297. 2001.

Laurent, G., Wehr, M., and Davidowitz, H. Temporal representations of odors in an olfactory network. *J. Neurosci.* 16: 3837-3847. 1996.

Long, M.A., Deans, M.R., Paul, D.L., and Connors, B.W. Rhythmicity without synchrony in the electrically uncoupled inferior olive. *J. Neurosci.* 22: 10898-10905. 2002.

Long, M.A., Landisman, C.E., and Connors, B.W. Small clusters of electrically coupled neurons generate synchronous rhythms in the thalamic reticular nucleus. *J. Neurosci.* 24: 341-349. 2004.

MacLeod, K., Baker, A., and Laurent, G. Who reads temporal information contained across synchronized and oscillatory spike train? *Nature.* 395: 693-698. 1998.



Mori, K., Nagao, H., and Yoshihara, Y. The olfactory bulb: coding and processing of odor molecule information. *Science*. 286: 711-715. 1999.

Miragall, F., Simburger, E., and Dernietzel, R. Mitral and tufted cells of the mouse olfactory bulb possess gap junctions and express connexin43 mRNA. *Neurosci. Letters*. 216: 199-202. 1996.

Nagy, J.I., and Rash, J.E. Connexins and gap junctions of astrocytes and oligodendrocytes in the CNS. *Brain Res. Rev.* 32: 29-44. 2000.

Paternostro, M.A., Reyher, C.K.H., and Brunjes, P.C. Intracellular injections of Lucifer Yellow into lightly fixed mitral cells reveal neuronal dye-coupling in the developing rat olfactory bulb. *Develop. Brain Research*. 84: 1-10. 1995.

Parenti R, Gulisano M, Zappala A, and Cicirata F. Expression of connexin36 mRNA in adult rodent brain. *Neuroreport*. 7: 1497-1502. 2000.

Pereda, A.E., Bell, T.D., and Faber, D.S. Retrograde synaptic communication via gap junctions coupling auditory afferents to the Mauthner cell. *J. Neurosci*. 15: 5943-5955. 1995.

Pinching, J., and Powell, T.P.S. The neuropil of the glomeruli of the olfactory bulb. *J. Cell Sci*. 9: 347-377. 1971.

Puopolo, M., and Belluzzi, O. NMDA-dependent, network-driven oscillatory activity induced by bicuculline or removal of  $Mg^{2+}$  in the rat olfactory bulb neurons. *European J. Neurosci.* 13: 92-102. 2001.

Rash, J.E., Staines, W.A., Yasumura, T., Furman, C.S., Stelmack, G.L. and Nagy, J.I. Immunogold evidence that neuronal gap junctions in adult rat brain and spinal cord contain connexin-36 but not connexin-32 or connexin-43. *Proc. Nat. Acad. Sci. USA.* 97: 7573-7578. 2000.

Salin, P.A., Lledo, P.M., Vincent, J.D., and Charpak, S. Dendritic glutamate autoreceptors modulate signal processing in rat mitral cells. *J Neurophysiol.* 85: 1275-1282. 2001.

Schmitz, D. Schuchmann, S., Fisahn, A., Draguhn, A., Buhl, E.H., Petrasch-Parwez, E., Dermietzel, R., Heinemann, U., and Traub, R.D. Axo-axonal coupling. a novel mechanism for ultrafast neuronal communication. *Neuron.* 31: 831-840. 2001.

Schoppa, N.E., and Westbrook, G.L. Glomerulus-specific synchronization of mitral cells in the olfactory bulb. *Neuron.* 31: 639-651. 2001.

Schoppa, N.E., and Westbrook, G.L. AMPA autoreceptors drive correlated spiking in olfactory bulb glomeruli. *Nat. Neurosci.* 5: 1194-1202. 2002.

Schoppa, N.E., and Urban, N.N. Dendritic processing within olfactory bulb circuits. *Trends Neurosci.* 26: 501-506. 2003.

Smith, M., and Pereda, A.E. Chemical synaptic activity modulates nearby electrical synapses. *Proc. Natl. Acad. Sci. USA.* 100: 4829-4854. 2003.

Srinivas, M., Rozental, R., Kojima, T., Dermietzel, R., Mehler, M., Condorelli, D.F., Kessler, J.A., and Spray, D.C. Functional properties of channels formed by the neuronal gap junction protein connexin36. *J. Neurosci.* 19: 9848-9855. 1999.

Stopfer, M., Bhagavan, S. Smith, B.H., and Laurent, G. Impaired odor discrimination on desynchronization of odor-encoding neural assemblies. *Nature.* 390: 70-74. 1997.

Teubner, B., Degen, J., Sohl, G., Guldenagel, M., Bukauskas, F.F., Trexler, E.B., Verselis, V.K., De Zeeuw, C.I., Lee, C.G., Kozak, C.A., Petrasch-Parwez, E., Dermietzel, R., and Willecke, K. Functional expression of the murine connexin 36 gene coding for a neuron-specific gap junctional protein. *Membrane Biology.* 176: 249-262. 2000.

Traub, R.D., Pais, I., Bibbing, A., LeBeau, F.E., Buhl, E.H., Hormuzdi, S.G., Monyer, H., and Whittington, M.A. Contrasting roles of axonal (pyramidal cell) and dendritic (interneuron) electrical coupling in the generation of neuronal network oscillations. *Proc. Nat. Acad. Sci. USA.* 100: 1370-1374. 2003.

Urban, N.N., and Sakmann, B. Reciprocal intraglomerular excitation and intra- and interglomerular lateral inhibition between mouse olfactory bulb mitral cells. *J. Physiol.* 542: 355-367. 2002.

Venance, L., Rozov A., Blatow, M. Burnashev, N. Feldmeyer, D. and Monyer, H. Connexin expression in electrically coupled postnatal rat brain neurons. *Proc. Natl. Acad. Sci. USA.* 97: 10260-10265. 2000.

Wehr, M., and Laurent, G. Odour encoding by temporal sequences of firing in oscillating neuronal assemblies. *Nature* 384: 162-166. 1996.

Xu, F., Greer, C.A., and Shepherd, G.M. Odor maps in the olfactory bulb. *J. Comp. Neurol.* 422: 489-495. 2000.

Zhang, C., and Restrepo, D. Expression of connexin 45 in the olfactory system. *Brain Research* 929: 37-47. 2002.

Zhang, C., and Restrepo, D. Heterogenous expression of connexin 36 in the olfactory epithelium and glomerular layer of the olfactory bulb. *J. Comp. Neurol.* 459: 426-439. 2003.

## Chapter 4

Arnth-Jensen, N., Jabaudon, D., and Scanziani, M. Cooperation between independent hippocampal synapses is controlled by glutamate uptake. *Nat. Neurosci.* 5: 325-331. 2002.

Aroniadou-Anderjaska, V., Ennis, M., and Shipley, M.T. Dendrodendritic recurrent excitation in mitral cells of the rat olfactory bulb. *J. Neurophysiol.* 82: 489-494. 1999.

Asztley, F., Erdemil, G., and Kullmann, D.M. Extrasynaptic glutamate spillover in the hippocampus: dependence on temperature and the role of active uptake. *Neuron.* 18: 281-293. 1997.

Barbour, B., and Hausser, M. Intersynaptic diffusion of neurotransmitter. *Trends Neurosci.* 20: 377-384. 1997.

Bennett, M.V., and Zukin, R.S. Electrical coupling and neuronal synchronization in the mammalian brain. *Neuron.* 41: 495-511. 2004.

Bergles, D.E., and Jahr, C.E. Glial contribution to glutamate uptake at schaffer collateral-commissural synapses in the hippocampus. *J. Neurosci.* 18: 7709-7716. 1998.

Carlson, G.C., Shipley, M.T., and Keller, A. Long-lasting depolarizations in mitral cells of the rat olfactory bulb. *J. Neurosci.* 20, 2011-2021. 2000.

Carter, A.G., and Regehr, W.G. Prolonged synaptic currents and glutamate spillover at the parallel fiber stellate cell synapse. *J. Neurosci.* 20: 4423-4434. 2000.

Chao, T.I., Kasa, P., and Wolff, J.R. Distribution of astroglia in glomeruli of the rat main olfactory bulb: exclusion from the sensory subcompartment of neuropil. *J. Comp. Neurol.* 388: 191-210. 1997.

Chen, S., and Diamond, J.S. Synaptically released glutamate activates extrasynaptic NMDA receptors on cells in the ganglion cell layer of the rat retina. *J. Neurosci.* 22: 2165-2173. 2002.

Christie, J.M., Bark, C., Hormuzdi, S.G., Helbig, I., Monyer, H., and Westbrook, G.L. Loss of correlated spiking in olfactory bulb mitral cells in connexin36 deficient mice. Submitted to *Neuron*. 2004.

Clark, B.A., and Cull-Candy, S.G. Activity-dependent recruitment of extrasynaptic NMDA receptor activation at an AMPA receptor-only synapse. *J. Neurosci.* 22: 4428-4436. 2002.

Connors, B.W., and Long, M.A. Electrical synapses in the mammalian brain. *Annu. Rev. Neurosci.* 27: 393-418. 2004.

Diamond, J.S. Neuronal glutamate transporters limit activation of NMDA receptors by neurotransmitter spillover on CA1 pyramidal cells. *J. Neurosci.* 21: 8328-8338. 2001.

DiGregorio, D.A., Nusser, Z., and Silver, R.A. Spillover of glutamate onto synaptic AMPA receptors enhances fast transmission at a cerebellar synapse. *Neuron.* 35: 521-533. 2002.

Giustetto, M., Bovolin, P., Fasolo, A., Bonino, M., Cantino, D., and Sassoe-Pognetto, M. Glutamate receptors in the olfactory bulb circuitry: heterogeneity and synaptic localization of N-methyl-D-aspartate receptor subunit 1 and AMP receptor subunit 1. *Neuroscience.* 76: 787-798. 1997.

Friedman, D., and Strowbridge, B.W. Functional role of NMDA autoreceptors in olfactory bulb mitral cells. *J. Neurophysiol.* 84: 39-50. 2000.

Hormuzdi, SG, Filippov, M.A., Mitropoulou, G., Monyer, H., and Bruzzone, R. Electrical synapses: a dynamic signaling system that shapes the activity of neuronal networks. *Biochim. Biophys. Acta.* 1662: 113-137. 2004.

Hormuzdi, S.G., Pais, I., LeBeau, F.E.N., Towers, S.K., Rozov, A., Buhl, E.H., Whittington, M.A., and Monyer, H. Impaired electrical signaling disrupts gamma frequency oscillations in connexin 36-deficient mice. *Neuron*. 31: 487-495. 2001.

Isaacson, J.S. Glutamate spillover mediates excitatory transmission in the rat olfactory bulb. *Neuron*. 23: 377-384. 1999.

Kasowski, H.J., Kim, H., Greer, C.A. Compartmental organization of the olfactory bulb glomerulus. *J. Comp. Neurol.* 407: 261-274. 1999.

Kinney, G.A., Overstreet, L.S., Slater, N.T. Prolonged physiological entrapment of glutamate in the synaptic cleft of cerebellar unipolar brush cells. *J. Neurophysiol.* 78: 1320-1333. 1997.

Kullmann, D.M., Erdemli, G., and Asztely, F. LTP of AMPA and NMDA receptor-mediated signals: evidence for presynaptic expression and extrasynaptic glutamate spillover. *Neuron*. 17: 461-474. 1996.

Laurent, G., Stopfer, M., Friedrich, R.W., Rabinovich, M.I., Volkovskii, A., and Abarbanel, H.D.I. Odor encoding as an active, dynamical process: experiments, computation, and theory. *Annu. Rev. Neurosci.* 24: 263-297. 2001.



Montague, A.A., and Greer, C.A. Differential distribution of ionotropic glutamate receptor subunits in the rat olfactory bulb. *J. Comp. Neurol.* 405: 233-246. 1999.

Nicoll, R.A., Jahr, C.E. Self-excitation of olfactory bulb neurons. *Nature.* 296: 441-444. 1982.

Otis, T.S., and Trussell, L.O. Inhibition of transmitter release shortens the duration of the excitatory synaptic current at a calyceal synapse. *J. Neurophysiol.* 76: 3584-3588. 1996.

Otis, T.S., Wu, Y.C., and Trussell, L.O. Delayed clearance of transmitter and the role of glutamate transporters at synapses with multiple release sites. *J. Neurosci.* 16: 1634-1644. 1996.

Overstreet, L.S., Kinney, G.A., Liu, Y., Bilups, D., Slater, N.T. Glutamate transporters contribute to the time course of synaptic transmission in cerebellar granule cells. *J. Neurosci.* 19: 9663-9673. 1999.

Patneau, D.K., and Mayer, M.L. Structure-activity relationships for amino acid transmitter candidates acting at N-methyl-D-aspartate and quisqualate receptors. *J. Neurosci.* 10: 2385-2399. 1990.

Pinching, J., and Powell, T.P.S. The neuropil of the glomeruli of the olfactory bulb. *J. Cell Sci.* 9: 347-377. 1971.

Price, J.L., and Powell, T.P.S. The mitral cell and short axon cells of the olfactory bulb. *J. Cell Sci.* 7: 631-651. 1970.

Puopolo, M., and Belluzzi, O. NMDA-dependent, network-driven oscillatory activity induced by bicuculline or removal of  $Mg^{2+}$  in the rat olfactory bulb neurons. *European J. Neurosci.* 13: 92-102. 2001.

Salin, P.A., Lledo, P.M., Vincent, J.D., and Charpak, S. Dendritic glutamate autoreceptors modulate signal processing in rat mitral cells. *J. Neurophysiol.* 85: 1275-1282. 2001.

Sassoe-Pognetto, M., Utvik, J.K., Camoletto, P., Watanabe, M., Stephenson, F.A., Bredt, D.S., and Otterson, O.P. Organization of postsynaptic density proteins and glutamate receptors in axodendritic and dendrodendritic synapses of the rat olfactory bulb. *J. Comp. Neurol.* 463: 237-248. 2003.

Schoppa, N.E., and Westbrook, G.L. Glomerulus-specific synchronization of mitral cells in the olfactory bulb. *Neuron.* 31: 639-651. 2001.

Schoppa, N.E., and Westbrook, G.L. AMPA autoreceptors drive correlated spiking in olfactory bulb glomeruli. *Nat. Neurosci.* 5: 1194-1202. 2002.

Schoppa, N.E., and Urban, N.N. Dendritic processing within olfactory bulb circuits. *Trends Neurosci.* 26: 501-506. 2003.

Shepherd, G.L., and Greer, C.A. *The Synaptic Organization of the Brain*. New York, NY. Oxford University Press. 1998.

Silver, R.A., Cull-Candy, S.G., and Takahashi, T. Non-NMDA glutamate receptor occupancy and open probability at a rat cerebellar synapse with single and multiple release sites. *J. Physiol.* 494: 231-250. 1996.

Urban, N.N., and Sakmann, B. Reciprocal intraglomerular excitation and and intra- and interglomerular lateral inhibition between mouse olfactory bulb mitral cells. *J. Physiol.* 542: 355-367. 2002.

Xu, F., Greer, C.A., and Shepherd, G.M. Odor maps in the olfactory bulb. *J. Comp. Neurol.* 422: 489-495. 2000.

Zhang, C., and Restrepo, D. Heterogenous expression of connexin 36 in the olfactory epithelium and glomerular layer of the olfactory bulb. *J. Comp. Neurol.* 459, 426-439. 2003.

Zou, Z., Horowitz, L.F., Montmayeur, J.P. Snapper, S., and Buck, L.B. Genetic tracing reveals a stereotyped sensory map in the olfactory cortex. *Nature.* 414: 173-179. 2001.

## **Discussion**

DiGregorio, D.A., Nusser, Z., and Silver, R.A. Spillover of glutamate onto synaptic AMPA receptors enhances fast transmission at a cerebellar synapse. *Neuron*. 35: 521-533. 2002.

Hoffman, D.A., Magee, J.C., Colbert, C.M., and Johnston, D. K<sup>+</sup> channel regulation of signal propagation in dendrites of hippocampal pyramidal neurons. *Nature*. 387: 869-875. 1997.

Kinney, G.A. Overstreet, L.S. and Slater, N.T. Prolonged physiological entrapment of glutamate in the synaptic cleft of cerebellar unipolar brush cells. *J. Neurophysiol.* 78: 1320-1333. 1997.

Marin, E.C., Jefferies, G.S., Komiyama, T., Zhu, H., and Luo, L. Spatial representation of the glomerular olfactory map in the Drosophila brain. *Cell*. 109: 243-255. 2002

Miragall, F., Simburger, E., and Dernietzel, R. Mitral and tufted cells of the mouse olfactory bulb possess gap junctions and express connexin43 mRNA. *Neurosci. Letters* 216: 199-202. 1996.

Otis, T.S. and Trussell, L.O. Inhibition of transmitter release shortens the duration of the excitatory synaptic current at a calyceal synapse. *J. Neurophysiol.* 76: 3584-3588. 1996.

Otis, T.S., Wu, Y.C. and Trussell, L.O. Delayed clearance of transmitter and the role of glutamate transporters at synapses with multiple release sites. *J. Neurosci.* 16: 1634-1644.

Overstreet, L.S., Kinney, G.A., Liu, Y., Bilups, D. and Slater, N.T. Glutamate transporters contribute to the time course of synaptic transmission in cerebellar granule cells. *J. Neurosci.* 19: 9663-9673. 1999.

Parenti, R., Gulisano, M., Zappala, A., and Cicirata, F. Expression of connexin36 mRNA in adult rodent brain. *Neuroreport* 7: 1497-1502. 2000.

Paternostro, M.A., Reyher, C.K.H., and Brunjes, P.C. Intracellular injections of Lucifer Yellow into lightly fixed mitral cells reveal neuronal dye-coupling in the developing rat olfactory bulb. *Develop. Brain Research* 84: 1-10. 1995.

Schoppa, N.E. and Westbrook, G.L. Glomerulus-specific synchronization of mitral cells in the olfactory bulb. *Neuron.* 31: 639-651. 2001.

Silver, R.A., Cull-Candy, S.G., and Takahashi, T. Non-NMDA glutamate receptor occupancy and open probability at a rat cerebellar synapse with single and multiple release sites. *J. Physiol.* 494: 231-250. 1996.

Teubner, B., Degen, J., Sohl, G., Guldenagel, M., Bukauskas, F.F., Trexler, E.B., Verselis, V.K., De Zeeuw, C.I., Lee, C.G., Kozak, C.A., Petrasch-Parwez, E., Dermietzel, R., and Willecke, K. Functional expression of the murine connexin 36 gene coding for a neuron-specific gap junctional protein. *Membrane Biology* 176: 249-262. 2000.

Urban, N.N., and Sakmann, B. Reciprocal intraglomerular excitation and and intra- and interglomerular lateral inhibition between mouse olfactory bulb mitral cells. *J. Physiol.* 542: 355-367. 2002.

Wong, A.M., Wang, J.W. and Axel, R. Representation of the glomerular map in *Drosophila protocerebrum*. *Cell*. 109: 229-241. 2002.

Zhang, C., and Restrepo, D. Expression of connexin 45 in the olfactory system. *Brain Research*. 929: 37-47. 2002.